Supporting information

for

Resorcin[4]arene-based multidentate phosphate ligands with superior binding affinity for nanocrystal surfaces

Suren J. Nemat,[a] Dietger Van den Eynden,[a] Loren Deblock,[a,b] Michael Heilmann,[a] Jesper M. Köster,[a] Mahsa Parvizian,[a] Konrad Tiefenbacher,[*a,c] Jonathan De Roo[*a]

[a]Department of Chemistry, University of Basel, Basel 4058, Switzerland

[b]Department of Chemistry, Ghent University, 9000 Gent, Belgium

[c]Department of Biosystems Science and Engineering, ETH Zürich, CH-4058 Basel, Switzerland

* Corresponding authors:

Jonathan De Roo, Jonathan.DeRoo@unibas.ch

Konrad Tiefenbacher, Konrad.Tiefenbacher@unibas.ch

Contents .....

1. Experimental Details

Materials for nanocrystal synthesis. $ZrCl_4$ (99.95%) was bought from Strem chemicals and used without purification. Oleic acid (technical, 90%), octylamine (99%), oleylamine (70%), benzylalcohol anhydrous (99.8%), dibenzylether (>98%) and $CHCl_3$ stabilized with ethanol (>99.5%) were purchased from Sigma Aldrich and used without purification. Diethylether BHT stabilized (CP), ethanol absolute dehydrated (CP-p) and acetone (CP) were bought from biosolve. THF-d_8 was bought from Eurisotop.

ZrO_2 nanocrystals. Oleic acid functionalized zirconia nanocrystals (diameter = 5 nm) were synthesized and purified according to De Roo *et al,*[1] which was an adaptation of Buha et al.[2] The procedure involves (i) a surfactant-free solvothermal synthesis and (ii) a post-synthetic de-aggregation step with oleic acid under basic conditions. Note that the direct stabilization of the ZrO_2 nanocrystals with ligand **1** or **2** (instead of oleic acid) was unsuccessful. First, one has to stabilize the nanocrystals with oleic acid and purify this complex mixture before exchanging oleate for ligand **1** or **2**.

Functionalization. To the ZrO_2 nanocrystal suspension (16.7 mg ZrO_2/mL, [oleic acid] = 14 mM) in 0.5 mL THF-d_8, was added one equivalent of ligand **1** or **2** as a solution in 0.5 mL THF-d_8. The dispersion was placed in an ultrasonic bath for a minute to overcome activation barriers.

Purification of nanocrystals, functionalized with ligand 1. The solvent was evaporated until the volume was reduced to 0.6 mL. Acetone (3mL) was added causing the nanocrystals to flocculate. The precipitate was compacted by centrifugation (5000 rpm = 3438 rcf, 3 min). The nanocrystals were suspended in 0.5 mL chloroform, precipitated with 2 mL of acetone and isolated by centrifugation (5000 rpm, 3 min). The nanocrystals were suspended in 0.5 mL THF, precipitated with 2 mL of acetone and isolated by centrifugation (5000 rpm, 3 min). The final nanocrystals were dispersed in THF-d_8.

Purification of nanocrystals, functionalized with ligand 2. The solvent was evaporated and the nanocrystals were dispersed in 0.25 mL distilled THF. Methanol (0.75 mL) was added causing the nanocrystals to flocculate. The precipitate was compacted by centrifugation (5000 rpm = 3438 rcf, 3 min). The nanocrystals were suspended in 0.25 mL distilled THF, precipitated with 0.75 mL of methanol and isolated by centrifugation (5000 rpm, 3 min). The final nanocrystals were dispersed in THF-d_8.

General considerations for macrocycle synthesis: All reactions were carried out using standard SCHLENK techniques with Argon (Ar 4.6) as inert gas. Unless indicated otherwise, glass equipment was dried under high vacuum (10^{-2} mbar) at 500–600 °C using a heat gun. Reactions at low temperatures were performed using cooling baths (−78 °C using dry ice/acetone, 0 °C using ice/water).

Materials for macrocycle synthesis: 3-methoxyphenol, dodecanal, boron trifluoride etherate, diethyl chlorophosphate, sodium hydride (NaH), 2,3 dihydrofurane, 1-iodohexane, diphenyl chlorophosphate and platinum(IV) oxide were purchased from SIGMA-ALDRICH. Bromotrimethylsilane (TMSBr) and potassium carbonate (K_2CO_3) were purchased from ACROS. Acetic acid was purchased from VWR. Reagents were used without prior purification. Anhydrous solvents were purchased from ACROS and were used without prior purification. Solvents for extractions, chromatography, filtrations and non-anhydrous reactions were purchased from VWR as HPLC grade solvents and were used without prior purification. NMR solvents were purchased from CAMBRIDGE ISOTOPE LABORATORIES and APOLLO and were used without prior purification.

Thin-Layer Chromatography (TLC): Analytical thin-layer chromatography (TLC) was performed on MERCK silica gel 60 F254 glass-baked plates, which were analyzed by fluorescence detection with UV-

light (λ = 254 nm, [UV]) and after exposure to standard staining reagents and subsequent heat treatment. The following staining solution was used: acidic cerium ammonium molybdate solution [CAM] (40 g ammonium heptamolybdate, 1.6 g cerium sulfate in 900 mL H_2O with 100 mL conc. H_2SO_4).

Flash Column Chromatography (FCC): Flash column chromatography was performed with MERCK silica 60 (230–240 mesh ASTM, pore size 40–63 µm).

Medium Pressure Liquid Chromatography (MPLC): Medium Pressure Liquid Chromatography (MPLC) was carried out with RediSep® Silica Gel Disposable Flash Columns SiO_2 columns (particle size 40-60 µm) (Table S1) on a Combi*Flash* NextGen 300+ version 5.0.55 by TELEDYNE ISCO with a fraction collector version 00.92.00, detector version 11, and a pump version: 1.47.

Table S1: Key parameters of the disposable SiO_2 columns used for MPLC.

Column Size	24g	40g
Column Volume (CV)/ml	33	48
Flow Rate /ml·min^{-1}	35	40

NMR-Spectroscopy: ^{1}H NMR spectra were recorded at 298 K at 500 MHz or 600 MHz on a BRUKER UltraShield 500 spectrometer or a 600 MHz BRUKER Avance III NMR spectrometer equipped with a cryogenic QCI-F probe, respectively. ^{13}C NMR spectra were recorded at 126 MHz or 151 MHz on a BRUKER UltraShield 500 spectrometer or a 600 MHz BRUKER Avance III NMR spectrometer equipped with a cryogenic QCI-F probe, respectively. ^{31}P NMR spectra were recorded at 202 MHz on a Bruker UltraShield 500 spectrometer. Chemical shifts of ^{1}H NMR and ^{13}C NMR spectra (measured at 298 K or 353 K) are given in ppm by using residual solvent signals as references ($CDCl_3$: 7.26 ppm and 77.16 ppm, respectively; DMSO−d_6: 2.50 ppm and 39.52 ppm, respectively; THF-d_8: 3.58 ppm and 67.57 ppm, respectively). Coupling constants (*J*) are reported in Hertz (Hz). Standard abbreviations indicating multiplicity were used as follows: s (singlet), d (doublet), t (triplet), q (quartet), p (pentet), s (sextet), h (septet), m (multiplet), b (broad).

For quantitative 1D 1H measurements, 64k data points were sampled with the spectral width set to 20 ppm and a relaxation delay of 30s. DOSY measurements were performed with a double stimulated echo and bipolar gradient pulses (dstebpgp3s). The gradient strength was varied quadratically from 5-95% of the probe's maximum value in 64 steps, with the gradient pulse duration and diffusion delay optimized to ensure a final attenuation of the signal in the final increment of less than 10% relative to the first increment. ^{31}P NMR measurement (for ligands bound to nanocrystals) were acquired with decoupling (zgpg30) and 4000 scans. The ^{31}P spectra were processed with a line broadening parameter of 50 Hz.

IR-Spectroscopy: Infrared (IR) spectra were recorded on a BRUKER ALPHA spectrometer (attenuated total reflection, ATR). Only selected absorbances (ν_{max}) are reported. Standard abbreviations indicating signal intensity were used as follows: s (strong), m (medium), w (weak), b (broad).

ESI-HRMS: High resolution mass spectra were obtained using the electrospray ionization (ESI) technique on a BRUKER maXis 4G mass spectrometer.

Melting Point (M.p.): Melting points (M.p.) were recorded on a BÜCHI Melting Point M-565 apparatus using open capillary tubes.

2. Supporting Figures

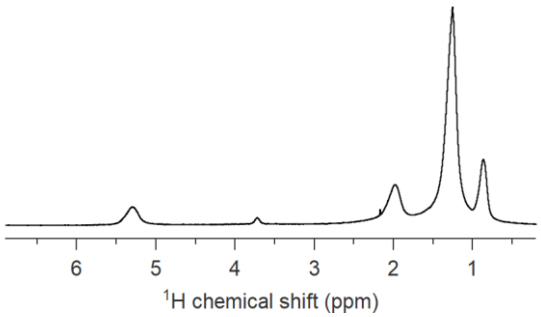

Figure S1: ^{1}H NMR spectrum of oleic acid capped ZrO_2 nanocrystals in $CDCl_3$, showing only bound ligands.

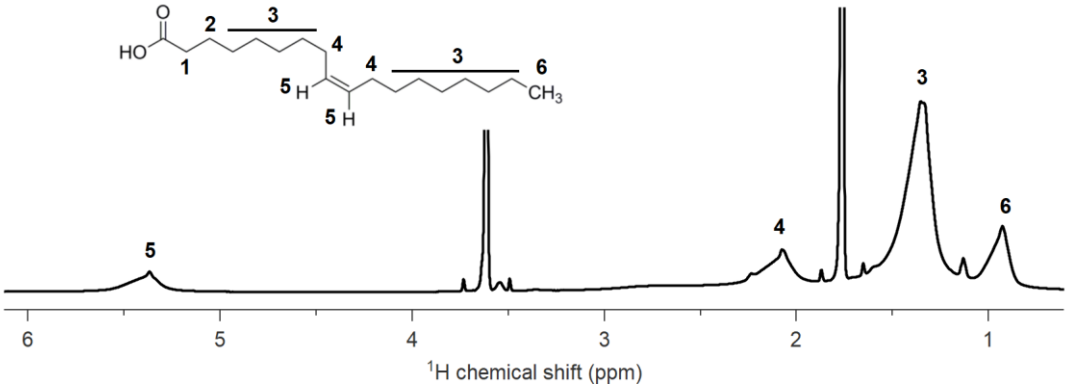

Figure S2: ^{1}H NMR spectrum of oleic acid capped ZrO_2 nanocrystals in THF-d_8, showing a small, sharper feature on top of the broad resonances, indicated a small amount of desorbed ligand.

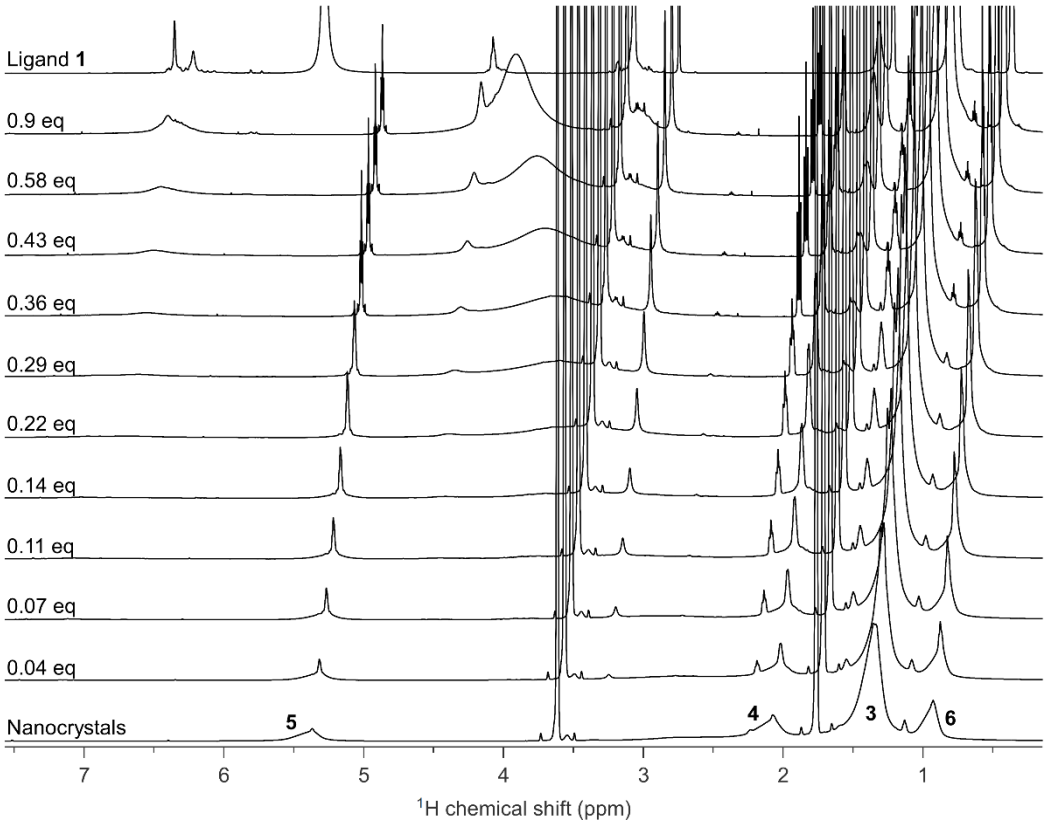

Figure S3: Waterfall plot of the ^{1}H NMR spectra of the titration of ligand **1** into a solution of oleic acid capped ZrO_2 nanocrystals (16.7 mg/mL), [oleic acid] = 14 mM). The ^{1}H NMR spectra of pure nanocrystals and pure **1** are also shown.

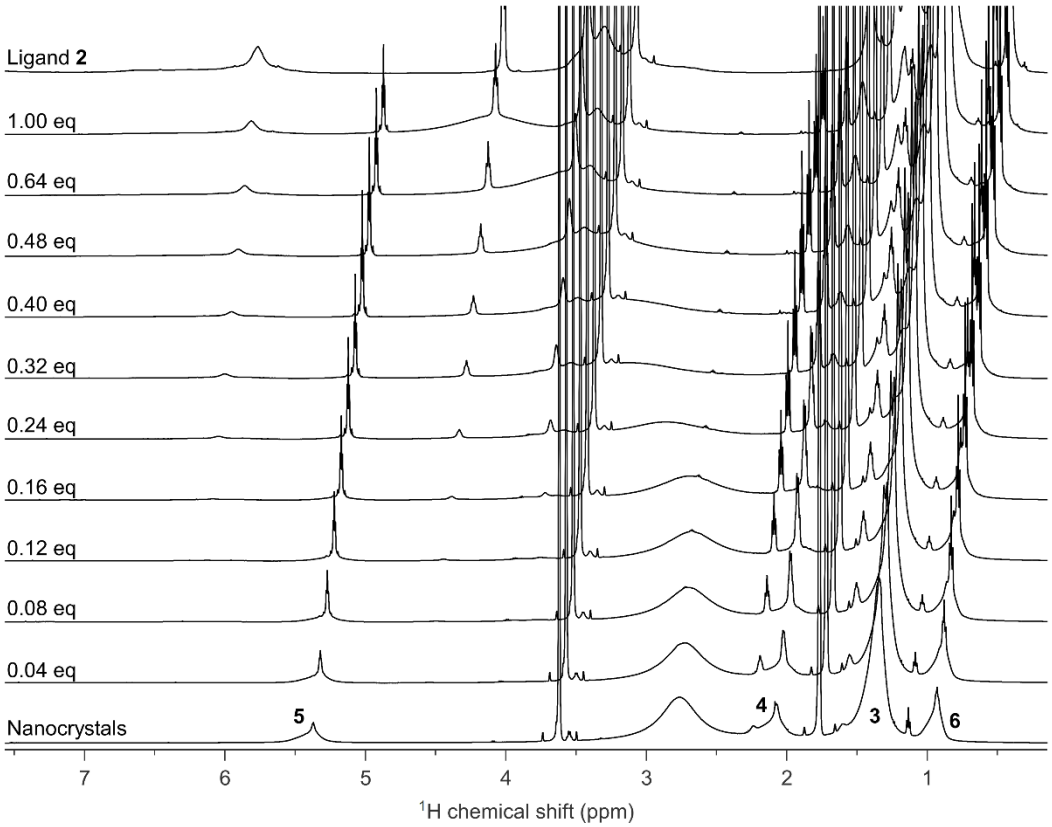

Figure S4: Waterfall plot of the ^{1}H NMR spectra of the titration of **2** into a solution of oleic acid capped ZrO_2 nanocrystals (16.7 mg/mL), [oleic acid] = 14 mM). The ^{1}H NMR spectra of pure nanocrystals and pure **2** are also shown.

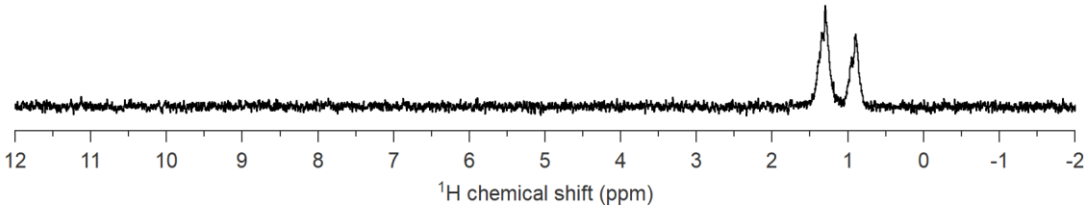

Figure S5: Diffusion filtered ^{1}H NMR spectrum after addition of 1 equivalent of **1** to oleic acid capped ZrO_2 nanocrystals.

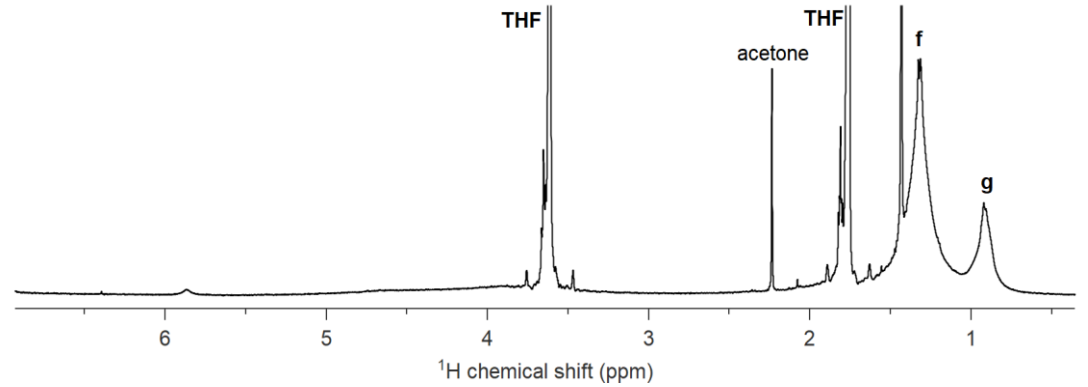

Figure S6: ^{1}H NMR spectrum of ZrO_2 nanocrystals capped with **1** in THF-d_8

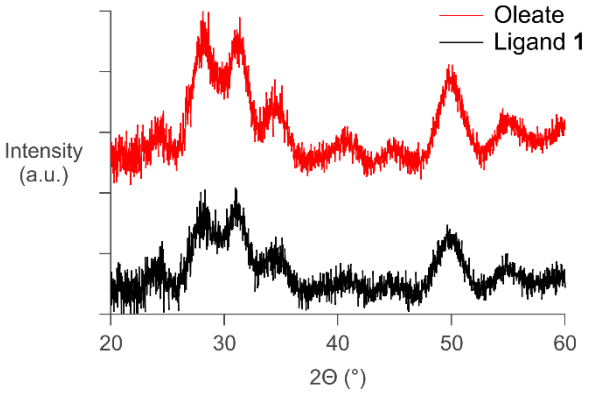

Figure S7: XRD diffractograms of the zirconia nanocrystals before and after ligand exchange with ligand 1. The nanocrystals have the monoclinic crystal structure as expected from literature.[1, 3]

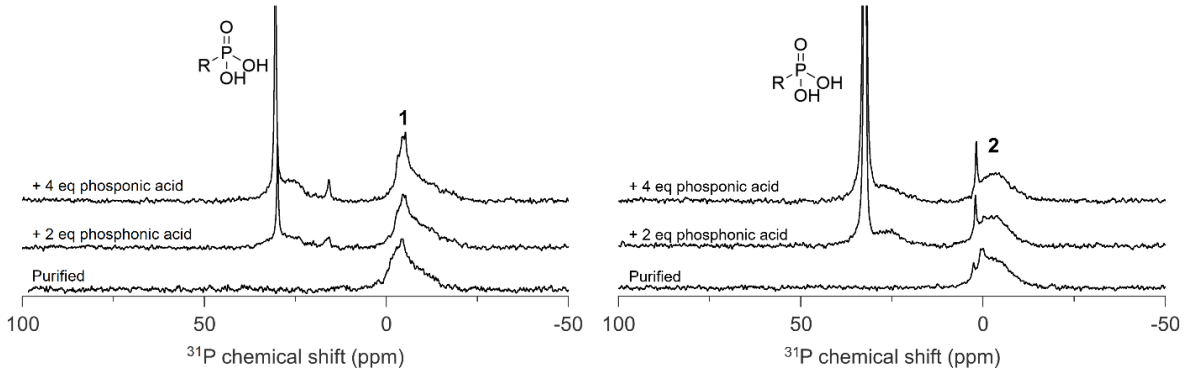

Figure S8: ^{31}P NMR spectrum of a purified ZrO_2 nanocrystal suspension, functionalized by **1** or **2** , after addition of 0, 2 or 4 equivalents oleylphosphonic acid.

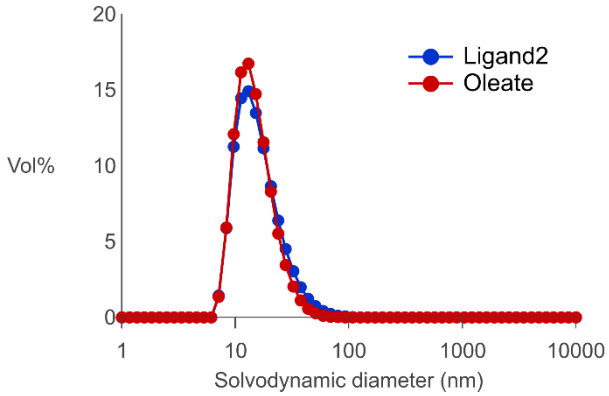

Figure S9: DLS measurements of oleate capped zirconia nanocrystals and purified nanocrystals functionalized with ligand **2** after one week of storage.

3. Synthetic Procedures and Analytical Data

3.1. Synthesis of Ligand 1

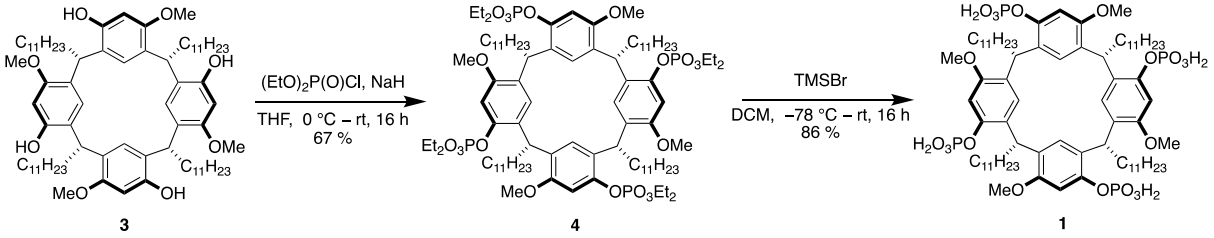

Scheme S1. Synthetic route to ligand **1**.

1^6,3^4,5^4,7^4-tetramethoxy-2,4,6,8-tetraundecyl-1,3,5,7(1,3)-tetrabenzenacyclo-octaphane-1^4,3^6,5^6,7^6-tetraol (3)

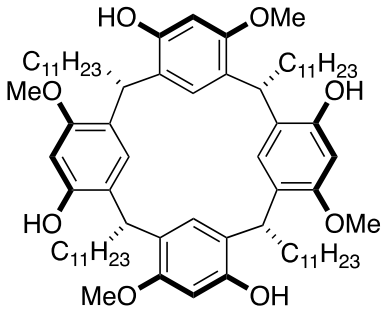

$C_{76}H_{120}O_8$
M = 1161.79 g/mol

Compound **3** was synthesized according to Nemat *et al*.[4]

octaethyl (1^6,3^4,5^4,7^4-tetramethoxy-2,4,6,8-tetraundecyl-1,3,5,7(1,3)-tetrabenzenacyclooctaphane-1^4,3^6,5^6,7^6-tetrayl) tetrakis(phosphate) (4)

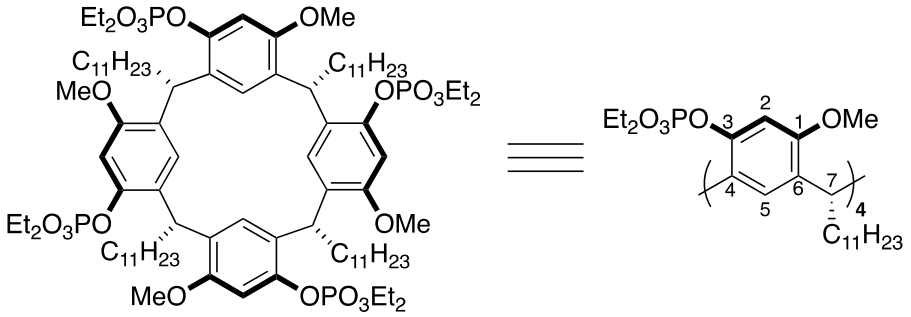

$C_{92}H_{156}O_{20}P_4$
M = 1706.14 g/mol

A one-neck 50 mL round-bottom flask was charged with **3** (1.00 g, 0.86 mmol, 1.00 equiv). The solid was dissolved in 10 mL dry THF and the solution was cooled to 0 °C. NaH (124 mg, 5.17 mmol, 6.01 equiv) was added, followed by dropwise addition of diethyl chlorophosphate (0.62 mL, 4.31 mmol, 5.01 equiv). The reaction mixture was allowed to warm to room temperature and stirred for 16 h. The reaction was quenched by addition of water (10 mL), transferred into a separatory funnel, followed by extraction with DCM (3 x 25 mL). The combined organic layers were dried with Na_2SO_4 and concentrated *in vacuo* at 40 °C. The crude product was purified by MPLC (RediSep® Column: Silica 40 g; 40 ml/min; DCM/DCM:MeOH (9:1) 100:0 to 0:100, 22.5 CV, 30.8 min) to obtain **4** (984 mg, 0.58 mmol, 67%) as a colourless oil which solidified to a white solid upon storage.

TLC: R_f = 0.38 (DCM/Acetone = 1/2) [UV, CAM].

M.p.: ϑ_m = 50-52 °C.
IR (ATR): ν [cm^{-1}] 2922 (m), 2852 (m), 1613 (w), 1585 (w), 1498 (m), 1465 (w), 1445 (w), 1284 (m), 1195 (w), 1164 (w), 1097 (w), 1026 (s), 957 (s), 852 (w), 820 (w), 758 (w).

^{1}H NMR (500 MHz, $CDCl_3$, 298 K, assignments based on COSY, HMQC and HMBC NMR spectra): δ [ppm] 6.88 (s, 4H, −C_2H), 6.66 (s, 4H, −C_5H), 4.48 (t, *J* = 7.4 Hz, 4H, −C_7H−), 4.23 – 4.08 (m, 8H, −PO(CH_2)CH_3), 4.02 (p, *J* = 7.3 Hz, 8H, −PO(CH_2)CH_3), 3.64 (s, 12H, −O*Me*), 1.90 – 1.75 (m, 8H, −(CH_2)$(CH_2)_9CH_3$), 1.3 – 1.2 (m, 96H, −(CH_2)(CH_2)$_9CH_3$ and -PO(CH_2)CH_3), 0.86 (t, *J* = 6.8 Hz, 12H, −$(CH_2)(CH_2)_9$CH_3).

^{13}C NMR (126 MHz, $CDCl_3$, 298 K): δ [ppm] 155.5 (d, J_{CP} = 1.3 Hz), 147.5 (d, J_{CP} = 6.8 Hz), 128.9 (s), 126.4 (s), 102.4 (s), 64.4 (d, J_{CP} = 6.2 Hz), 55.6 (s), 35.9 (s), 34.8 (s), 32.1 (s), 30.1 (s), 30.0 (s), 29.9 (s), 29.9 (s), 29.9 (s), 29.5 (s), 28.3 (s), 22.8 (s), 16.3 (d, J_{CP} = 6.7 Hz), 16.2 (d, J_{CP} = 6.7 Hz), 14.2 (s).

^{31}P NMR (202 MHz, $CDCl_3$, 298 K): δ [ppm] −6.83.

HR-MS (ESI, 5.0 eV): m/z calcd. for $C_{92}H_{156}O_{20}P_4Na$ $[(M+Na)]^+$: 1728.0033; measd.: 1728.0025.

Note: Diethyl chlorophosphate is a highly toxic and corrosive reagent that should be handled with great care in a well-ventilated fume hood.

1^6,3^4,5^4,7^4-tetramethoxy-2,4,6,8-tetraundecyl-1,3,5,7(1,3)-tetrabenzenacyclooctaphane-1^4,3^6,5^6,7^6-tetrayl tetrakis(dihydrogen phosphate) (1)

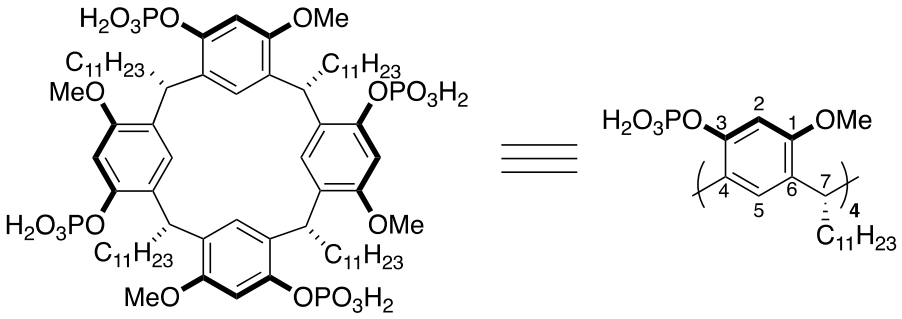

$C_{76}H_{124}O_{20}P_4$
M = 1481.70 g/mol

A one-neck 50 mL round-bottom flask was charged with **4** (200 mg, 117 μmol, 1.00 equiv). The solid was dissolved in 10 mL dry DCM and the solution was cooled to −78 °C. TMSBr (0.31 ml, 2.34 mmol,

20.0 equiv) was added dropwise. The reaction mixture was allowed to warm to room temperature and stirred for 48 h. The reaction was concentrated *in vacuo* at 40 °C, followed by dissolving the crude in 10 mL MeOH. The solution was stirred for 1 h at room temperature. After removing the solvent *in vacuo* at 50 °C, the crude was suspended in H_2O (10 mL) and lyophilized to obtain **1** (150 mg, 101 μmol, 86%) as an off-white powder.

M.p.: ϑ_m = 214-215 °C (decomposition).
IR (ATR): ν [cm^{-1}] 2922 (s), 2852 (s), 1497 (w), 1464 (w), 1286 (w), 1193 (w), 1151 (w), 1091 (w), 1012 (m), 965 (m), 842 (w), 737 (w).

^{1}H NMR (600 MHz, DMSO-d_6, 298 K, assignments based on COSY, NOESY, HMQC and HMBC NMR spectra): δ [ppm] 6.90 (s, 4H, −C_5H), 6.82 (s, 4H, −C_2H), 4.60 (t, *J* = 7.6 Hz, 4H, −C_7H), 3.61 (s, 12H, −O*Me*), 1.82 – 1.70 (m, 8H, −(C*H*$_2$)(CH$_2$)$_9$CH$_3$), 1.20 (m, 72H, −(CH$_2$)(*CH*$_2$)$_9$CH$_3$), 0.83 (t, *J* = 6.9 Hz, 12H, −(CH$_2$)(CH$_2$)$_9$*CH*$_3$).

^{13}C NMR (151 MHz, DMSO-d_6, 298 K): δ [ppm] 154.8 (s), 147.8 (s), 127.6 (s), 126.2 (s), 125.6 (s), 102.8 (s), 55.5 (s), 35.5 (s), 34.0 (s), 31.4 (s), 29.6 (s), 29.4 (s), 29.2 (s), 28.9 (s), 27.7 (s), 22.2 (s), 14.0 (s).

^{31}P NMR (202 MHz, DMSO-d_6, 298 K): δ [ppm] −6.14.

^{1}H NMR (500 MHz, THF-d_8, 298 K, assignments based on COSY, NOESY, HMQC and HMBC NMR spectra): δ [ppm] 6.88 (bs, 4H, −C_2H), 6.77 (bs, 4H, −C_5H), 4.63 (t, *J* = 7.4 Hz, 4H, −C_7H), 3.51 (bs, 12H, −O*Me*), 1.82 (s, 8H, −(C*H*$_2$)(CH$_2$)$_9$CH$_3$), 1.28 (s, 72H, −(CH$_2$)(*CH*$_2$)$_9$CH$_3$), 0.88 (t, *J* = 6.7 Hz, 12H, −(CH$_2$)(CH$_2$)$_9$*CH*$_3$).

^{13}C NMR (126 MHz, THF-d_8, 298 K): 156.9 (s), 148.9 (s), 126.7 (s), 104.3 (s), 56.6 (s), 36.3 (s), 33.1 (s), 31.3 (s), 31.1 (s), 31.0 (s), 31.0 (s), 30.9 (s), 30.6 (s), 29.3 (s), 26.0 (s), 23.7 (s), 14.6 (s).

^{31}P NMR (202 MHz, THF-d_8, 298 K): δ [ppm] −4.36.

HR-MS (ESI, 5.0 eV): m/z calcd. for $C_{76}H_{123}O_{20}P_4Na$ $[(M+2Na-H)]^+$: 1525.7348; measd.: 1525.7319.

Note: The carbon atoms C_2 and C_5 could not be resolved in the ^{13}C NMR in THF-d_8 as they are significantly broadened at 298 K. For further details, see Section 3.4.

3.2. Synthesis of Ligand 2

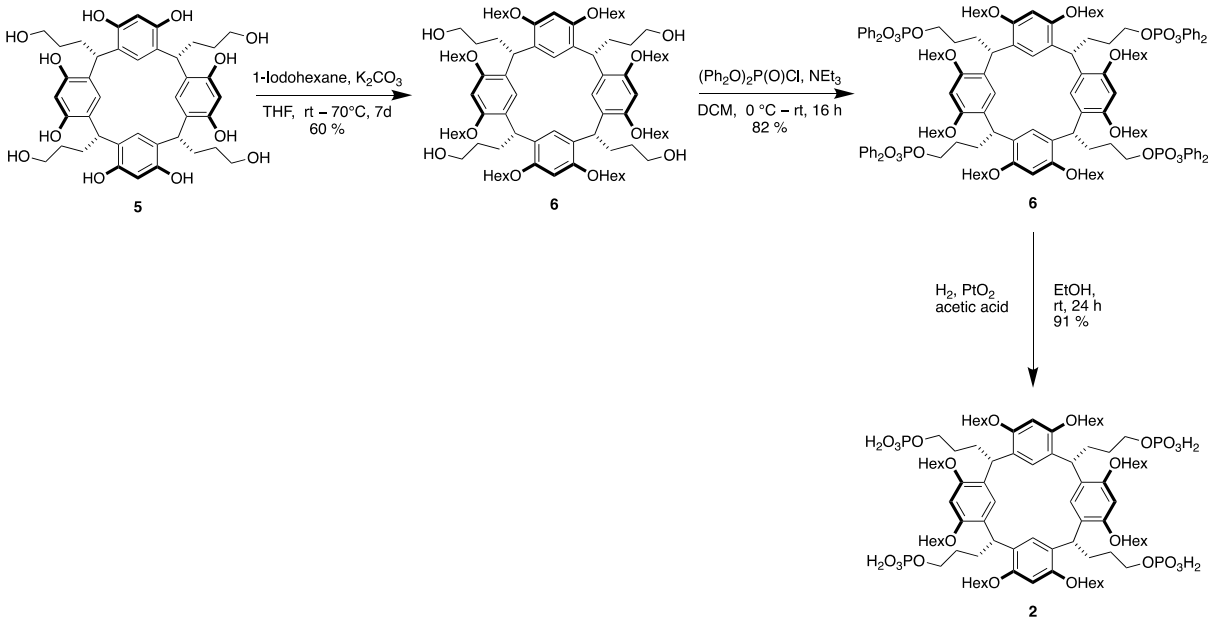

Scheme S2. Synthetic route to ligand **2**.

2,4,6,8-tetrakis(3-hydroxypropyl)-1,3,5,7(1,3)-tetrabenzenacyclooctaphan-1^4,1^6,3^4,3^6,5^4,5^6,7^4,7^6-octaol (5)

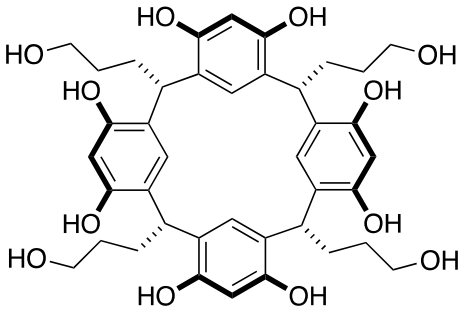

$C_{40}H_{48}O_{12}$
M = 720.81 g/mol

Compound **5** was synthesized according to Gibb *et al.*[5]

3,3',3'',3'''-((2*s*,4*s*,6*s*,8*s*)-1^4,1^6,3^4,3^6,5^4,5^6,7^4,7^6-octakis(hexyloxy)-1,3,5,7(1,3)-tetrabenzenacyclooctaphane-2,4,6,8-tetrayl)tetrakis(propan-1-ol) (6)

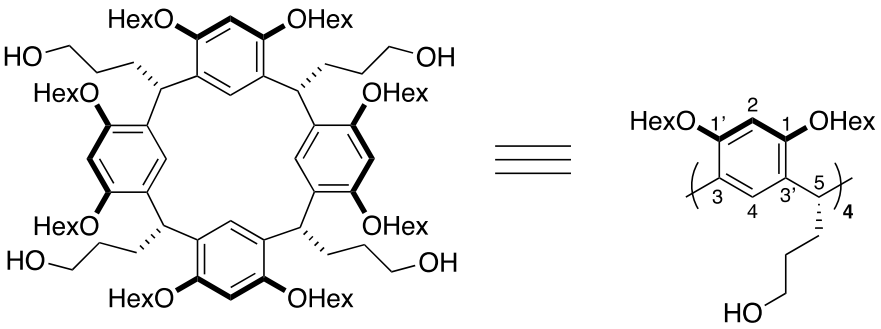

$C_{88}H_{144}O_{12}$
M = 1394.11 g/mol

A one-neck 250 mL round-bottom flask was charged with **5** (689 mg, 0.96 mmol, 1.00 equiv) and K_2CO_3 (2.21 g, 16.0 mmol, 16.7 equiv). 80 mL acetone were added and the resulting suspension was stirred for 1 h at room temperature. Then, 1-iodohexane (1.47 mL, 10.0 mmol, 10.4 equiv) was added dropwise. The reaction mixture was heated to 70 °C and stirred for 7 d. After cooling to room temperature, the solvent was removed and the remaining solid suspended in DCM (100 mL). The solid was filtered off, washed with DCM (3 x 10 mL) and the combined filtrates were concentrated *in vacuo* at 50 °C. The crude product was purified by flash column chromatography (250 g silica gel, DCM/acetone = 4/1 → 3/1) to obtain **6** (802 mg, 0.58 mmol, 60%) as a white solid.

TLC: R_f = 0.68 (DCM/Acetone = 1/2) [UV, CAM].

M.p.: ϑ_m = 139−140 °C.

IR (ATR): ν [cm^{-1}] 3293 (bw), 2930 (s), 2860 (s), 1611 (w), 1582 (w), 1500 (m), 1468 (m), 1411 (w), 1383 (w), 1300 (s), 1186 (s), 1118 (m), 1105 (m), 1049 (m), 937 (w), 912 (w), 813 (w).

^{1}H NMR (500 MHz, DMSO-d_6, 298 K, assignments based on COSY, HMQC and HMBC NMR spectra): δ [ppm] 6.55 (bs, 4H, −C$_4$*H*), 6.32 (s, 4H, −C$_2$*H*), 4.45 (t, *J* = 7.5 Hz, 4H, −C$_5$*H*−), 4.28 (t, *J* = 5.2 Hz, 4H, −(CH$_2$)(CH$_2$)(CH$_2$)O*H*), 3.82 (bs, 8H, −ArO(C*H*$_2$)(CH$_2$)(CH$_2$)$_3$CH$_3$), 3.59 (bs, 8H, −ArO(C*H*$_2$)(CH$_2$)(CH$_2$)$_3$CH$_3$), 3.36 (q, *J* = 6.3 Hz, 8H, −(CH$_2$)(CH$_2$)(C*H*$_2$)OH), 1.70 (q, *J* = 7.7 Hz, 8H, −(C*H*$_2$)(CH$_2$)(CH$_2$)OH), 1.56 (s, 16H, −ArO(CH$_2$)(C*H*$_2$)(CH$_2$)$_3$CH$_3$), 1.41 – 1.22 (m, 56H, −(CH$_2$)(C*H*$_2$)(CH$_2$)OH and −ArO(CH$_2$)(CH$_2$)(C*H*$_2$)$_3$CH$_3$), 0.87 (t, *J* = 6.6 Hz, 24H, −ArO(CH$_2$)(CH$_2$)(CH$_2$)$_3$C*H*$_3$).

^{13}C NMR (126 MHz, DMSO-d_6, 298 K): δ [ppm] 154.8 (s), 125.3 (s), 97.6 (s), 67.8 (s), 61.2 (s), 34.5 (s), 31.5 (s), 31.3 (s), 29.2 (s), 25.3 (s), 22.1 (s), 13.9 (s).

HR-MS (ESI, 4.0 eV): m/z calcd. for $C_{88}H_{145}O_{12}$ [(M+H)]$^+$: 1394.0731; measd.: 1394.0717.

Note: The carbon atom C_4 could not be resolved in the ^{13}C NMR as it is significantly broadened at 298 K. For further details see Section 3.4.

(1⁴,1⁶,3⁴,3⁶,5⁴,5⁶,7⁴,7⁶-octakis(hexyloxy)-1,3,5,7(1,3)-tetrabenzenacyclooctaphane-2,4,6,8-tetrayl)tetrakis(propane-3,1-diyl) octaphenyl tetrakis(phosphate) (7)

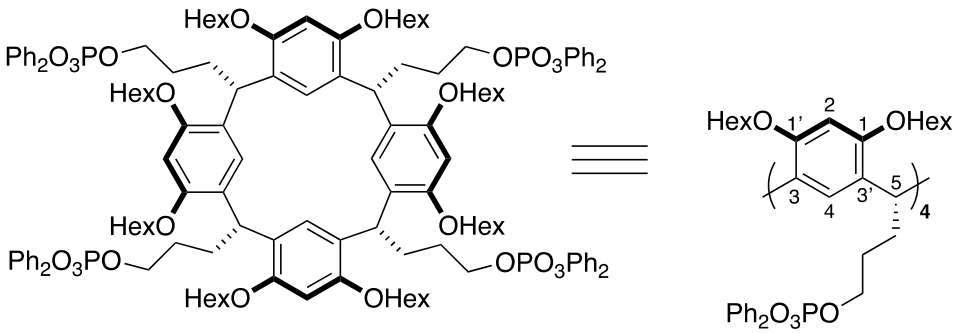

$C_{136}H_{180}O_{24}P_4$
M = 2322.81 g/mol

A one-neck 50 mL round-bottom flask was charged with **6** (976 mg, 700 μmol, 1.00 equiv). The solid was dissolved in 15 mL dry DCM and the solution was cooled to 0 °C. NEt_3 (0.58 ml, 4.20 mmol, 6.00 equiv) was added, followed by dropwise addition of diphenyl chlorophosphate (0.87 mL, 4.20 mmol, 6.00 equiv). The reaction mixture was allowed to warm to room temperature and stirred for 16 h. The reaction mixture was poured into sat. NH_4Cl (100 mL), transferred into a separatory funnel, followed by extraction with DCM (3 x 100 mL). The combined organic layers were dried with Na_2SO_4 and concentrated *in vacuo* at 40 °C. The crude product was purified by MPLC (RediSep® Column: Silica 24 g; 35 ml/min; DCM/EtOAc 100:0 to 90:10, 22.7 CV, 21.9 min) to obtain **7** (1.34 g, 577 μmol, 82%) as a colourless oil.

TLC: R_f = 0.19 (Cyclohexane/EtOAc = 2/1) [UV, CAM].

IR (ATR): ν [cm^{-1}] 2930 (m), 2858 (w), 1589 (w), 1490 (s), 1469 (m), 1411 (w), 1293 (s), 1189 (s), 1023 (s), 944 (s), 768 (m), 754 (m), 688 (m).

^{1}H NMR (500 MHz, DMSO-d_6, 298 K, assignments based on COSY, HMQC and HMBC NMR spectra): δ [ppm] 7.29 (t, *J* = 8.0 Hz, 16H, −Ar*H*), 7.15 (t, *J* = 7.4 Hz, 8H, −Ar*H*), 7.08 (d, *J* = 8.5 Hz, 16H, −Ar*H*), 6.61 (bs, 4H, −C_4H), 6.37 (s, 4H, −C_2H), 4.50 (t, *J* = 7.6 Hz, 4H, −C_5H−), 4.17 (q, *J* = 7.0 Hz, 8H, −$(CH_2)(CH_2)(CH_2)OPO_3Ph_2$), 3.83 (bs, 8H, $ArO(CH_2)(CH_2)(CH_2)_3CH_3$), 3.60 (bs, 8H, $ArO(CH_2)(CH_2)(CH_2)_3CH_3$), 1.87 – 1.73 (m, 8H, −$(CH_2)(CH_2)(CH_2)OPO_3Ph_2$), 1.59 – 1.52 (m, 16H, $ArO(CH_2)(CH_2)(CH_2)_3CH_3$), 1.45 – 1.02 (m, 56H, −$(CH_2)(CH_2)(CH_2)OPO_3Ph_2$ and −$ArO(CH_2)(CH_2)(CH_2)_3CH_3$), 0.82 (t, *J* = 6.8 Hz, 24H, −$ArO(CH_2)(CH_2)(CH_2)_3CH_3$).

^{13}C NMR (126 MHz, DMSO-d_6, 298 K): δ [ppm] 155.0 (s), 150.0 (d, J_{CP} = 7.0 Hz), 129.8 (s), 125.3 (s), 125.1 (s), 119.7 (d, J_{CP} = 4.7 Hz), 119.7 (s), 69.2 (s), 67.8 (s), 33.8 (s), 31.2 (s), 30.2 (s), 29.1 (s), 28.3 (s), 25.3 (s), 22.1 (s), 13.9 (s).

^{31}P NMR (202 MHz, DMSO-d_6, 298 K): δ [ppm] −11.88.

HR-MS (ESI, 4.0 eV): m/z calcd. for $C_{136}H_{180}O_{24}P_4Na_2$ $[(M+2Na)]^{2+}$: 183.5800; measd.: 1183.5809.

Note: The carbon atoms C_2 and C_4 could not be resolved in the ^{13}C NMR as they are significantly broadened at 298 K. C_2H (2.37 ppm) shows a cross peak in the HMQC spectrum which leads to the assumption, that C_2H is located at 97.9 ppm. For further details see Section 3.4.

(1⁴,1⁶,3⁴,3⁶,5⁴,5⁶,7⁴,7⁶-octakis(hexyloxy)-1,3,5,7(1,3)-tetrabenzenacyclooctaphane-2,4,6,8-tetrayl)tetrakis(propane-3,1-diyl) tetrakis(dihydrogen phosphate) (2)

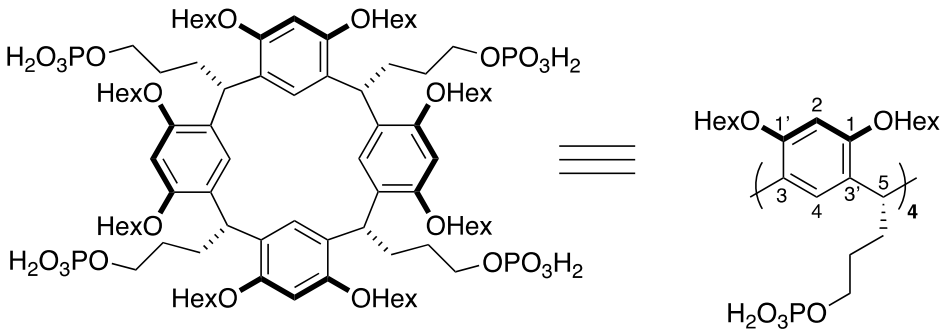

$C_{88}H_{148}O_{24}P_4$
M = 1714.02 g/mol

A one-neck 25 mL round-bottom flask was charged with **7** (232 mg, 100 μmol, 1.00 equiv). The solid was dissolved in 8 mL ethanol, followed by the addition of acetic acid (57.7 μmL, 1.00 mmol, 10.0 equiv). Platinum(IV) oxide (22.7 mg, 100 μmol, 1.00 equiv) was added in one portion and the resulting suspension was stirred vigorously. The reaction mixture was purged with three balloons of H_2 and then kept under H_2 atmosphere (1 bar) for 24 h at room temperature while stirring vigorously. The suspension was filtered through a pad of Celite®, washed with ethanol (3 x 10 mL) and the combined filtrates were concentrated *in vacuo* at 40 °C. The crude was suspended in H_2O (10 mL) and lyophilized to obtain **1** (156 mg, 91 μmol, 91%) as brown solid.

M.p.: ϑ_m = 177-179 °C (decomposition).
IR (ATR): ν [cm^{-1}] 2928 (m), 2858 (m), 2345 (w), 1610 (w), 1583 (w), 1501 (m), 1469 (m), 1410 (w), 1388 (w), 1293 (m), 1184 (s), 1015 (s), 812 (m), 736 (s).

^{1}H NMR (500 MHz, DMSO-d_6, 353 K, assignments based on COSY, NOESY, HMQC and HMBC NMR spectra): δ [ppm] 7.14 (bs, 8H, −PO*H*), 6.62 (s, 4H, −C_4H), 6.35 (s, 4H, −C_2H), 4.48 (t, *J* = 7.3 Hz, 4H, −C_5H), 3.93 – 3.74 (m, 16H, −ArO(CH_2)(CH_2)(CH_2)$_3CH_3$), 3.63 (q, *J* = 7.4 Hz, 8H, −(CH_2)(CH_2)(CH_2)OPO_3Ph_2), 1.80 (q, *J* = 8.3, 7.6 Hz, 8H, −(CH_2)(CH_2)(CH_2)OPO_3Ph_2), 1.67 – 1.55 (m, 16H, −ArO(CH_2)(CH_2)(CH_2)$_3CH_3$), 1.55 – 1.47 (m, 8H, −(CH_2)(CH_2)(CH_2)OPO_3Ph_2), 1.41 – 1.27 (m, 48H, −ArO(CH_2)(CH_2)(CH_2)$_3CH_3$), 0.89 (t, *J* = 6.7 Hz, 24H, −ArO(CH_2)(CH_2)(CH_2)$_3CH_3$).

^{13}C NMR (126 MHz, DMSO-d_6, 353 K): δ [ppm] 154.6 (s), 125.1 (s), 124.6 (s), 98.1 (s), 67.8 (s), 65.3 (s), 34.4 (s), 30.7 (s), 30.7 (s), 28.8 (s), 28.7 (s), 24.8 (s), 21.5 (s), 13.3 (s).

^{31}P NMR (202 MHz, DMSO-d_6, 298 K): δ [ppm] −6.14.

^{1}H NMR (500 MHz, THF-d_8, 298 K, assignments based on COSY, NOESY, HMQC and HMQC NMR spectra): δ [ppm] 9.29 (bs, 8H, −PO*H*), 7.41 – 5.90 (m, 8H, −C_2H and −C_4H), 4.53 (t, *J* = 7.5 Hz, 4H, −C_7H), 4.21 – 3.60 (m, 24H, −ArO(CH_2)(CH_2)(CH_2)$_3CH_3$ and −(CH_2)(CH_2)(CH_2)OPO_3Ph_2), 1.91 (s, 8H, −(CH_2)(CH_2)(CH_2)OPO_3Ph_2), 1.63 (bs, 24H, −(CH_2)(CH_2)(CH_2)OPO_3Ph_2 and −ArO(CH_2)(CH_2)(CH_2)$_3CH_3$), 1.56 – 1.18 (m, 48H, −ArO(CH_2)(CH_2)(CH_2)$_3CH_3$), 0.92 (t, *J* = 6.6 Hz, 24H, −ArO(CH_2)(CH_2)(CH_2)$_3CH_3$).

^{13}C NMR (126 MHz, THF-d_8, 298 K): 156.4 (s), 126.8 (s), 98.4 (s), 69.1 (s), 36.5 (s), 33.0 (s), 32.6 (s), 31.0 (s), 30.3 (s), 30.3 (s), 27.1 (s), 23.8 (s), 14.7 (s).

^{31}P NMR (202 MHz, THF-d_8, 298 K): δ [ppm] 1.48.

HR-MS (ESI, 5.0 eV): m/z calcd. for $C_{88}H_{149}O_{24}P_4$ $[(M+H)]^+$: 1713.9384; measd.: 1713.9357.

Note: The carbon atom C_4 could not be resolved in the ^{13}C NMR as it is significantly broadened at in THF-d_8 298 K. For further details see Section 3.4.

3.3. Assignment of NMR Signals of Ligands 1 and 2

Ligand 1

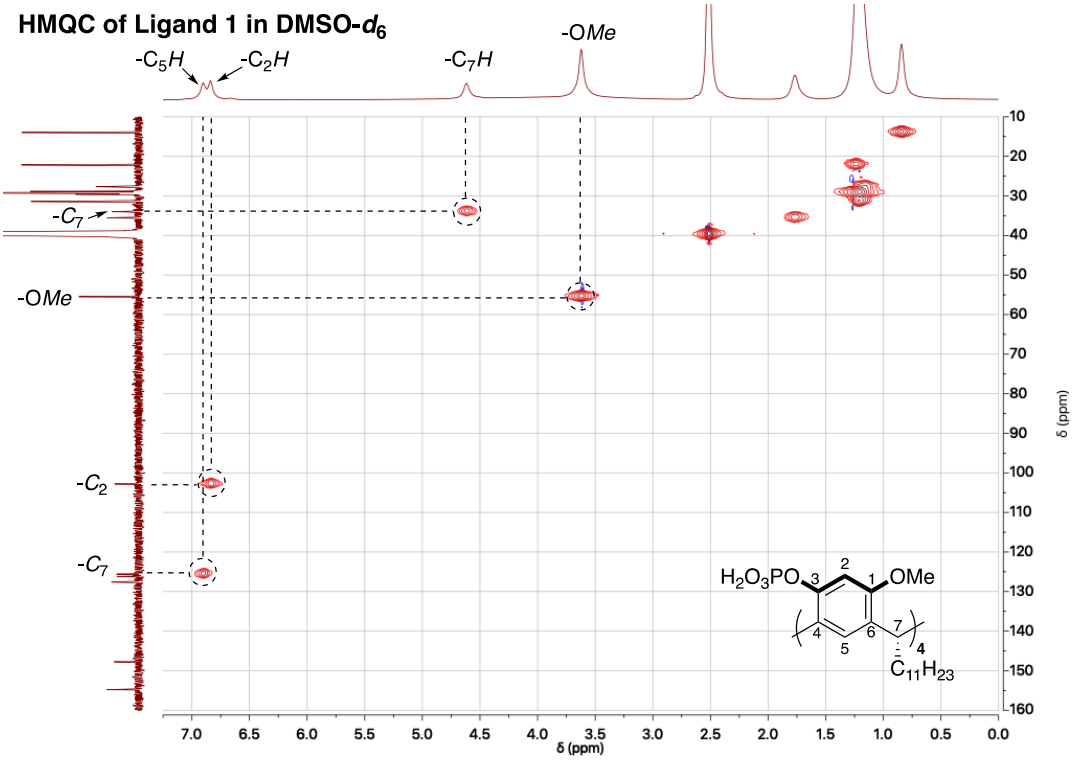

Figure S10: Section of HMQC (at 298 K) of ligand **1** in DMSO-d_6 used for the assignment of NMR peaks.

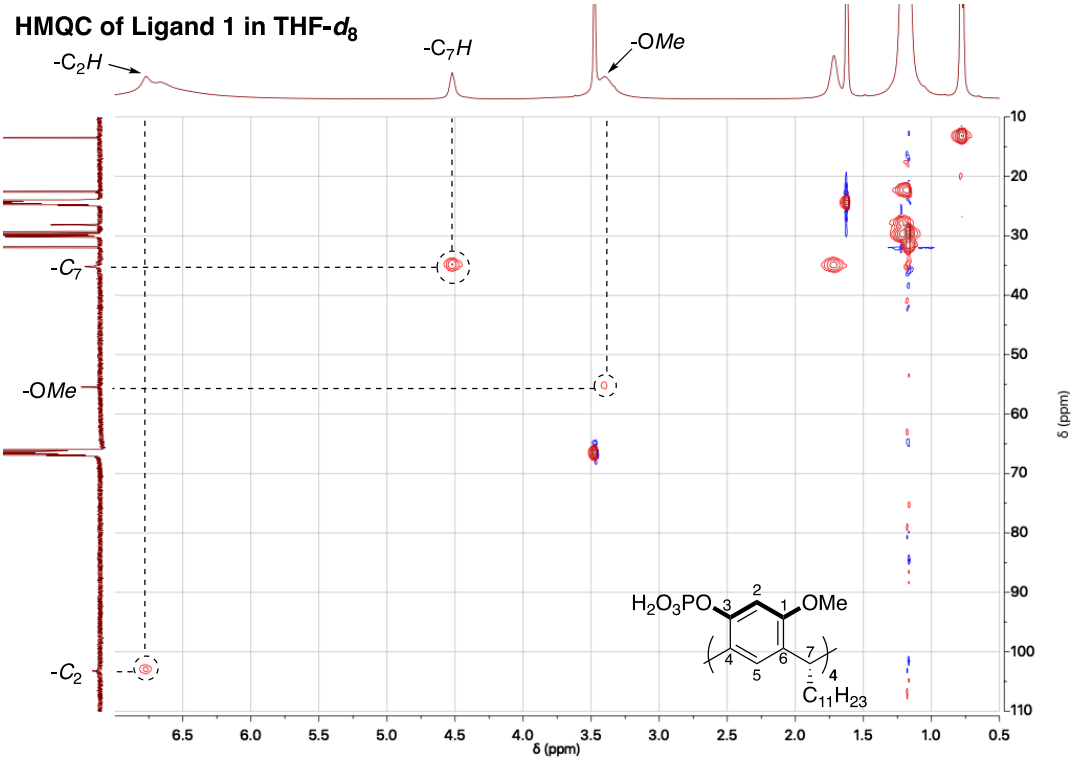

Figure S11: Section of HMQC (at 298 K) of ligand **1** in THF-d_8 used for the assignment of NMR peaks.

Ligand 2

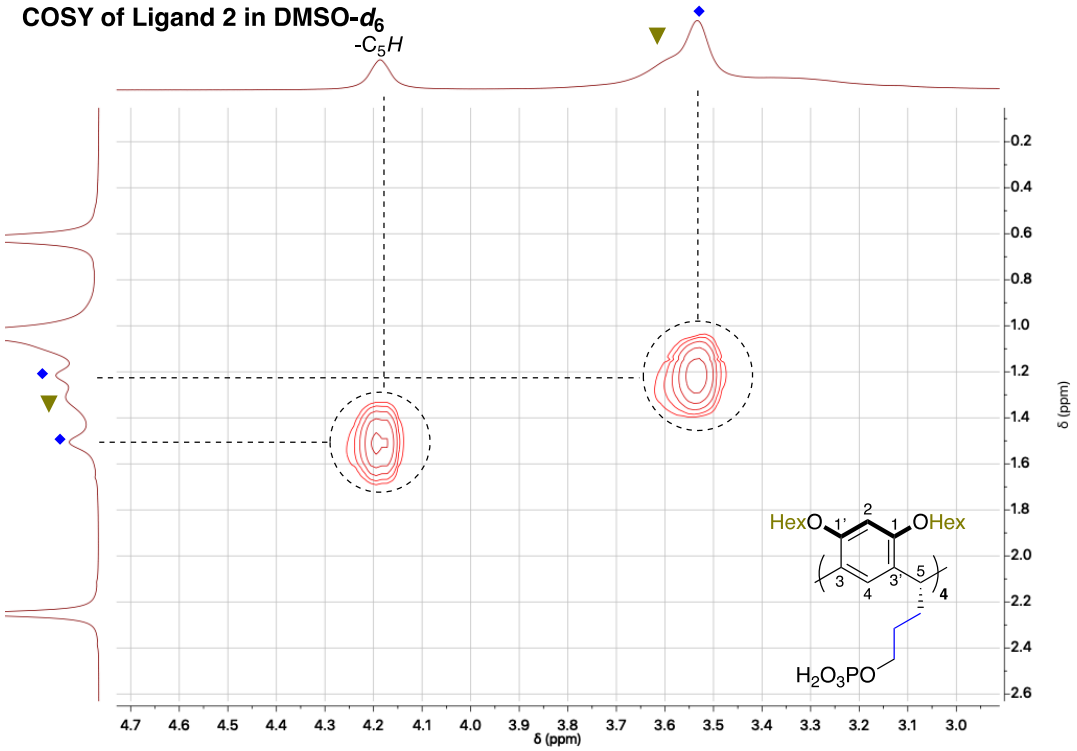

Figure S12: Section of COSY (at 298 K) of ligand 2 in DMSO-d_6 used for the assignment of NMR peaks. ◆= alkyl feet signals. ▼= upper rim hexyl groups.

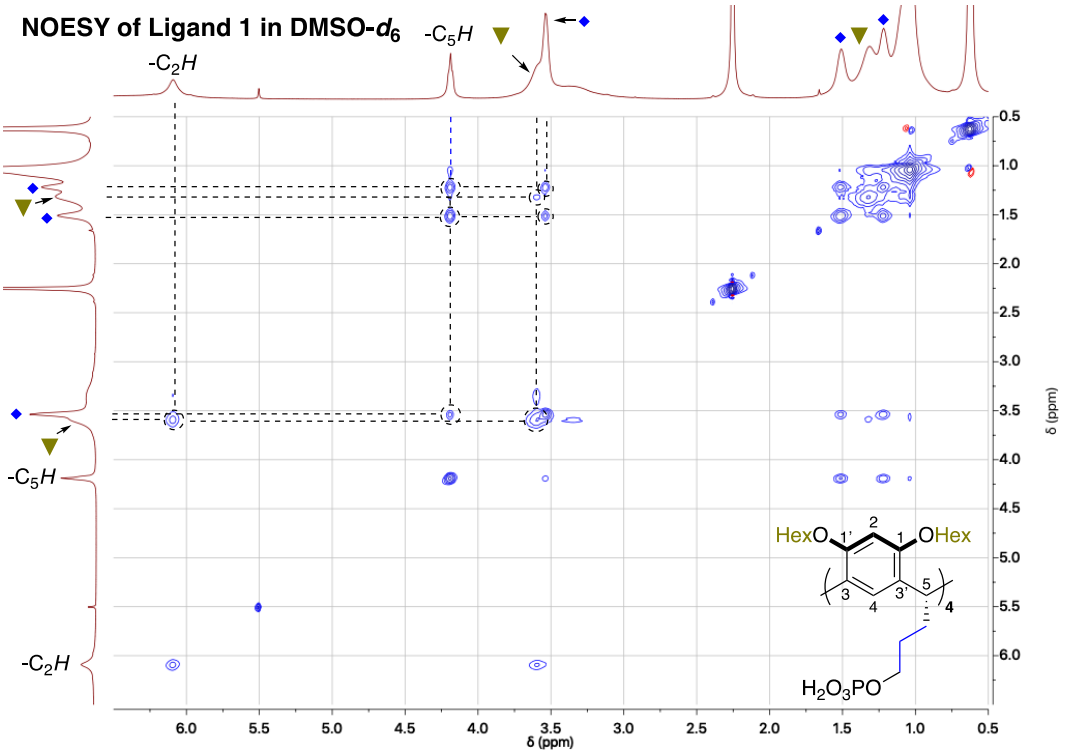

Figure S13: Section of NOESY (at 298 K) of ligand **2** in DMSO-d_6 used for the assignment of NMR peaks. ◆= alkyl feet signals. ▼= upper rim hexyl groups.

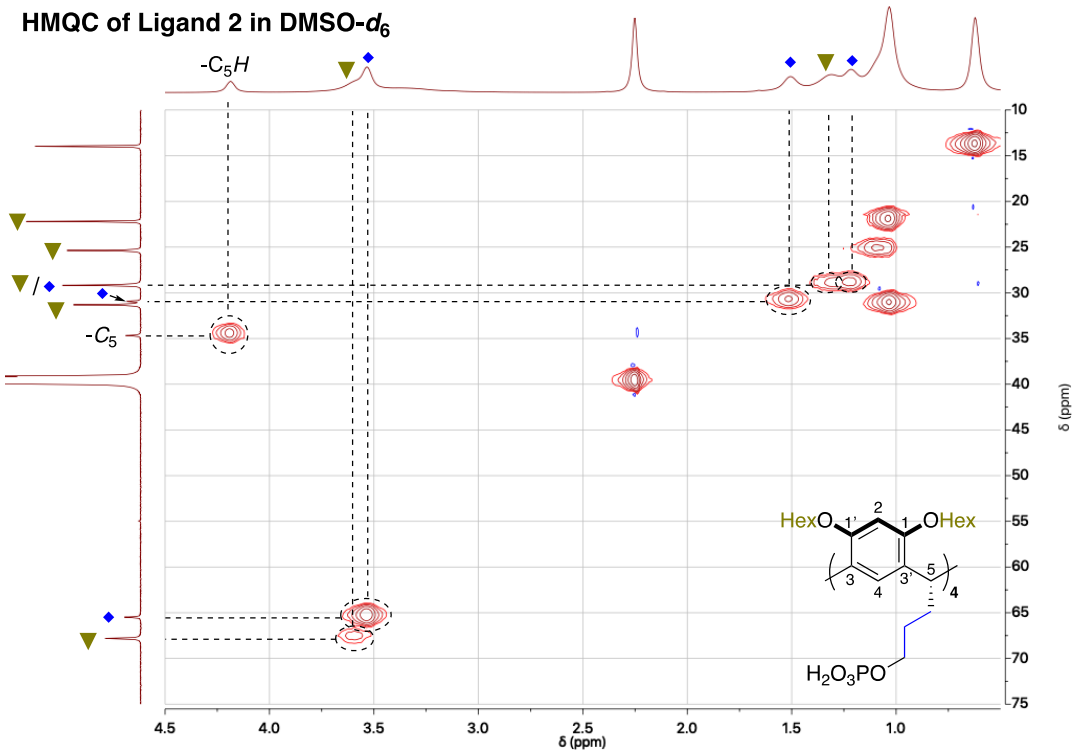

Figure S14: Section of HMQC (at 298 K) of ligand **2** in DMSO-d_6 used for the assignment of NMR peaks. ◆= alkyl feet signals. ▼= upper rim hexyl groups.

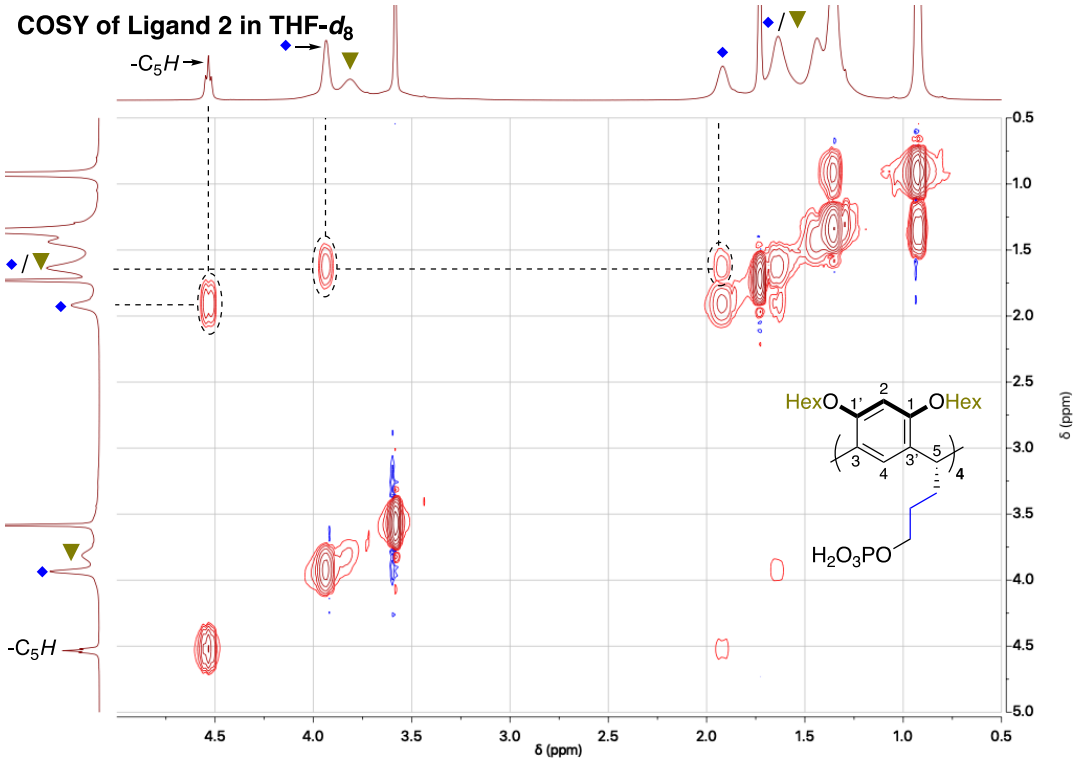

Figure S15: Section of COSY (at 298 K) of ligand **2** in THF-d_8 used for the assignment of NMR peaks. ◆= alkyl feet signals. ▼= upper rim hexyl groups.

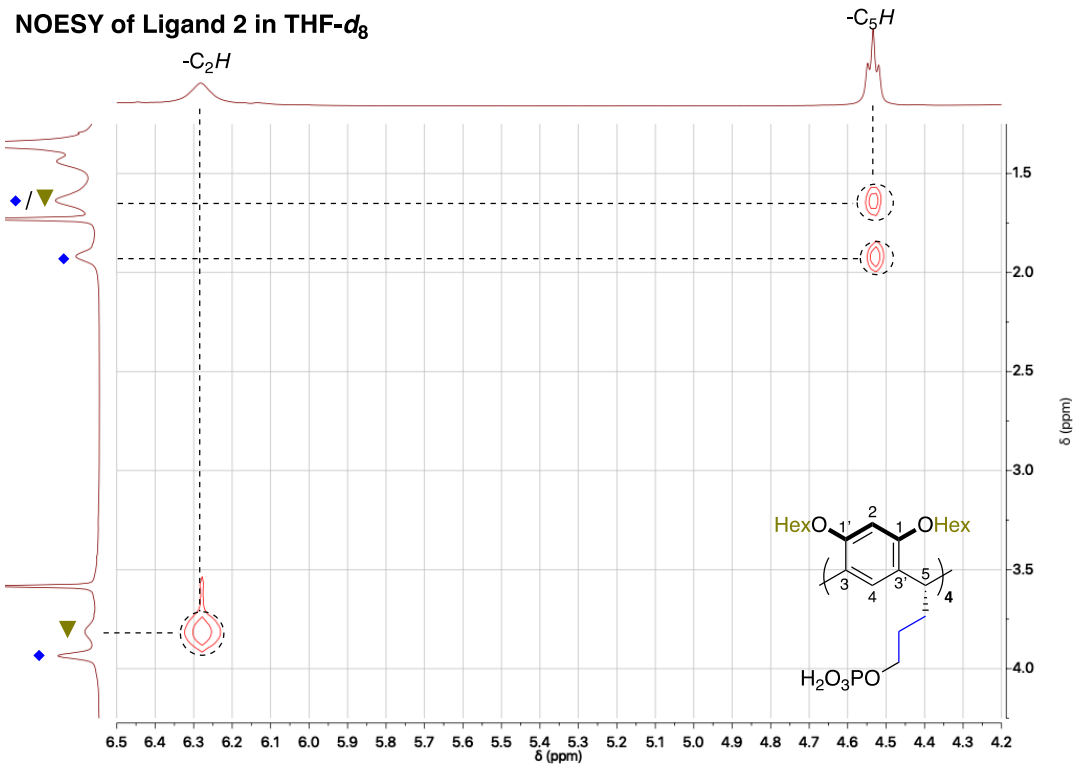

Figure S16: Section of NOESY (at 298 K) of ligand **2** in THF-d_8 used for the assignment of NMR peaks. ◆= alkyl feet signals. ▼= upper rim hexyl groups.

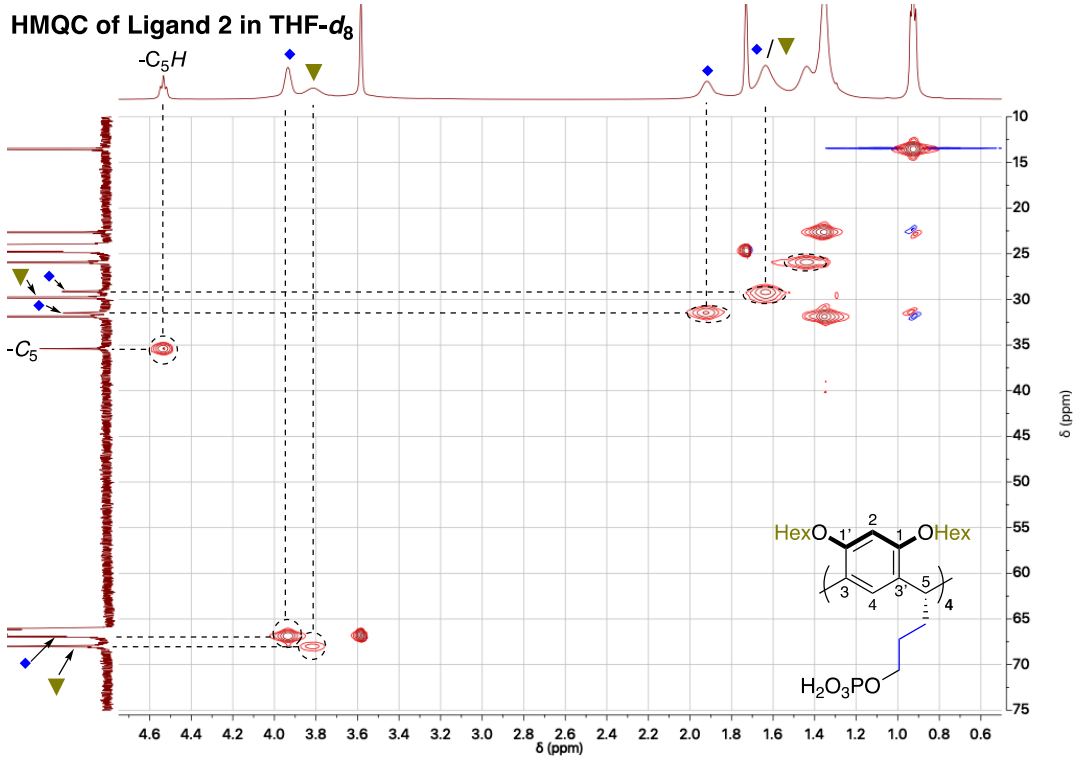

Figure S17: Section of HMQC (at 298 K) of ligand **2** in THF-d_8 used for the assignment of NMR peaks. ◆= alkyl feet signals. ▼= upper rim hexyl groups.

3.4. Behavior of Ligands 1 and 2 in solution and VT-NMR of Ligand 2

^{1}H-NMR spectra of ligands **1** and **2** at 298 K show a significant broadening for signals on or attached to the aromatic units of the macrocyclic frameworks (Figure S18). In the case of ligand **1** the aromatic protons −C_2H/−C_5H as well as the methoxy substituent −O*Me* are the signals most affected by this. For ligand **2**, the aromatic protons −C_2H/−C_4H as well as the upper rim hexyl chains (▼) show significant broadening.

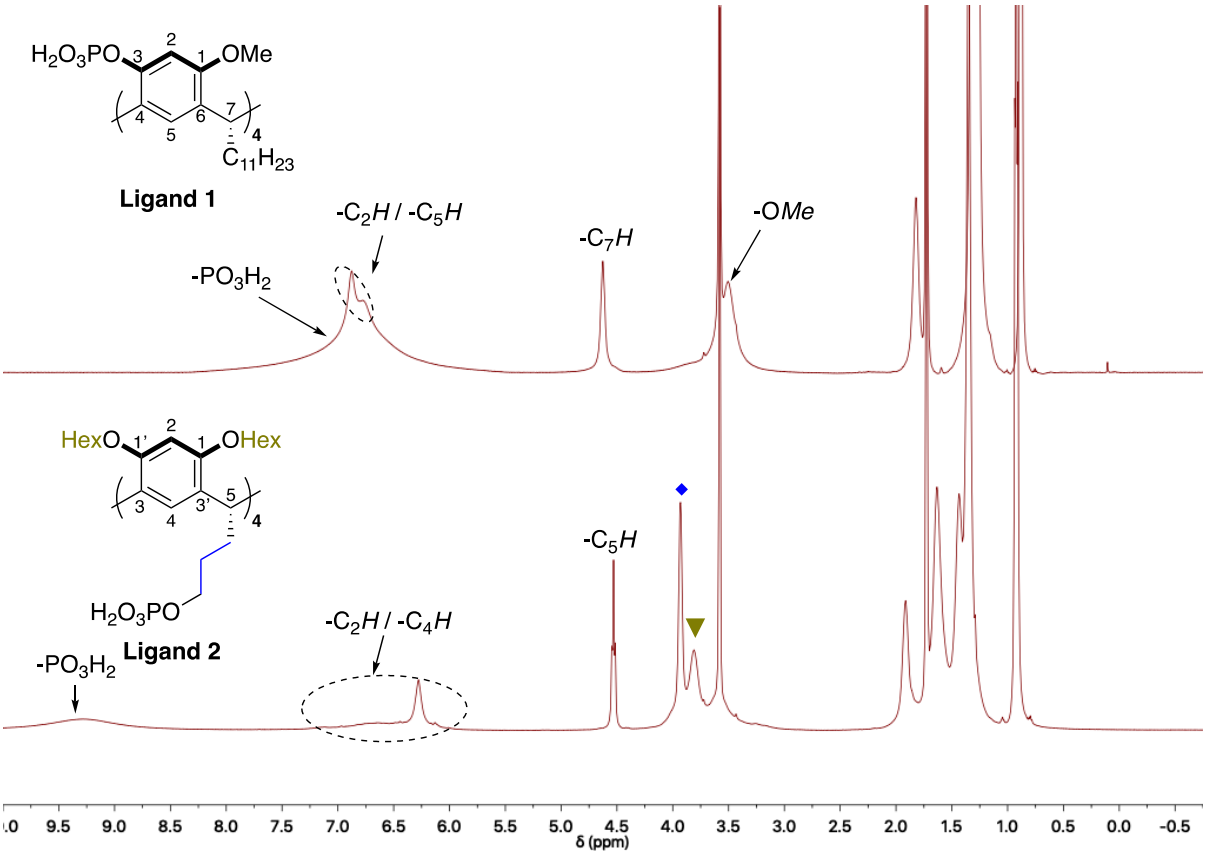

Figure S18: ^{1}H-NMR of ligands **1** (top) and **2** (bottom) in THF-d_8 at 298 K with important signals marked in the spectra. ◆= alkyl feet signals of **2**. ▼= upper rim hexyl groups of **2**.

Resorcin[4]arene derivatives are known to adopt different conformations in solution, such as the crown or the boat conformation (Figure S19).[6]

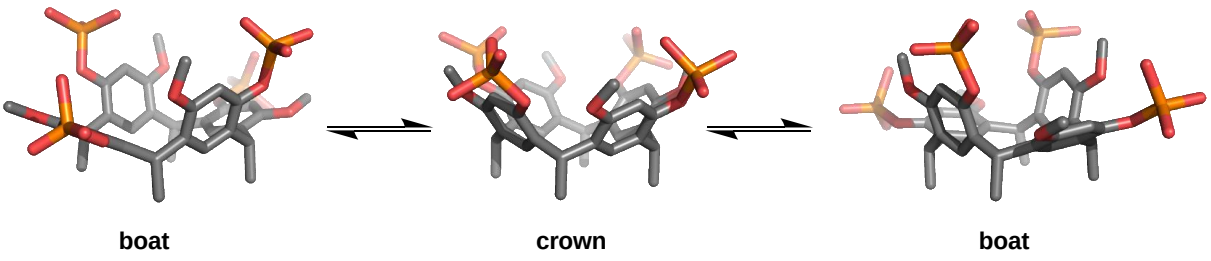

Figure S19: Proposed boat to boat interconversion of ligand **1**. Hydrogen atoms and alkyl feet omitted for clarity.

If the macrocyclic framework allows for rapid interconversion between these two conformations, this will be reflected in sharp NMR signals devoid of signal splitting expected for the boat conformation.

Sterically demanding substituents on the aromatic resorcin[4]arene units, such as the phosphate in ligand **1** or the hexyl groups in ligand **2**, may slow down this fast equilibrium, which can lead to signal broadening or signal splitting. The former is observed for the ligands **1** and **2**, which leads us to propose a decelerated interconversion between the boat and the crown conformation. This results in NMR signal broadening in both the ^{1}H-NMR and ^{13}C-NMR spectra. The broad NMR signals coalesce with increasing temperature, as shown for ^{1}H-NMR (Figure S20) and ^{13}C-NMR (Figure S21) of ligand **2**.

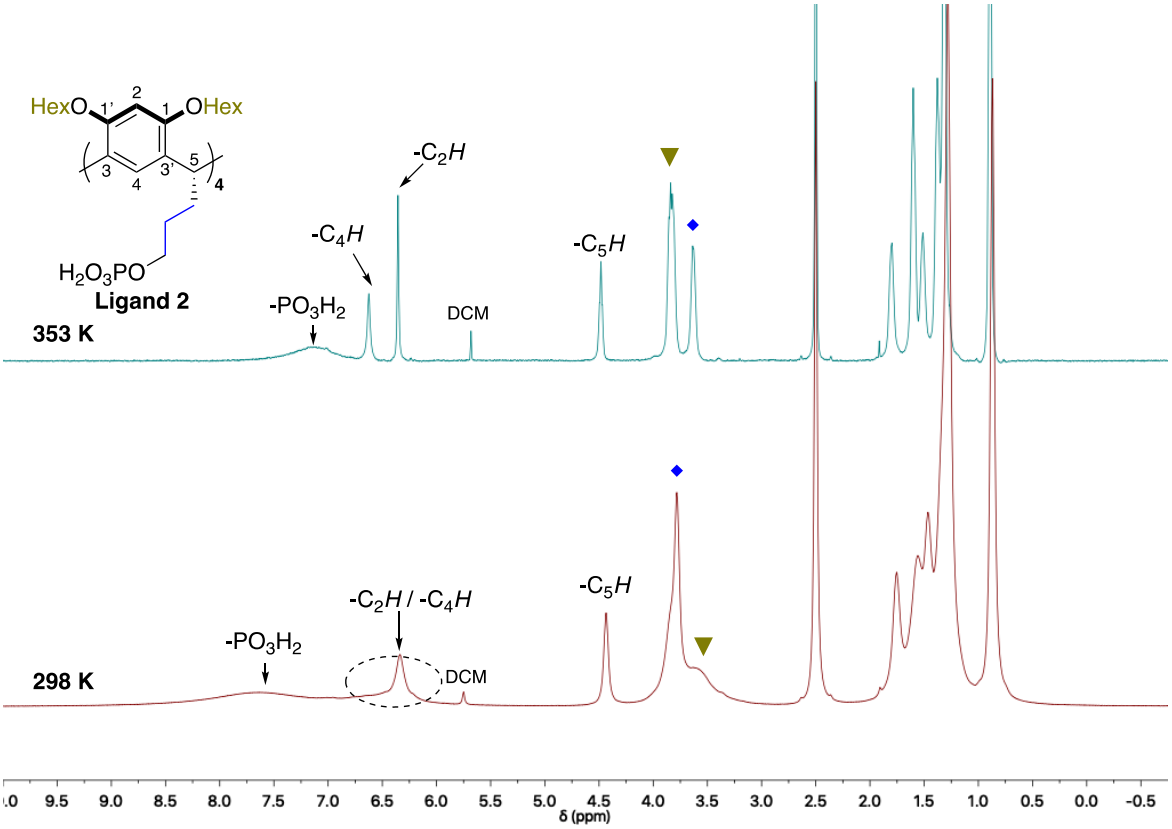

Figure S20: ^{1}H-NMR of ligand **2** in DMSO-d_6 at 353 K (top) and 298 K (bottom) with important signals marked in the spectra. ◆= alkyl feet signals of **2**. ▼= upper rim hexyl groups of **2**.

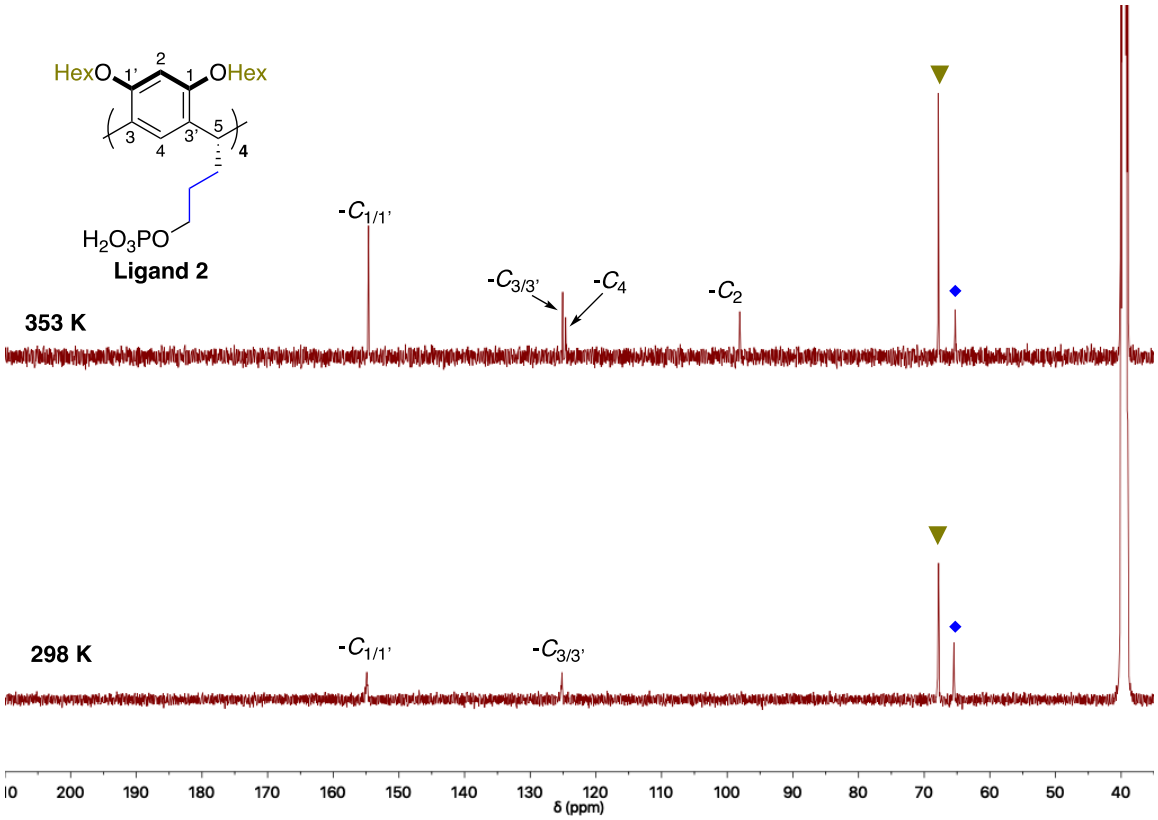

Figure S21: ^{13}C-NMR of ligand **2** in DMSO-d_6 at 353 K (top) and 298 K (bottom) with important signals marked in the spectra. ◆= alkyl feet signals of **2**. ▼= upper rim hexyl groups of **2**.

3.5. Stability of Ligands 1 and 2 in solution and as solid

Our previously developed anthracene 1,8 diphosphoric acids are highly light sensitive and need to be stored in the dark.[7] Samples of ligands **1** and **2** were stored as solution in DMSO-d_6 under air without any precaution concerning light. Additionally, a sample of ligand **1** was kept in a transparent flask under air without any precaution concerning light. The stability was determined by comparing the initial ^{1}H-NMR (Figure S22 and Figure S25) and ^{31}P-NMR (Figure S23, Figure S24, Figure S26, Figure S27) spectra to spectra recorded after the indicated time. Both ligands proved to be stable over long periods of time (> 2 months). Ligand **1** proved to be robust towards air and light as a solid over long periods of time (> 2 months). No significant changes were observed in the NMR spectra.

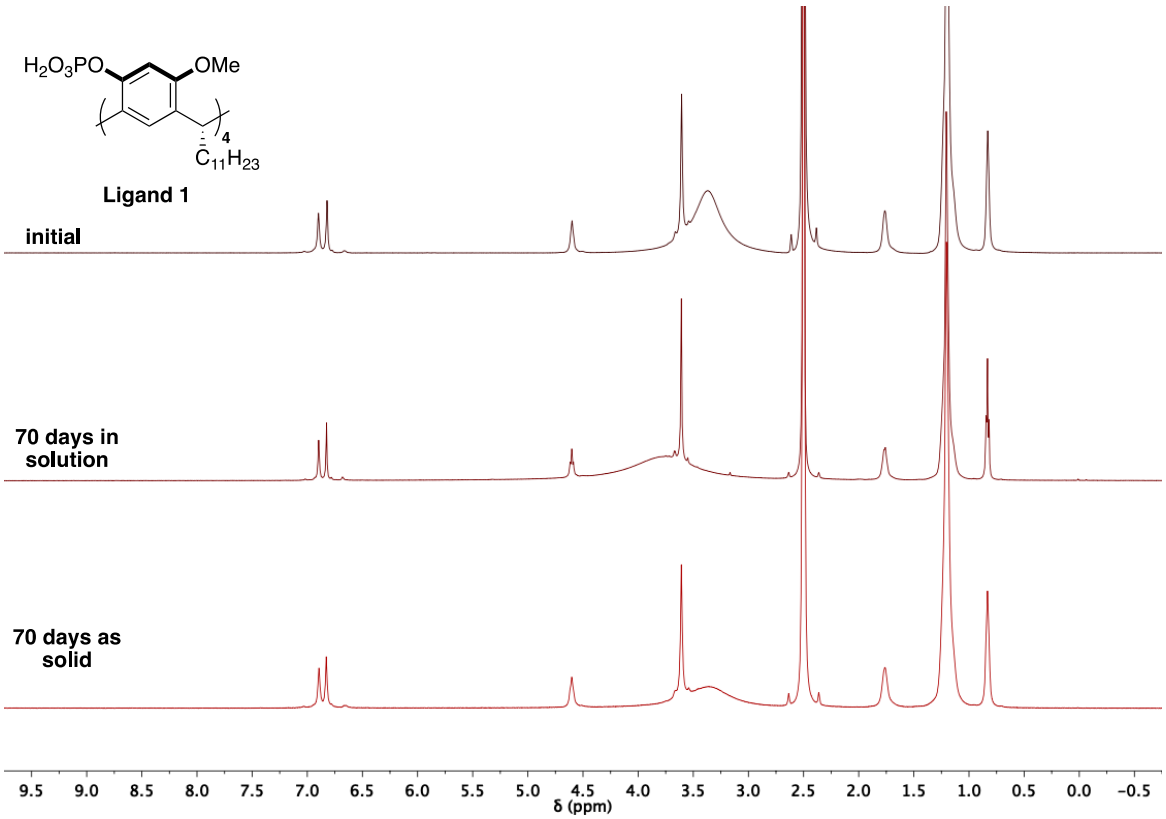

Figure S22: ^{1}H-NMRs of freshly prepared ligand **1** in DMSO-d_6 (top), after 70 days stored as solution (middle) and after 70 days stored as solid (bottom). The solution and the solid sample were exposed to air and light.

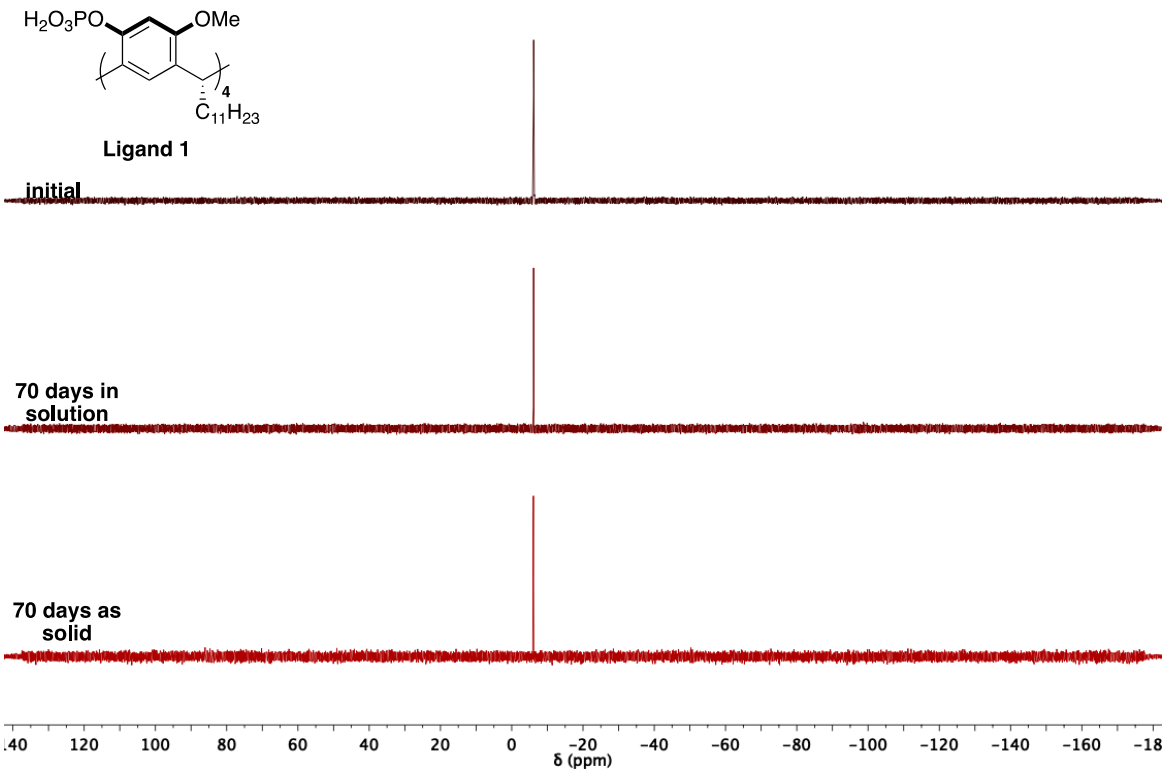

Figure S23: Full ^{31}P-NMRs of freshly prepared ligand **1** in DMSO-d_6 (top), after 70 days stored as solution (middle) and after 70 days stored as solid (bottom). The solution and the solid sample were exposed to air and light.

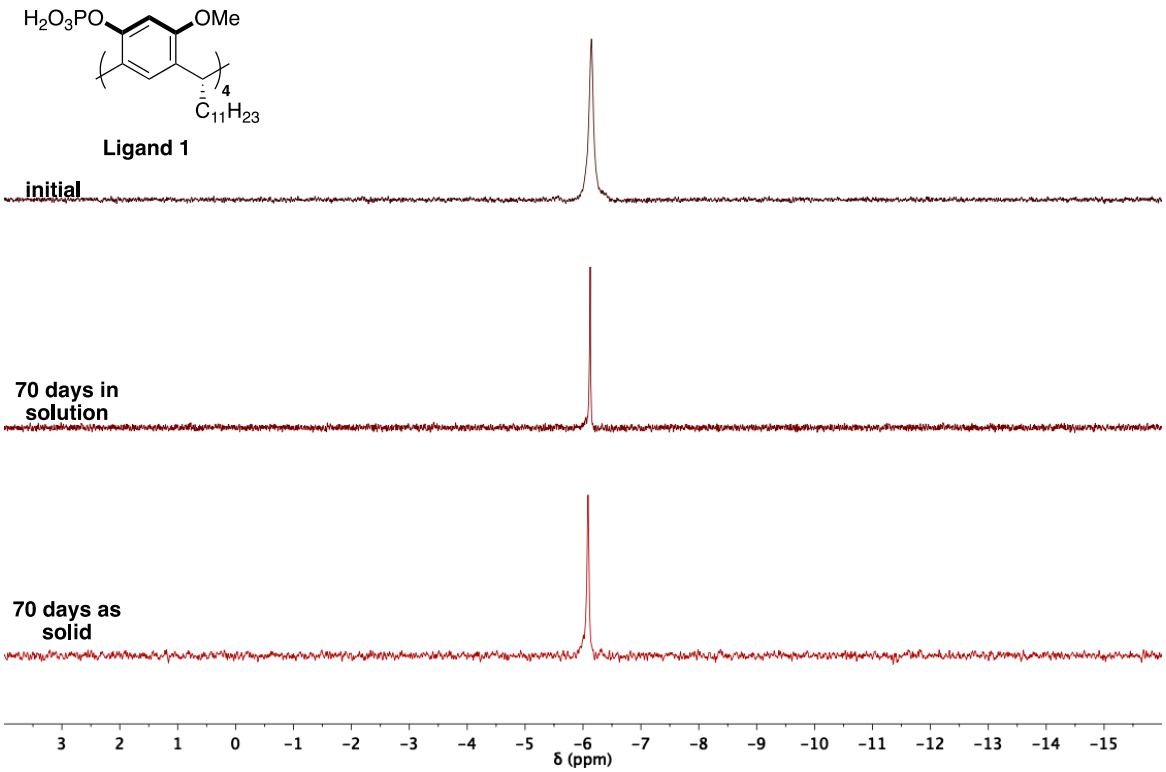

Figure S24: Detailed ^{31}P-NMRs of freshly prepared ligand **1** in DMSO-d_6 (top), after 70 days stored as solution (middle) and after 70 days stored as solid (bottom). The solution and the solid sample were exposed to air and light.

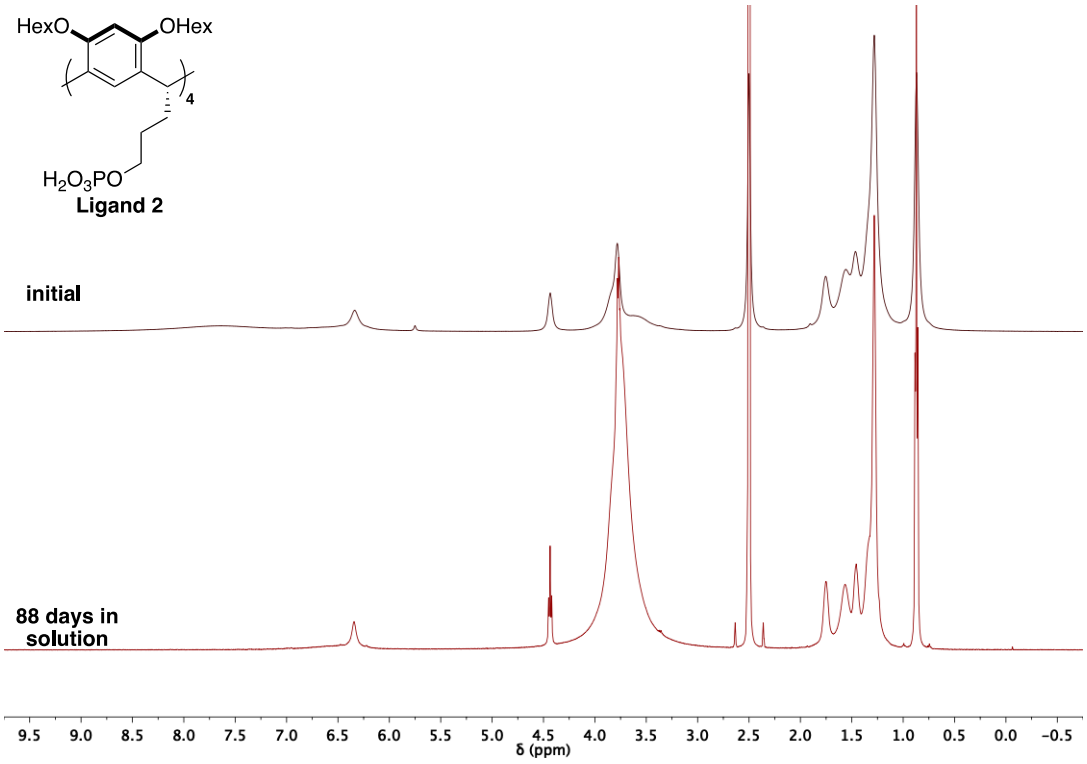

Figure S25: ^{1}H-NMRs of freshly prepared ligand **1** in DMSO-d_6 (top), after 88 days stored as solution (bottom). The solid sample was exposed to air and light.

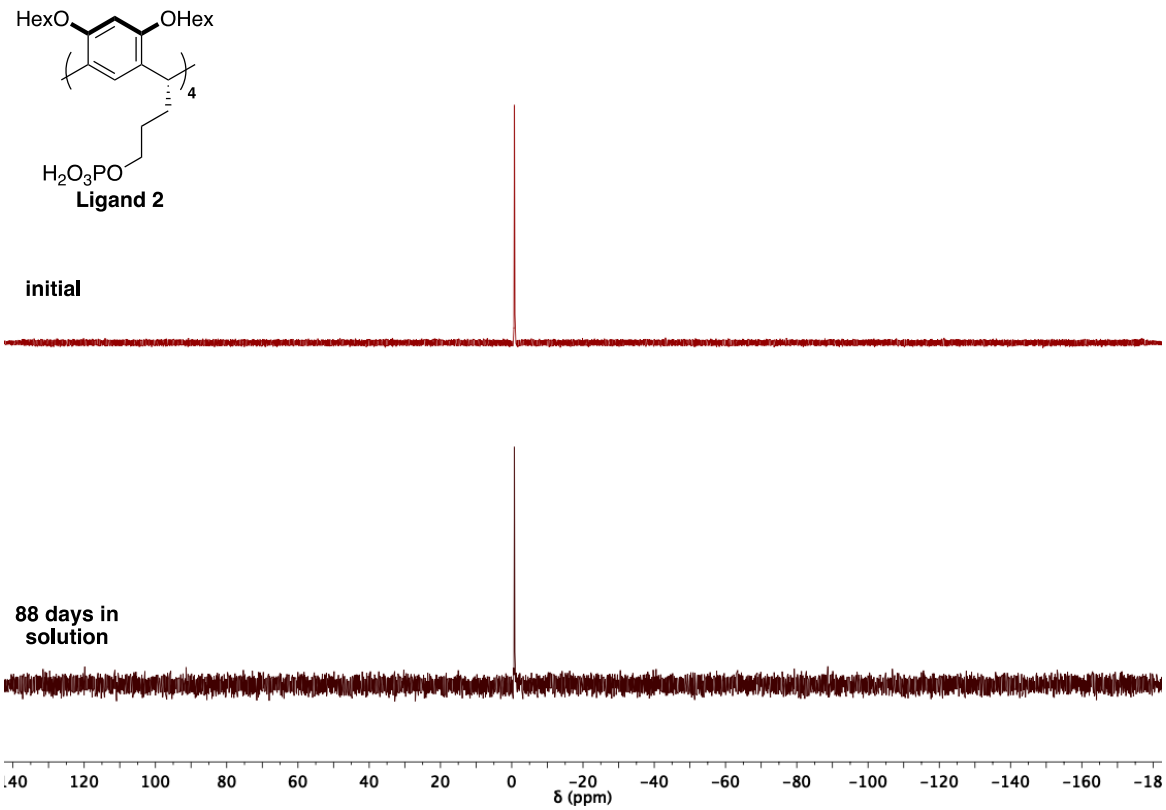

Figure S26: Full ^{31}P-NMRs of freshly prepared ligand **2** in DMSO-d_6 (top), after 88 days stored as solution (bottom). The solution and the solid sample were exposed to air and light.

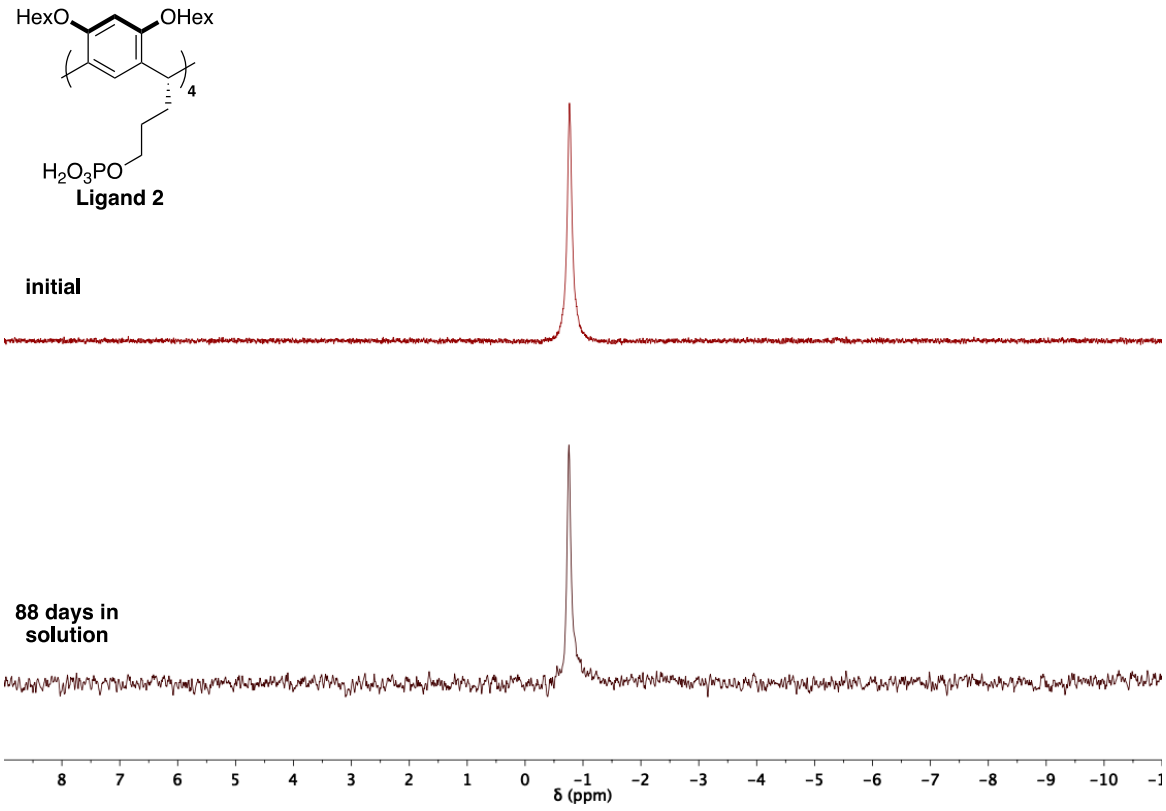

Figure S27: Detailed ^{31}P-NMRs of freshly prepared ligand **2** in DMSO-d_6 (top), after 88 days stored as solution (bottom). The solution and the solid sample were exposed to air and light.

4. Design and Models of Ligands 1 and 2

The following calculations on the equilibrium geometry of ligands **1** and **2** were performed first by the semi-empirical PM6 method, followed by the density functional theory (DFT) approach using the SPARTAN 18 program suite. The latter DFT optimization was executed with the B3LYP functional, employing the 6-31G* basis set. For the calculations, the undecyl feet of ligand **1** were replaced by methyl feet and reinserted into the final model. Using simplified model compounds is a common approach for ab initio calculations.[8-10]

When designing **1** and **2**, our goal was to create tetraphosphate substituted resorcin[4]arenes of similar dimensions. At the same time, their phosphate substituents were to show different degrees of flexibility and therefore different binding abilities to the nanocrystal surface.

To that end, two structures **1** and **2** emerged that possessed roughly the same molecular weight (MW), a similar molecular formula and a comparable length *H* from the top of the upper rim substituents to the end of the alkyl feet (Table S2, Figure S28). *H* can be seen as the height of the ligand attached to the nanocrystal surface.

Table S2: Structural parameters (molecular formula, molecular weight (MW), *H*) of ligands **1** and **2.**

Ligand	Formula	MW [g/mol]	*H* [Å]
1	$C_{76}H_{124}O_{20}P_4$	1481.70	18.163
2	$C_{88}H_{148}O_{24}P_4$	1714.02	17.989

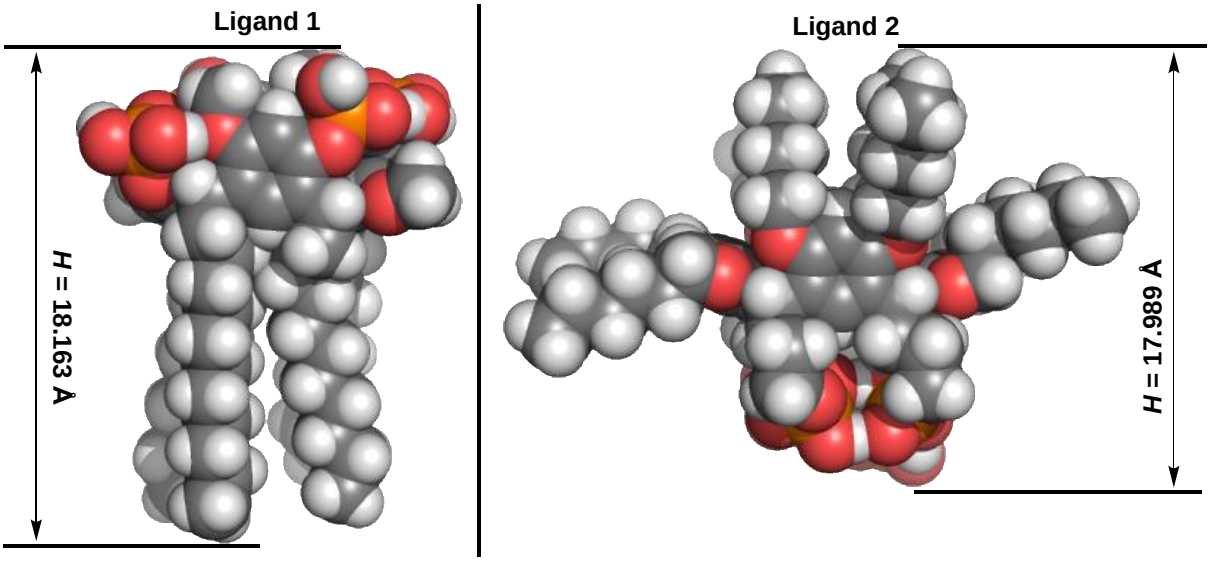

Figure S28: B3LYP/6-31G* DFT models of ligand **1** (left) and **2** (right) viewed from the side. Value *H* indicates the distance between the top of the upper rim substituents and the end of the alkyl feet (indicated by black arrows).

5. References

1. J. De Roo, F. Van den Broeck, K. De Keukeleere, J. C. Martins, I. Van Driessche and Z. Hens, *J. Am. Chem. Soc.*, 2014, **136**, 9650-9657.
2. J. Buha, D. Arcon, M. Niederberger and I. Djerdj, *Phys. Chem. Chem. Phys.*, 2010, **12**, 15537-15543.
3. K. De Keukeleere, J. De Roo, P. Lommens, J. C. Martins, P. Van der Voort and I. Van Driessche, *Inorg. Chem.*, 2015, **54**, 3469-3476.
4. S. J. Nemat, H. Jędrzejewska, A. Prescimone, A. Szumna and K. Tiefenbacher, *Organic Letters*, 2020, **22**, 5506-5510.
5. B. C. Gibb, R. G. Chapman and J. C. Sherman, *The Journal of Organic Chemistry*, 1996, **61**, 1505-1509.
6. P. Kumar and P. Venkatakrishnan, *Organic Letters*, 2018, **20**, 1295-1299.
7. J. De Roo, Z. Huang, N. J. Schuster, L. S. Hamachi, D. N. Congreve, Z. Xu, P. Xia, D. A. Fishman, T. Lian, J. S. Owen and M. L. Tang, *Chem. Mat.*, 2020, **32**, 1461-1466.
8. B. Kuberski, M. Pecul and A. Szumna, *European Journal of Organic Chemistry*, 2008, **2008**, 3069-3078.
9. W. Iwanek, K. Stefańska, A. Szumna and M. Wierzbicki, *RSC Adv.*, 2016, **6**, 13027-13031.
10. M. Wierzbicki, A. A. Głowacka, M. P. Szymański and A. Szumna, *Chem. Commun.*, 2017, **53**, 5200-5203.

Appendix A: NMR Spectra of New and Key Compounds

Appendix A.1: ^{1}H, ^{13}C and ^{31}P NMR Spectra of New and Key Compounds

3-^{1}H ($CDCl_3$, 298 K)

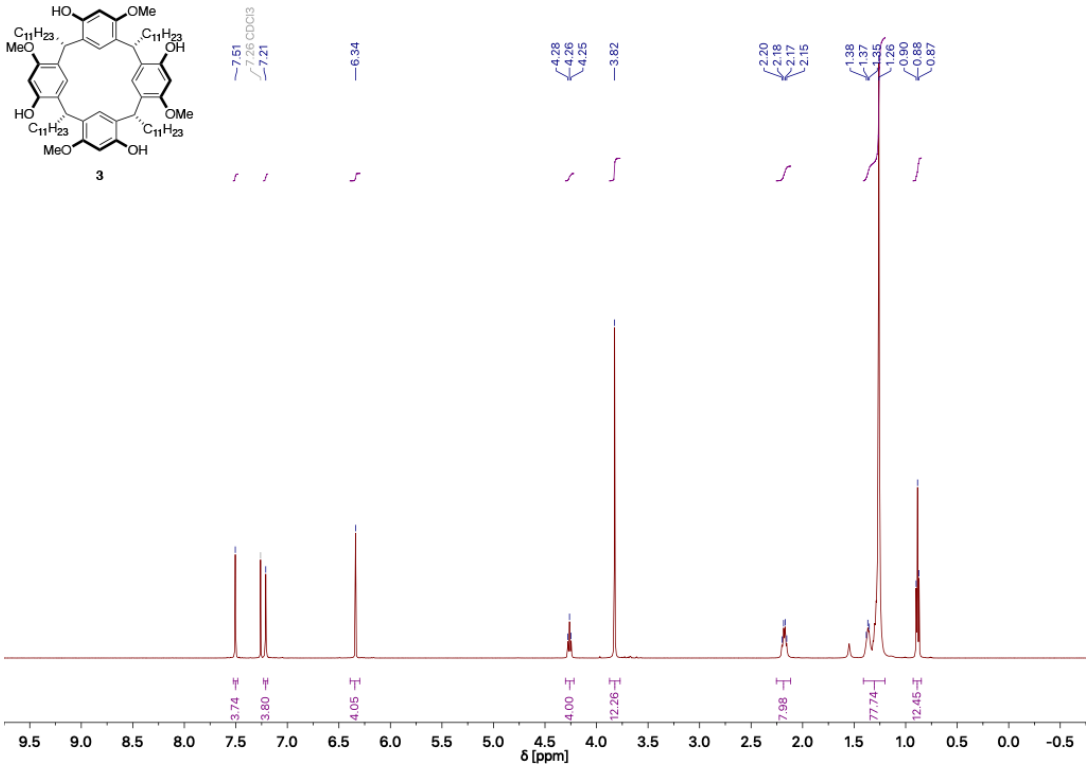

3-^{13}C ($CDCl_3$, 298 K)

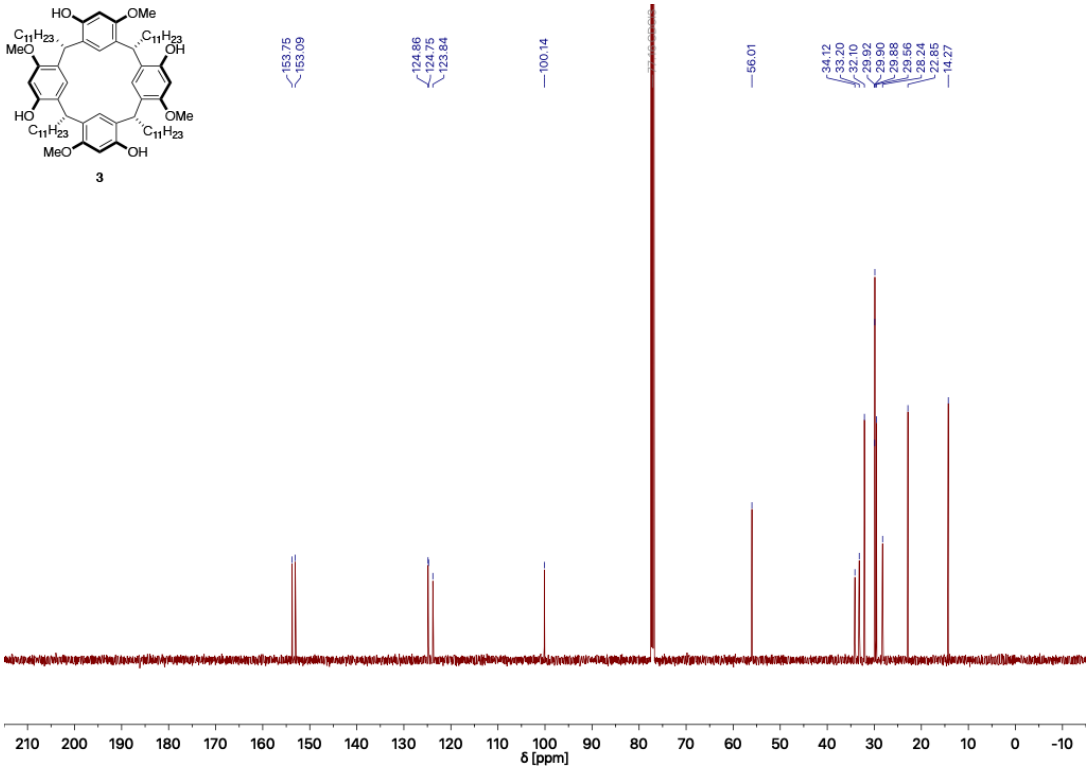

4-^{1}H ($CDCl_3$, 298 K)

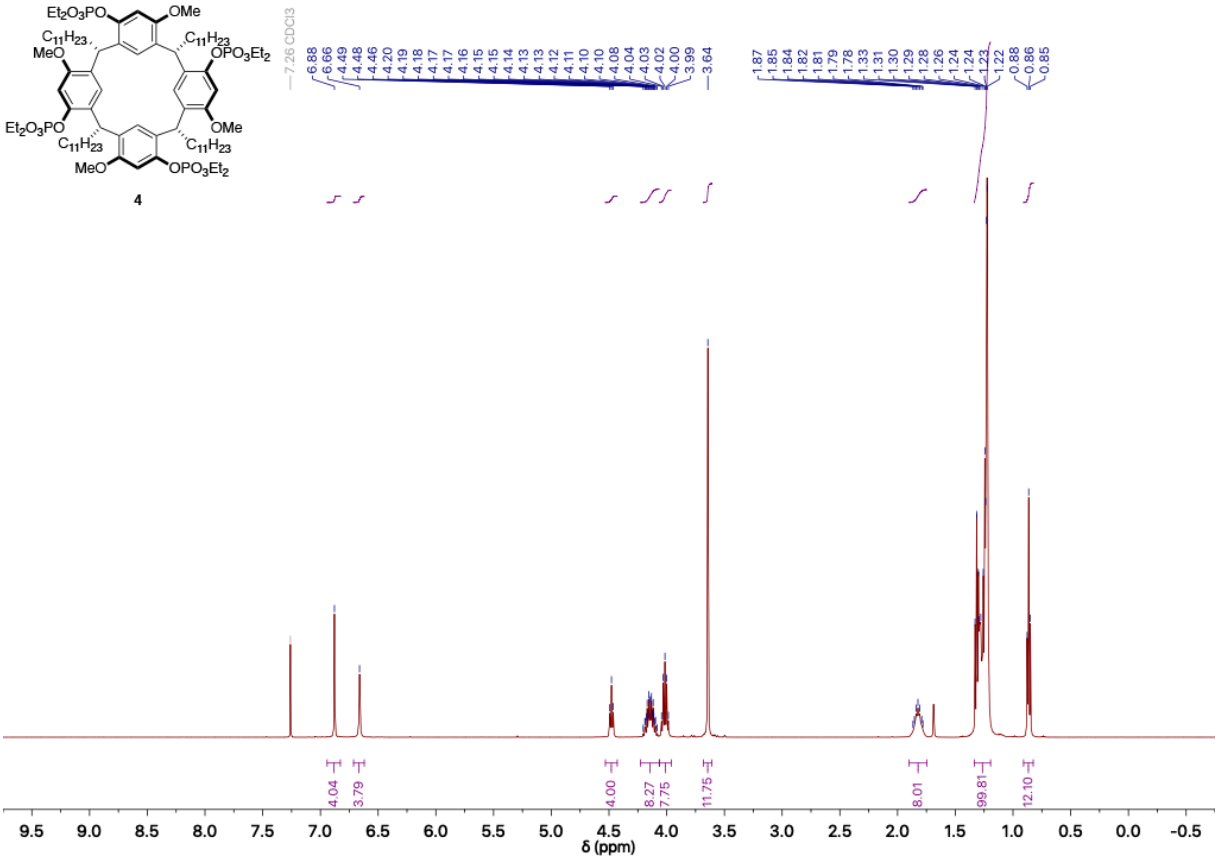

4-^{13}C ($CDCl_3$, 298 K)

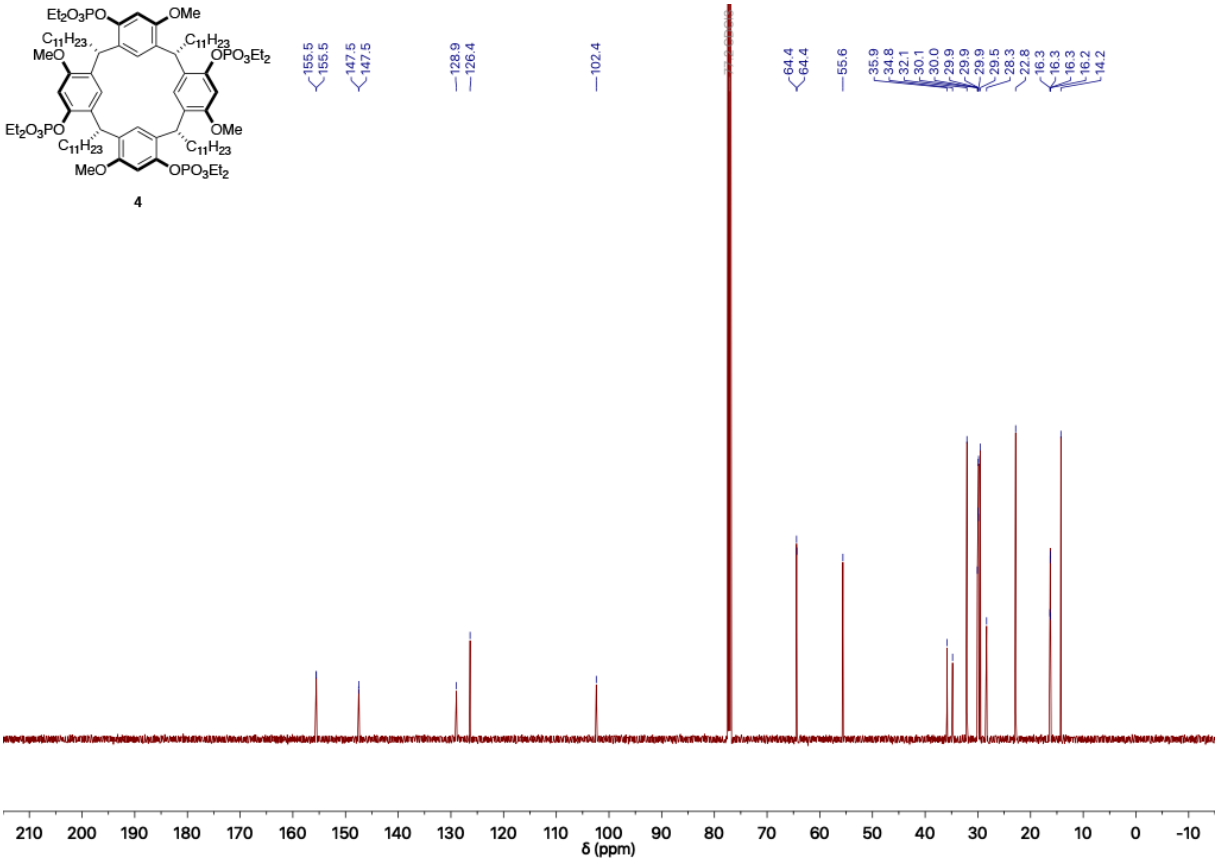

4-^{31}P ($CDCl_3$, 298 K)

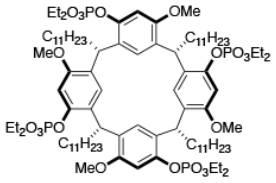

4

5-^{1}H (DMSO-d_6, 298 K)

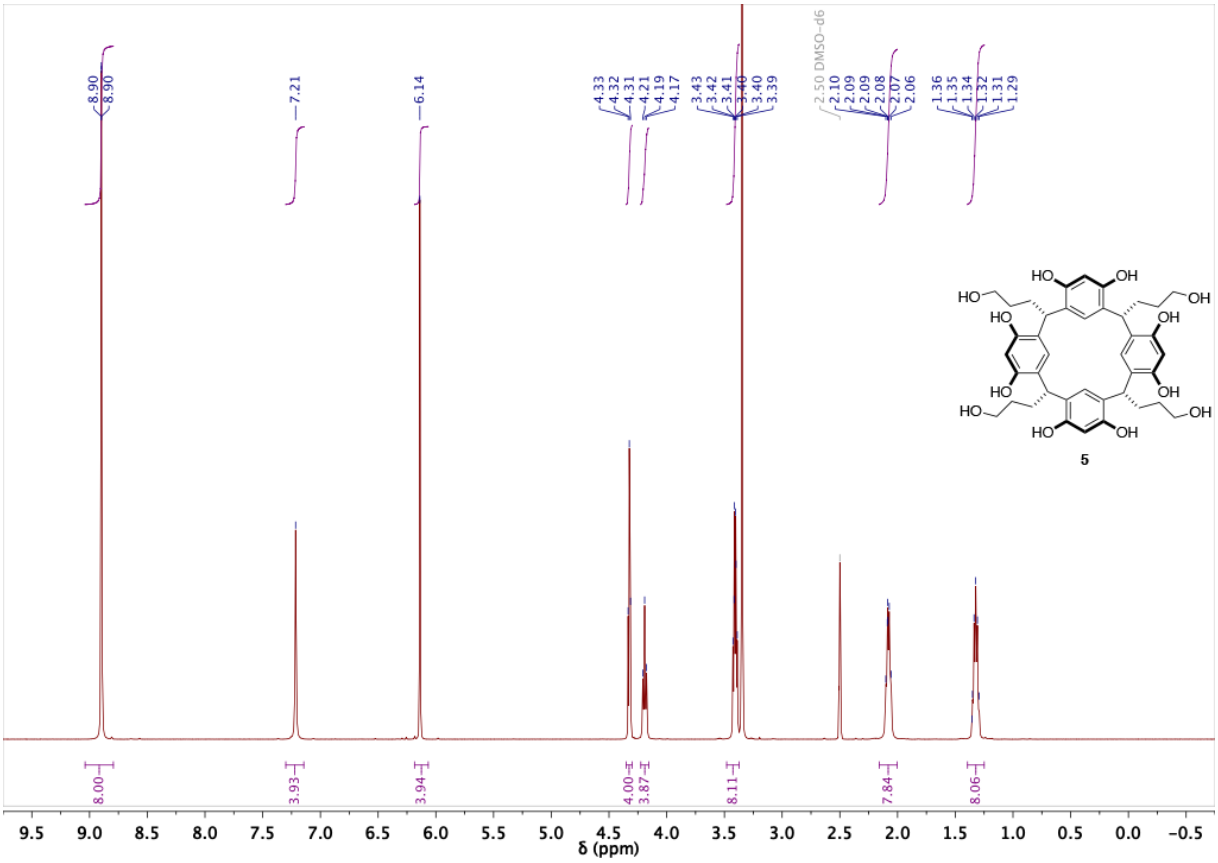

5

5-^{13}C (DMSO-d_6, 298 K)

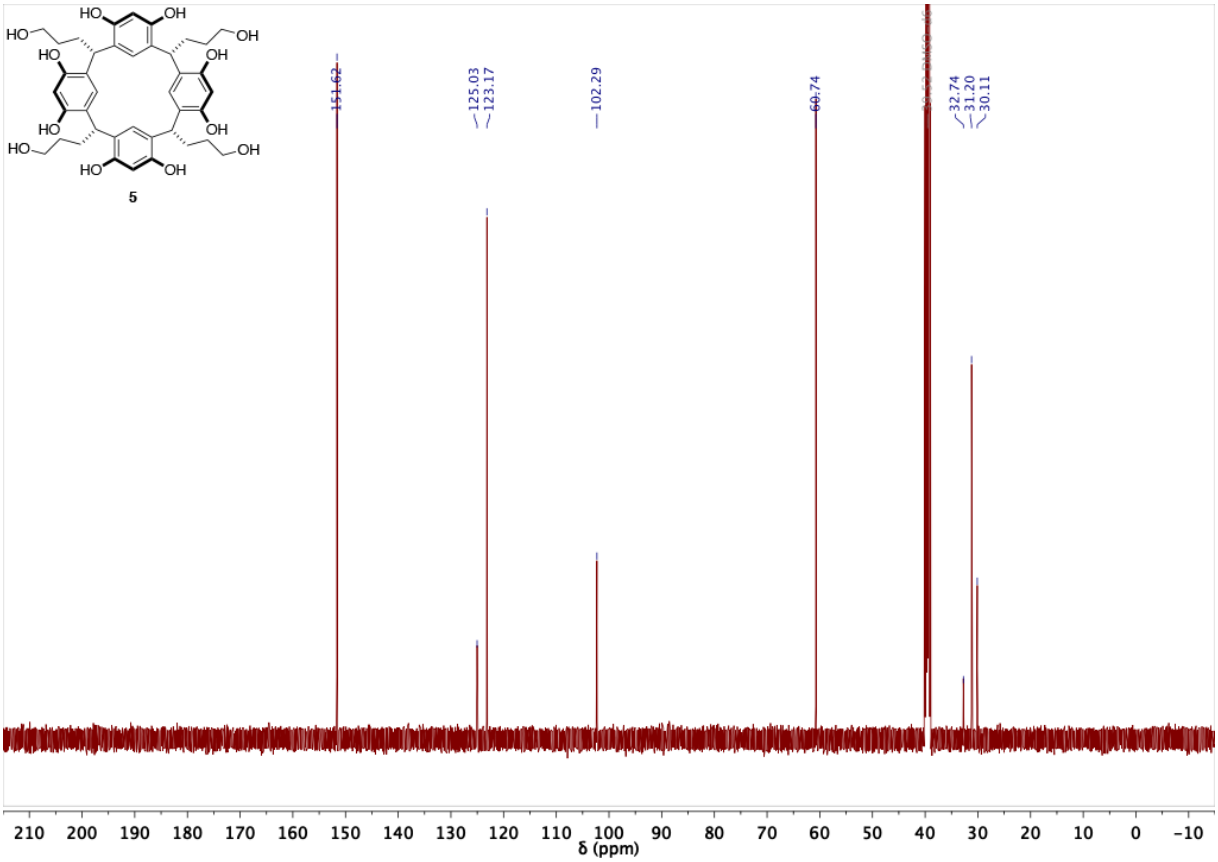

6-^{1}H (DMSO-d_6, 298 K)

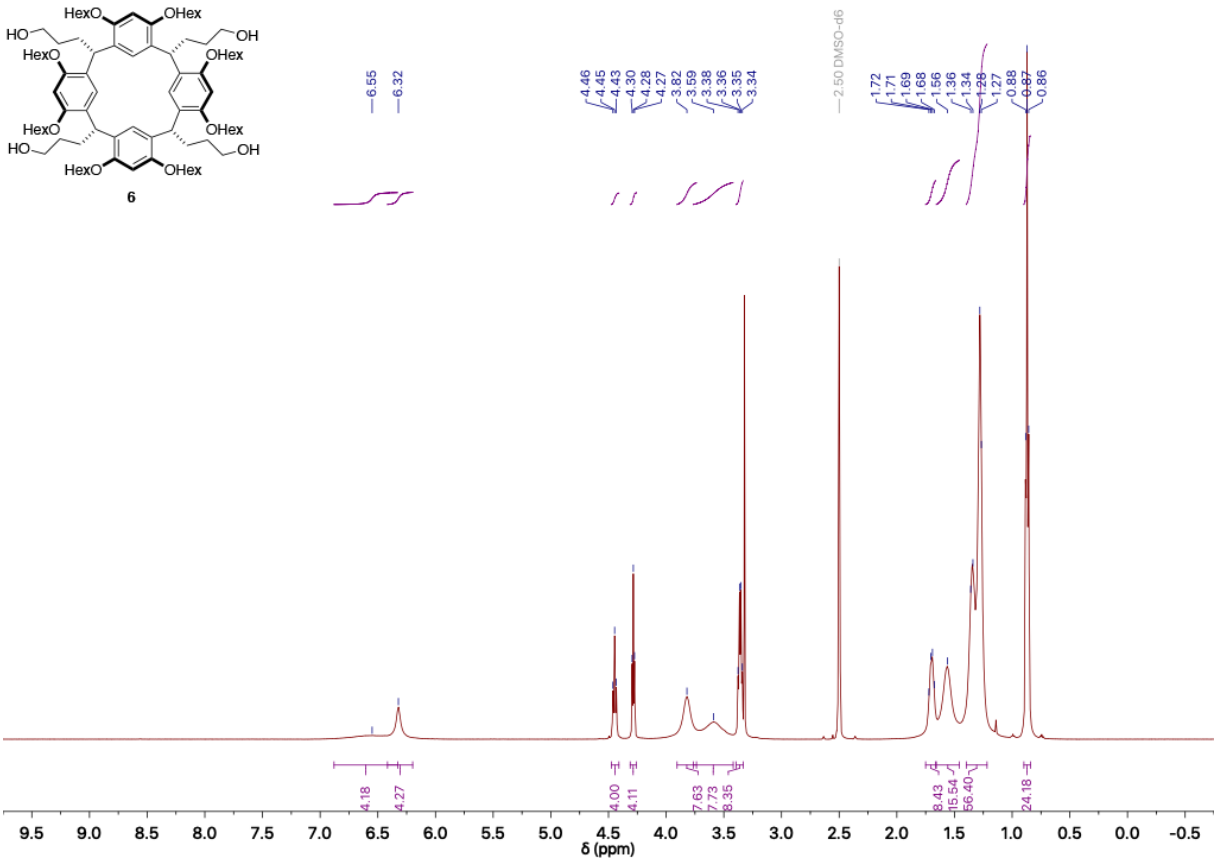

6-^{13}C (DMSO-d_6, 298 K)

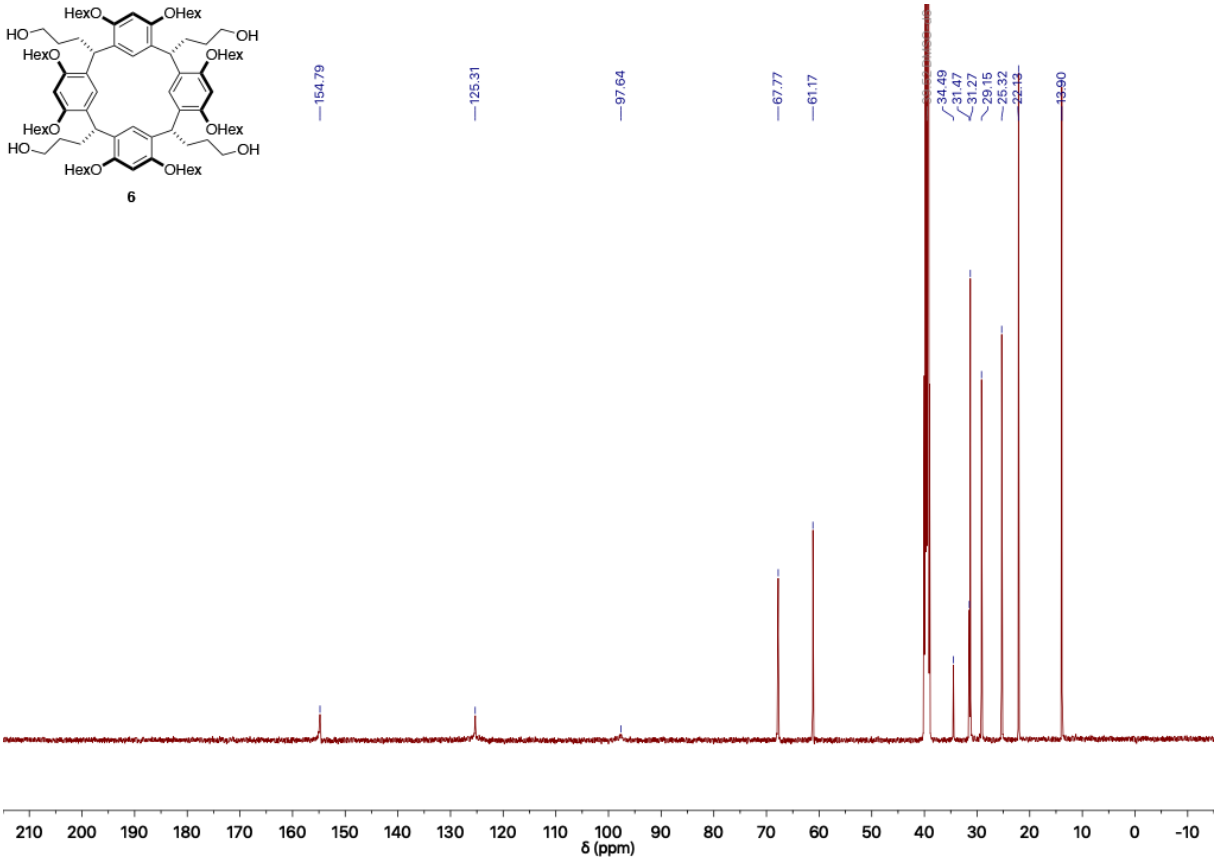

7-^{1}H (DMSO-d_6, 298 K)

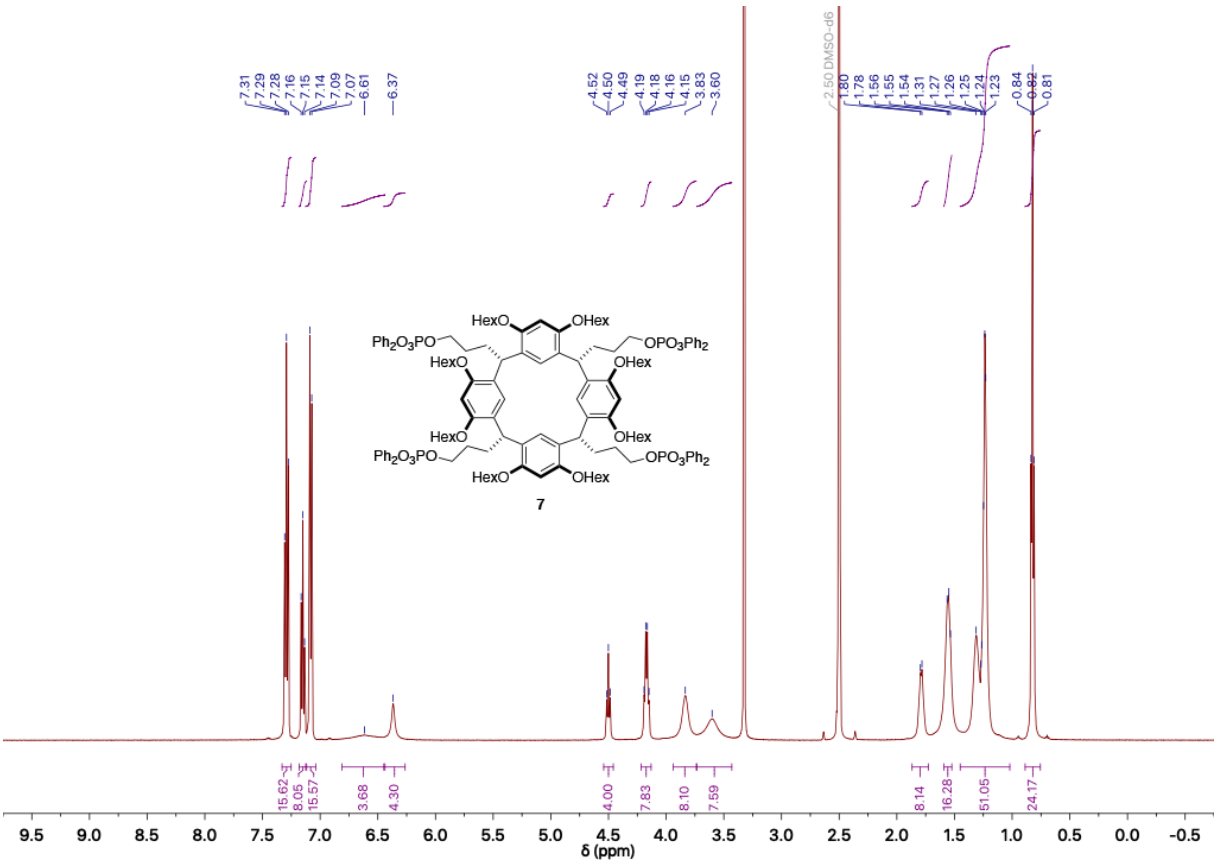

7-^{13}C (DMSO-d_6, 298 K)

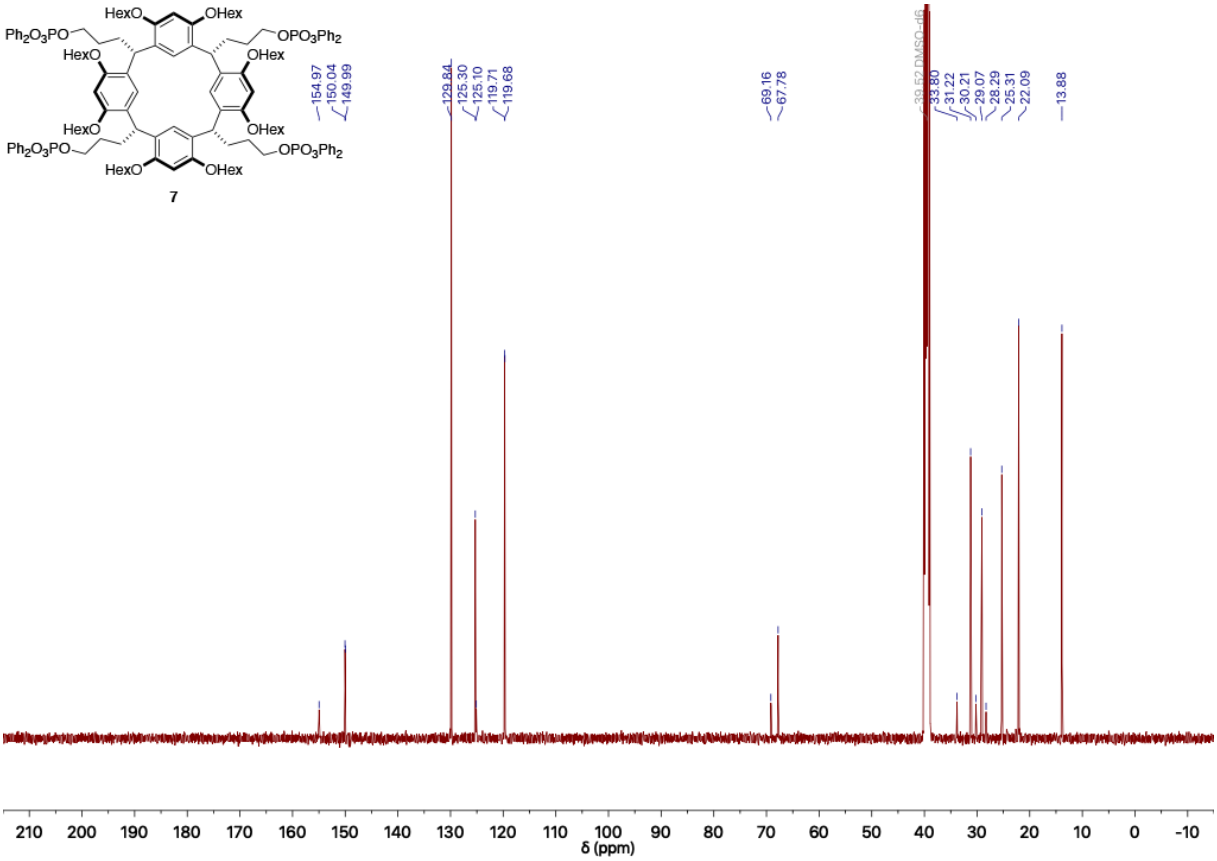

7

7-^{31}P (DMSO-d_6, 298 K)

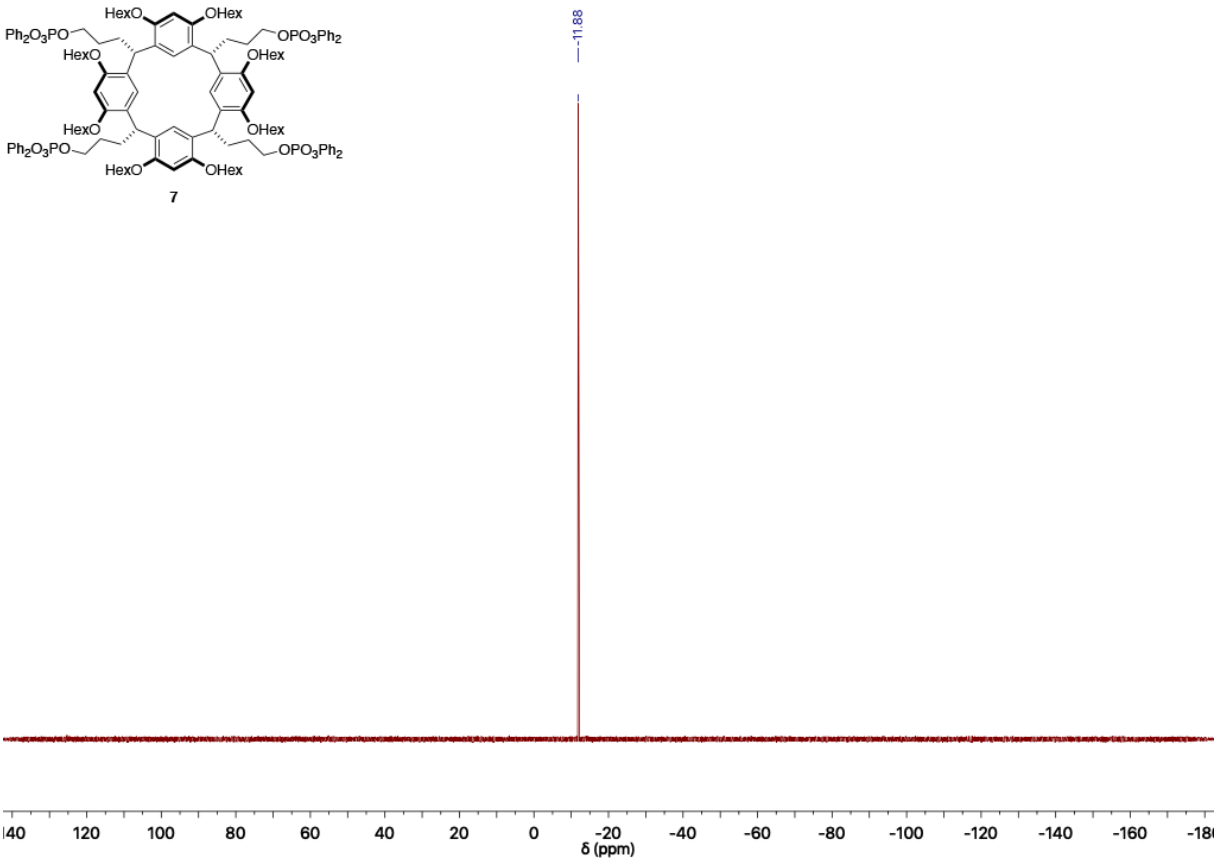

7

1-^{1}H (DMSO-d_6, 298 K)

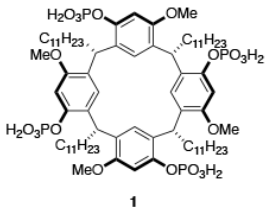

1

1-^{13}C (DMSO-d_6, 298 K)

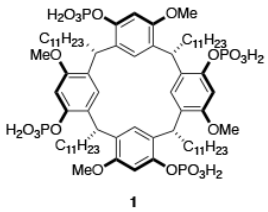

1

1-^{31}P (DMSO-d_6, 298 K)

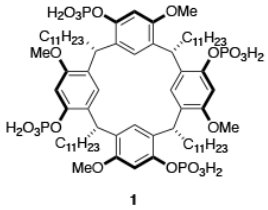

1

1-^{1}H (THF-d_8, 298 K)

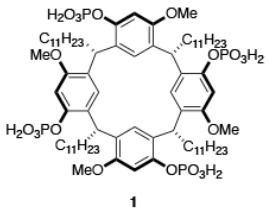

1

1-^{13}C (THF-d_8, 298 K)

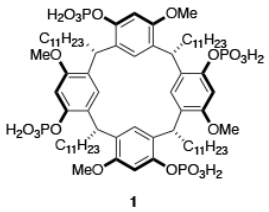

1

1-^{31}P (THF-d_8, 298 K)

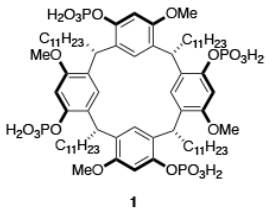

1

2-^{1}H (DMSO-d_6, 353 K)

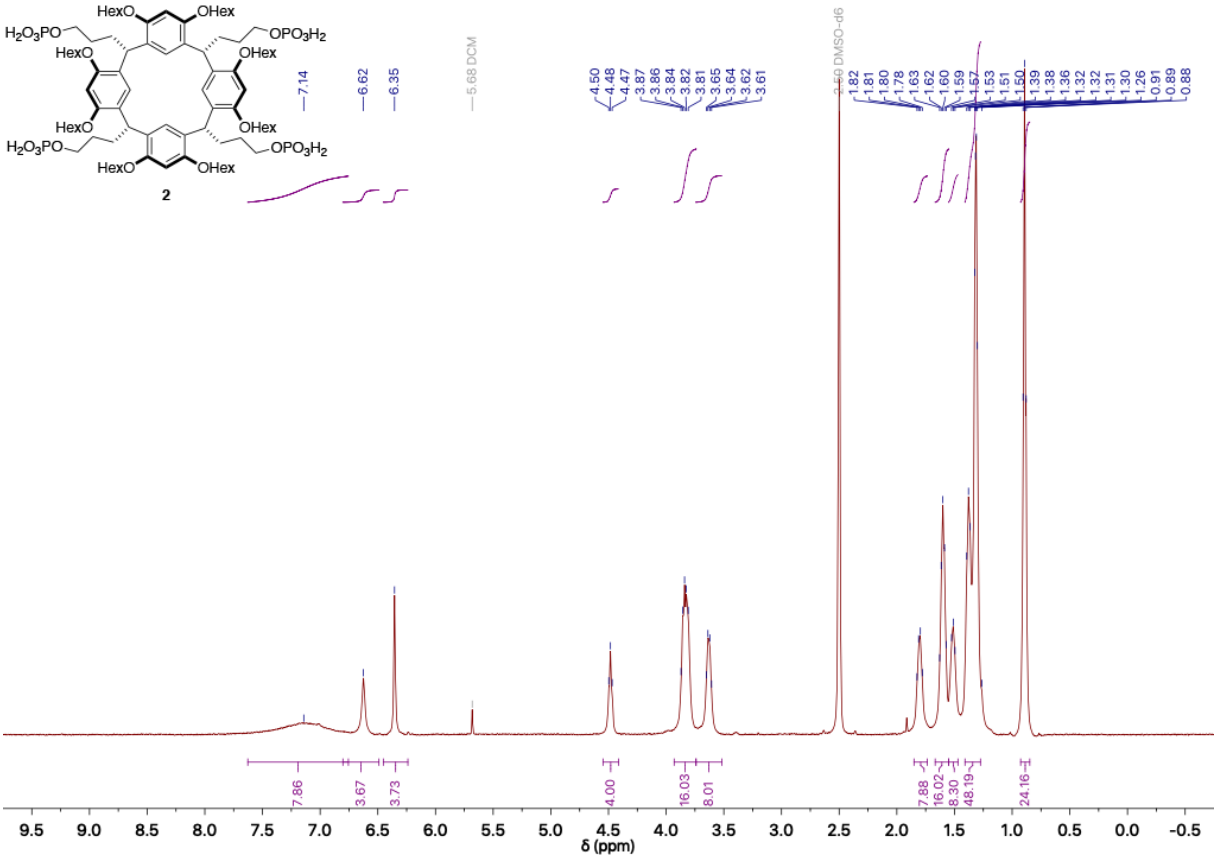

2-^{13}C (DMSO-d_6, 353 K)

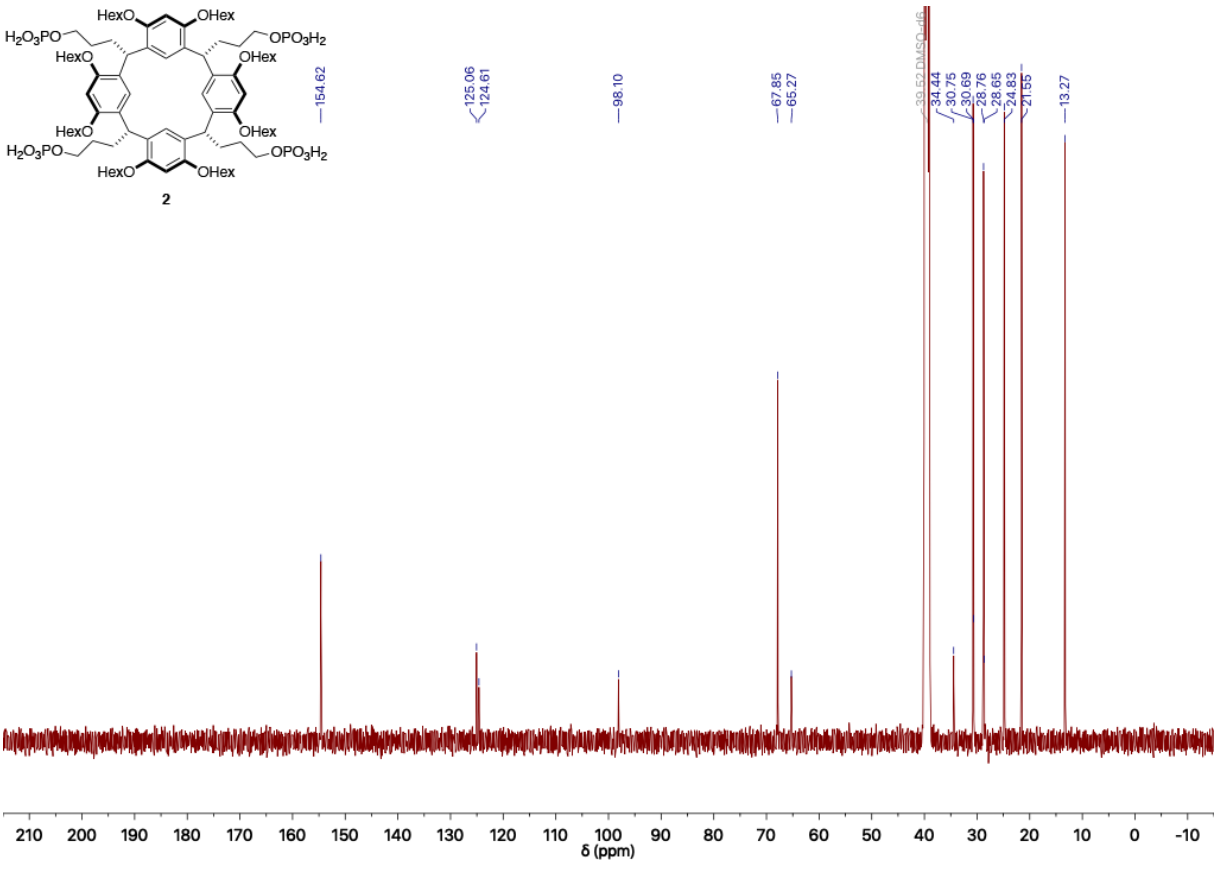

2-^{31}P (DMSO-d_6, 298 K)

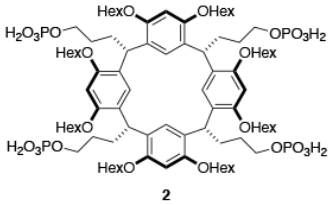

2-^{1}H (THF-d_8, 298 K)

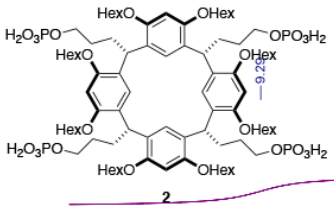

2-^{13}C (THF-d_8, 298 K)

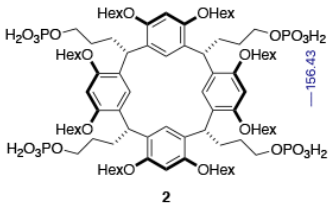

2

2-^{31}P (THF-d_8, 298 K)

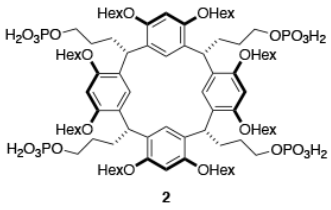

2

Appendix A.2: 2D NMR Spectra of New Compounds

4-COSY ($CDCl_3$, 298 K)

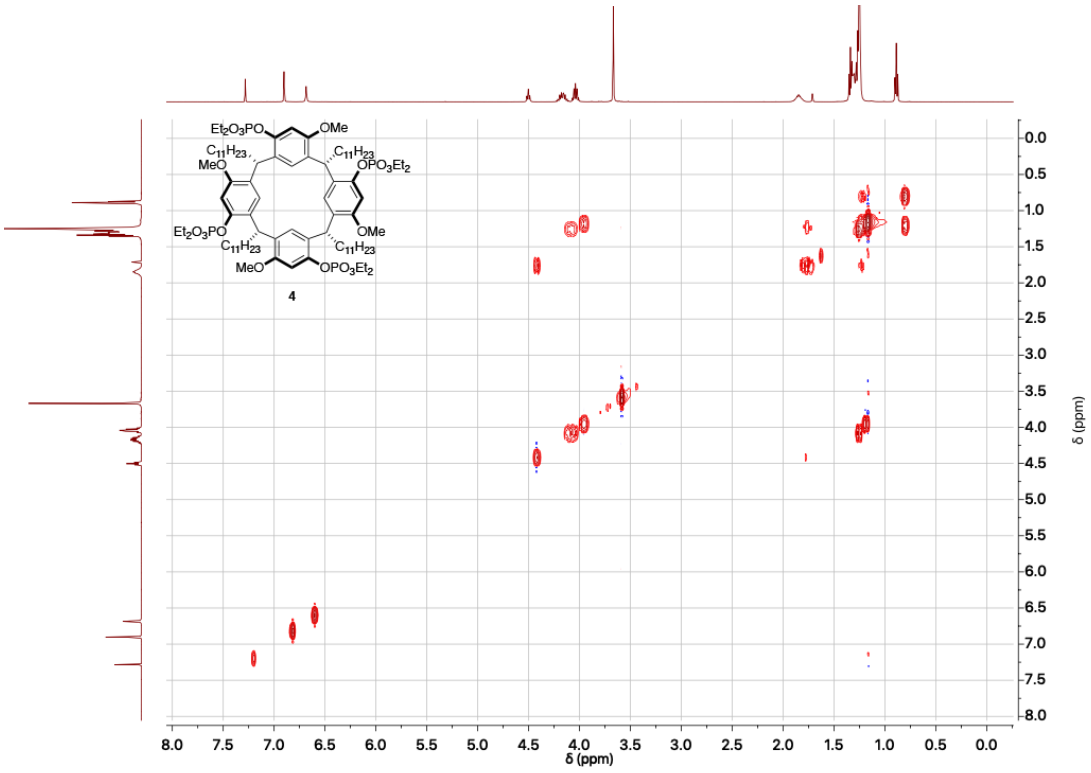

4-HMQC ($CDCl_3$, 298 K)

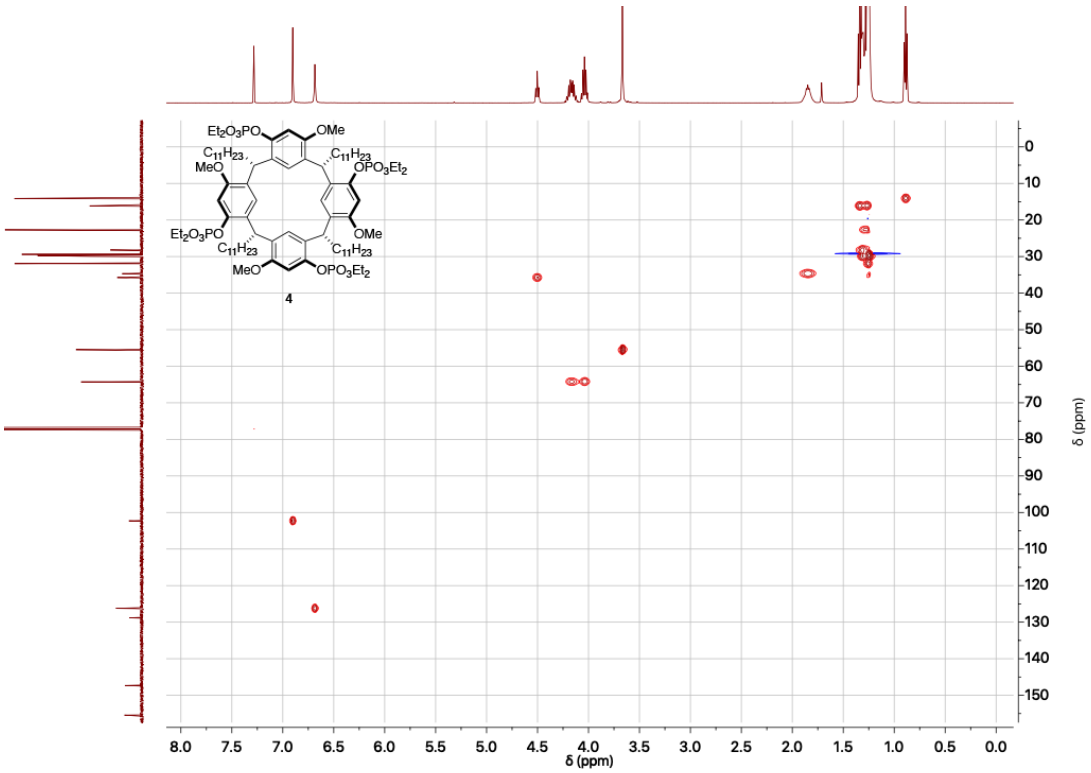

4-HMBC ($CDCl_3$, 298 K)

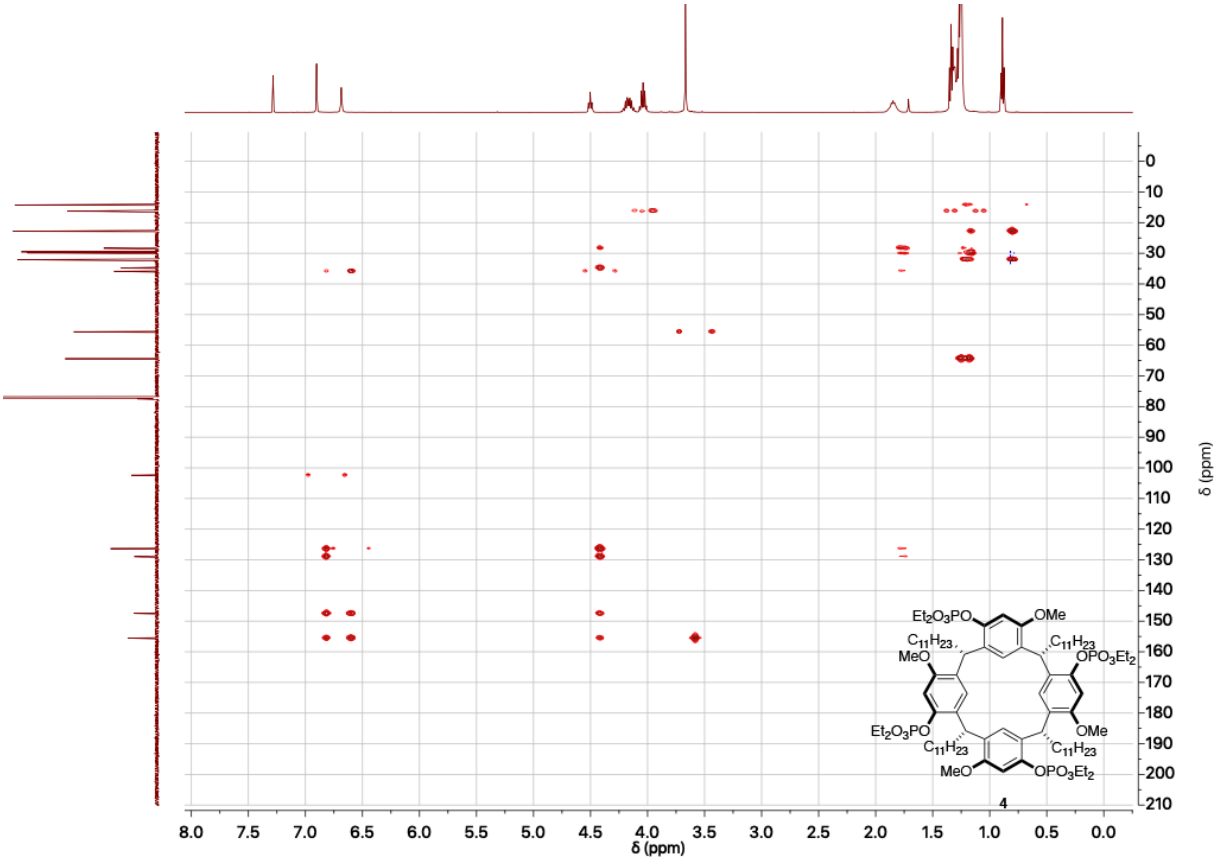

6-COSY (DMSO-d_6, 298 K)

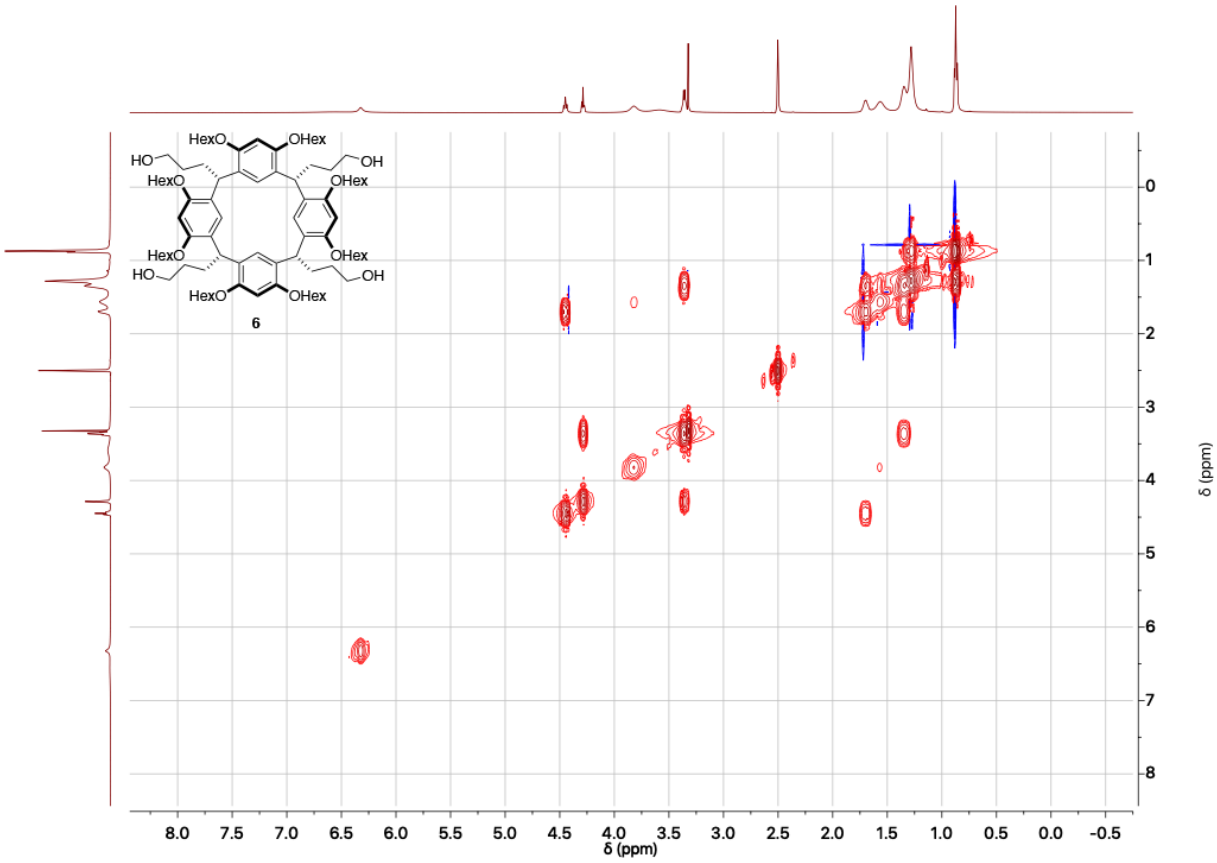

6-HMQC (DMSO-d_6, 298 K)

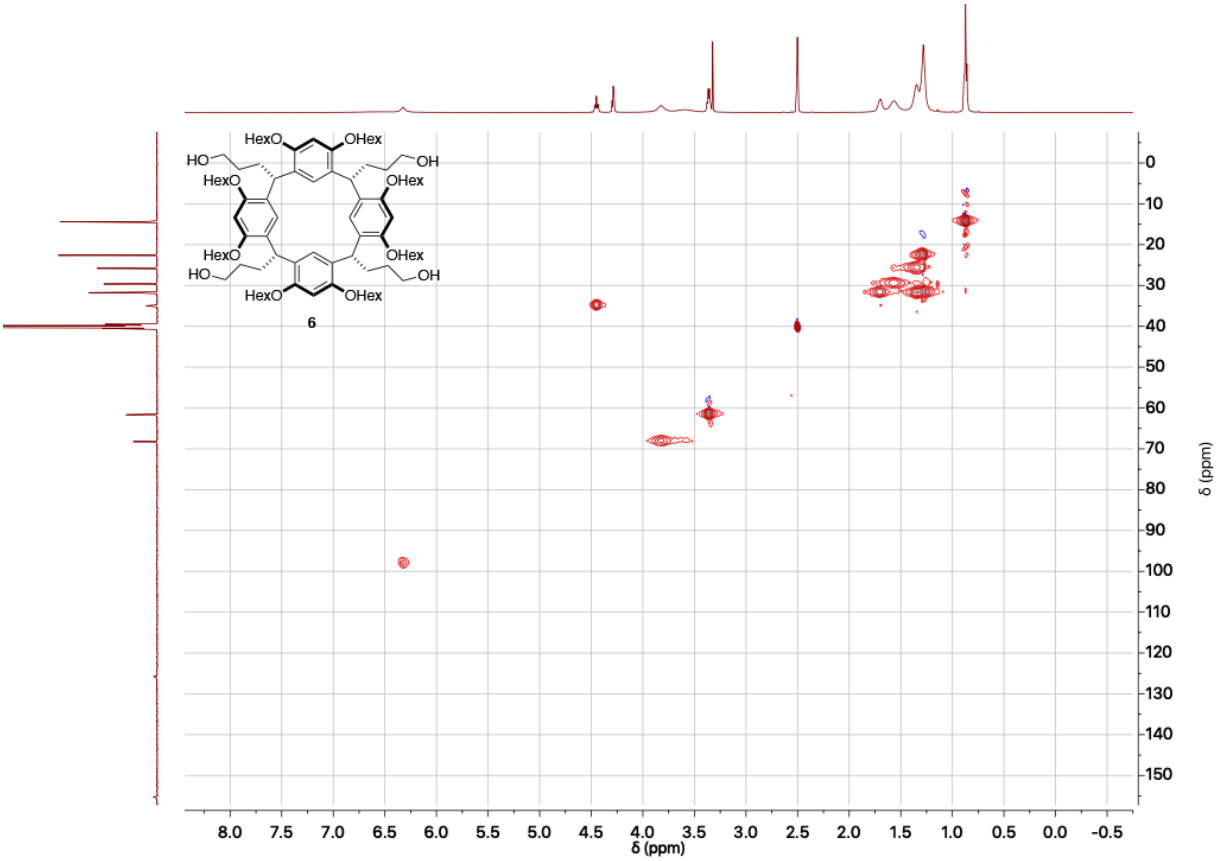

6-HMBC (DMSO-d_6, 298 K)

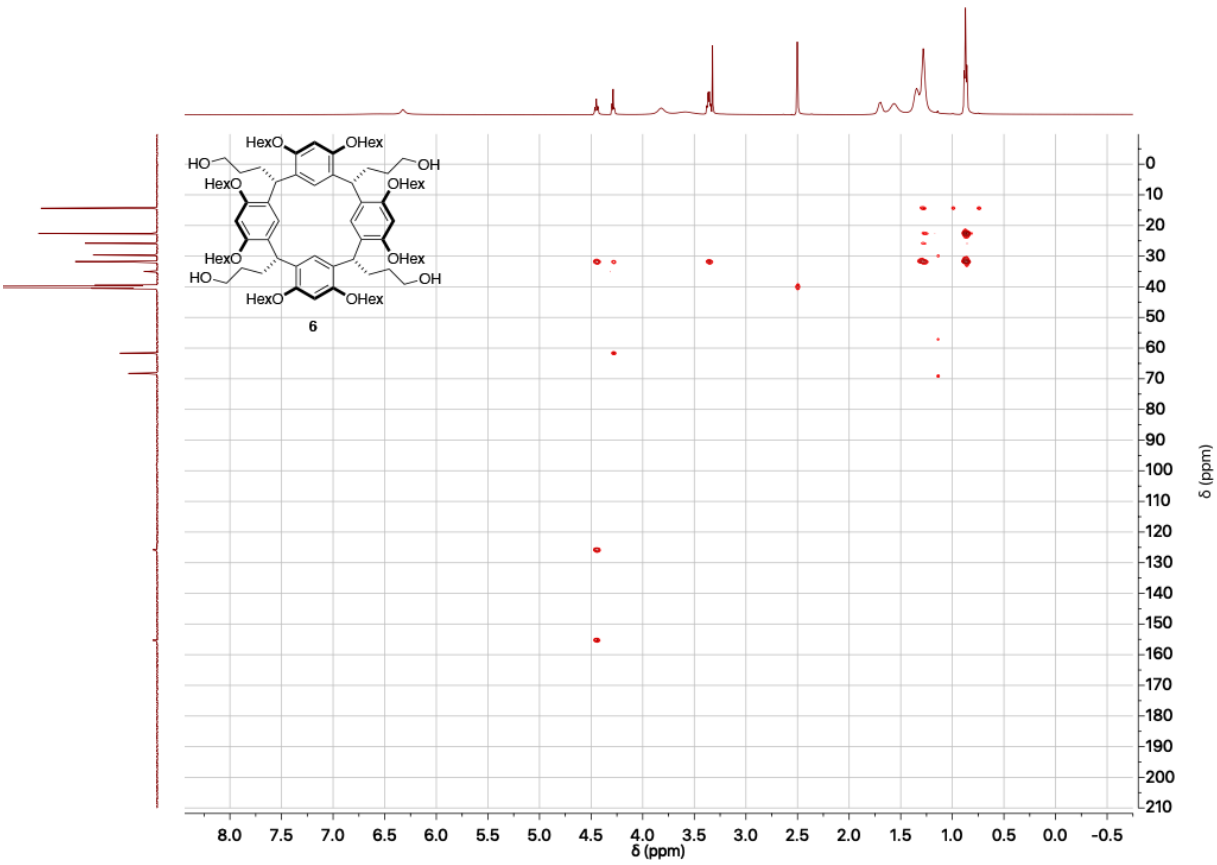

7-COSY (DMSO-d_6, 298 K)

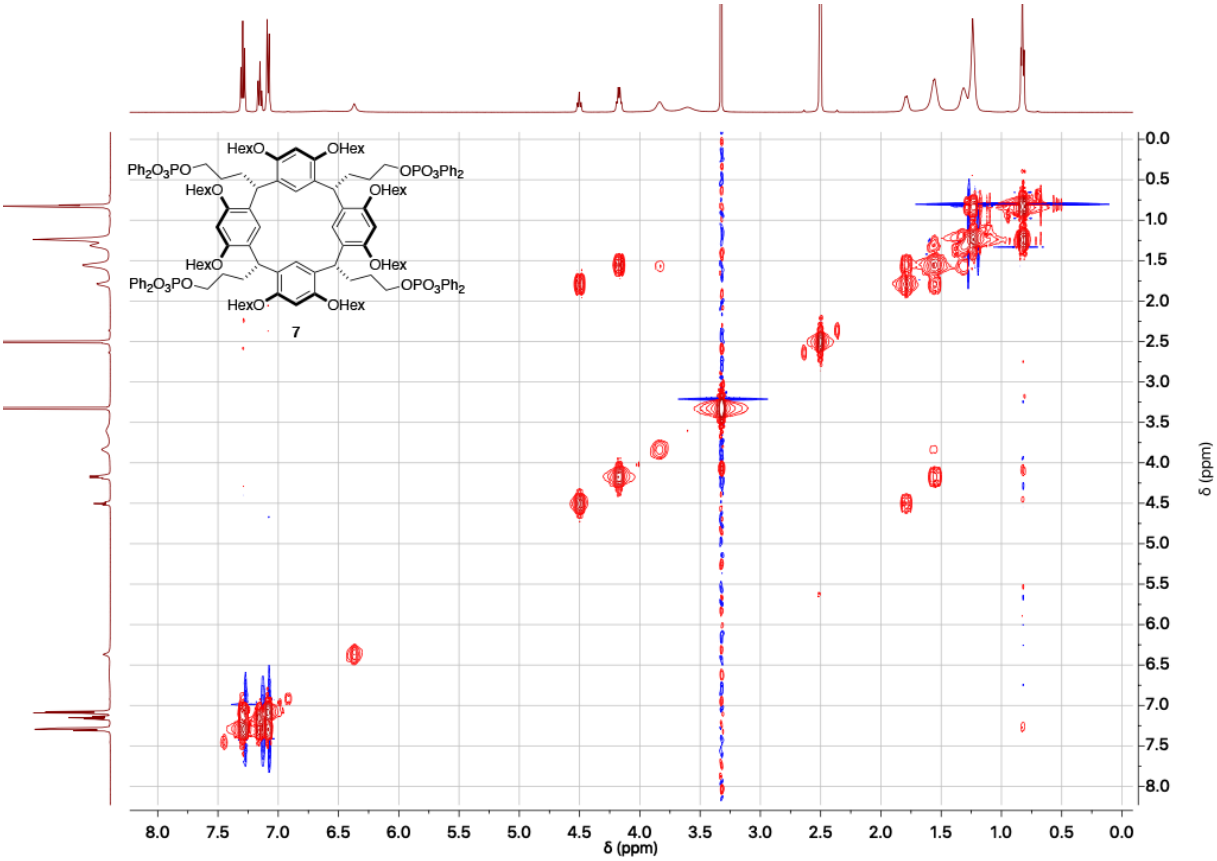

7-HMQC (DMSO-d_6, 298 K)

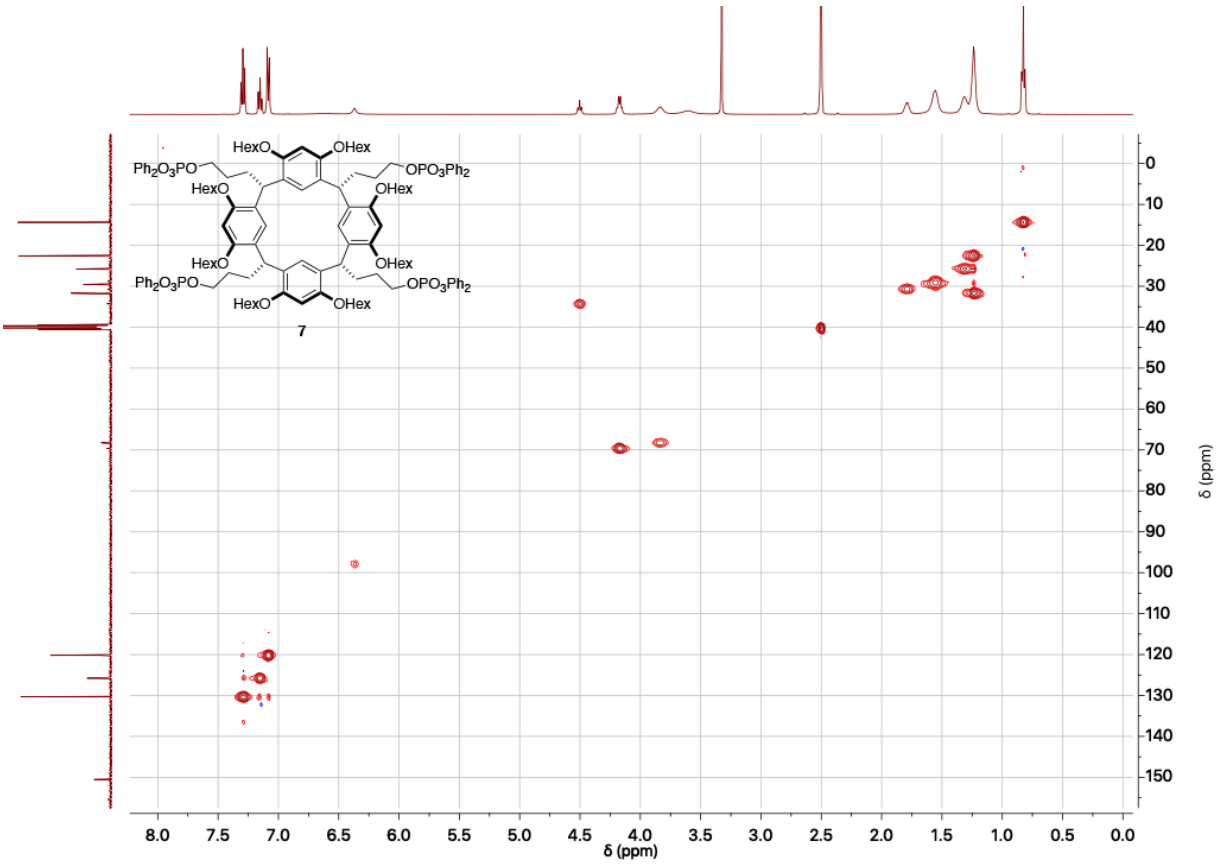

7-HMBC (DMSO-d_6, 298 K)

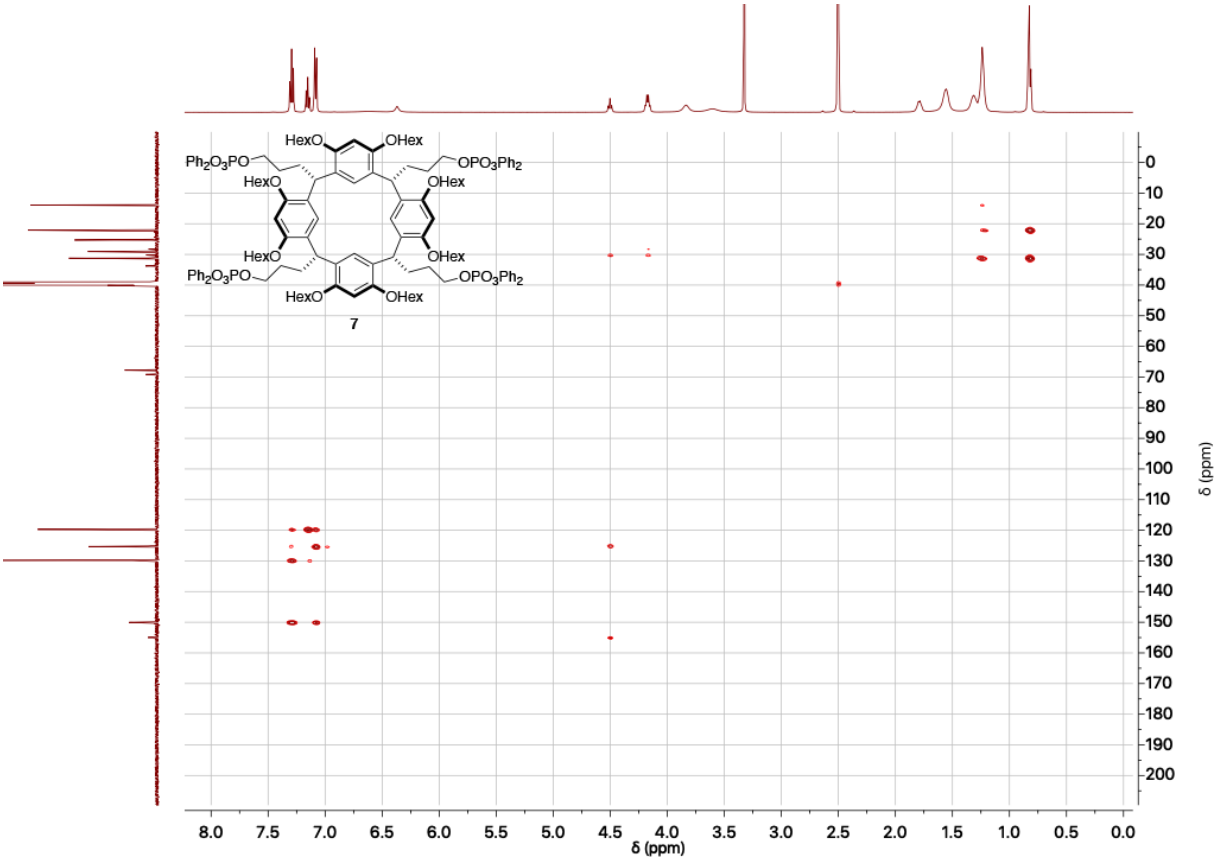

1-COSY (DMSO-d_6, 298 K)

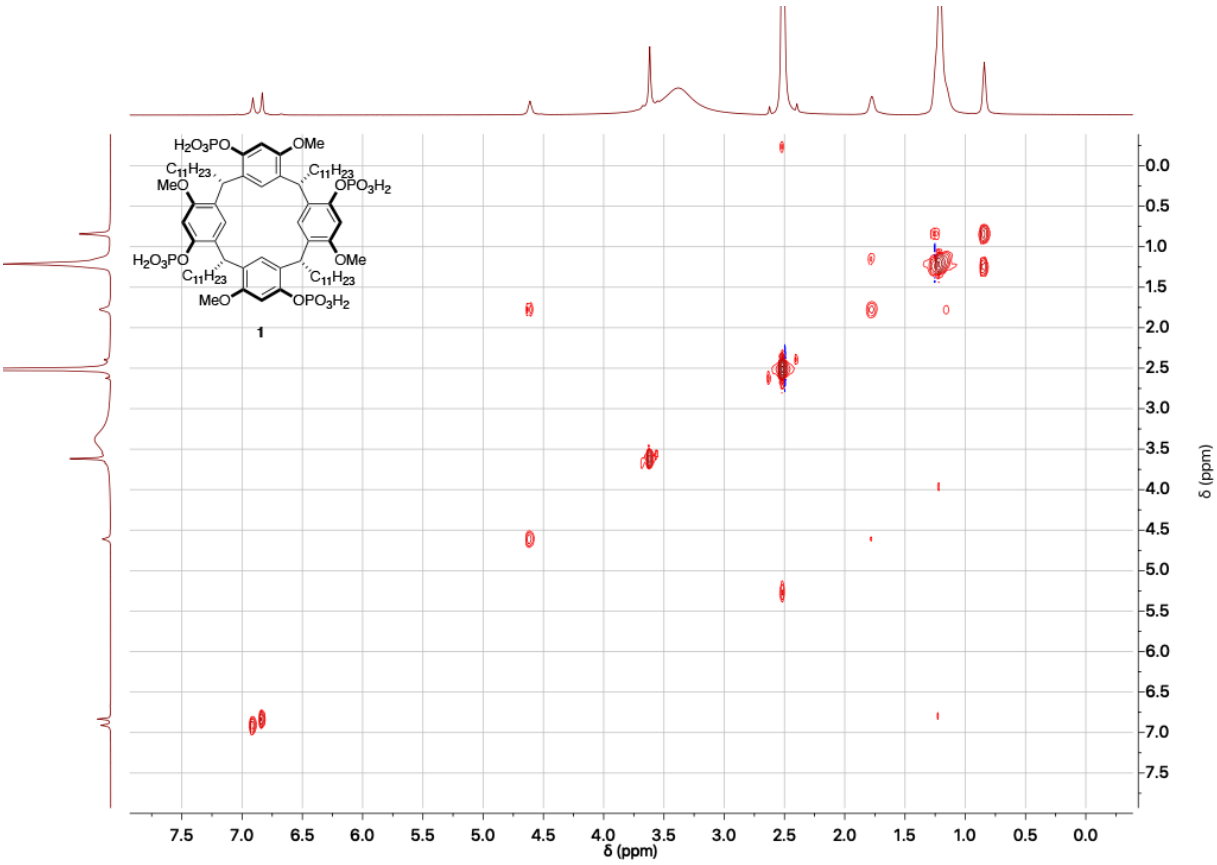

1-NOESY (DMSO-d_6, 298 K)

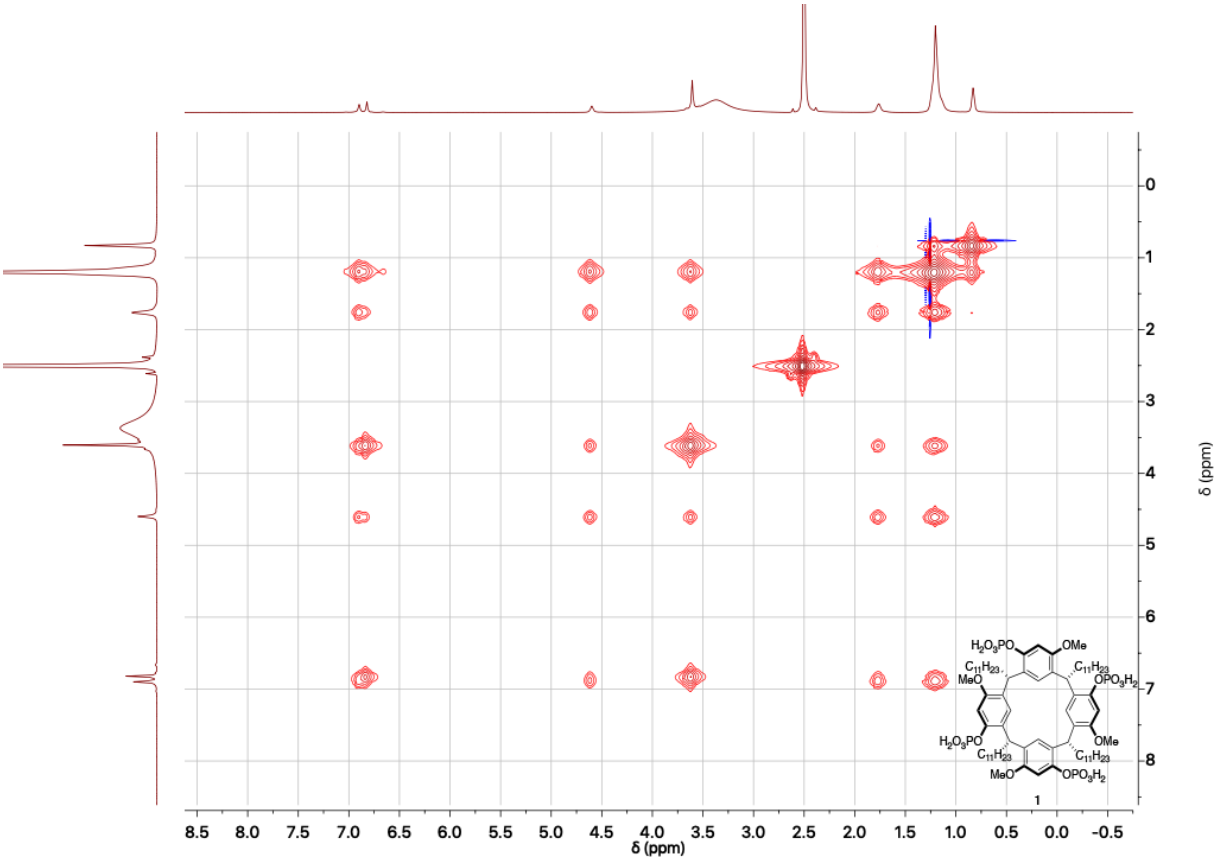

1-HMQC (DMSO-d_6, 298 K)

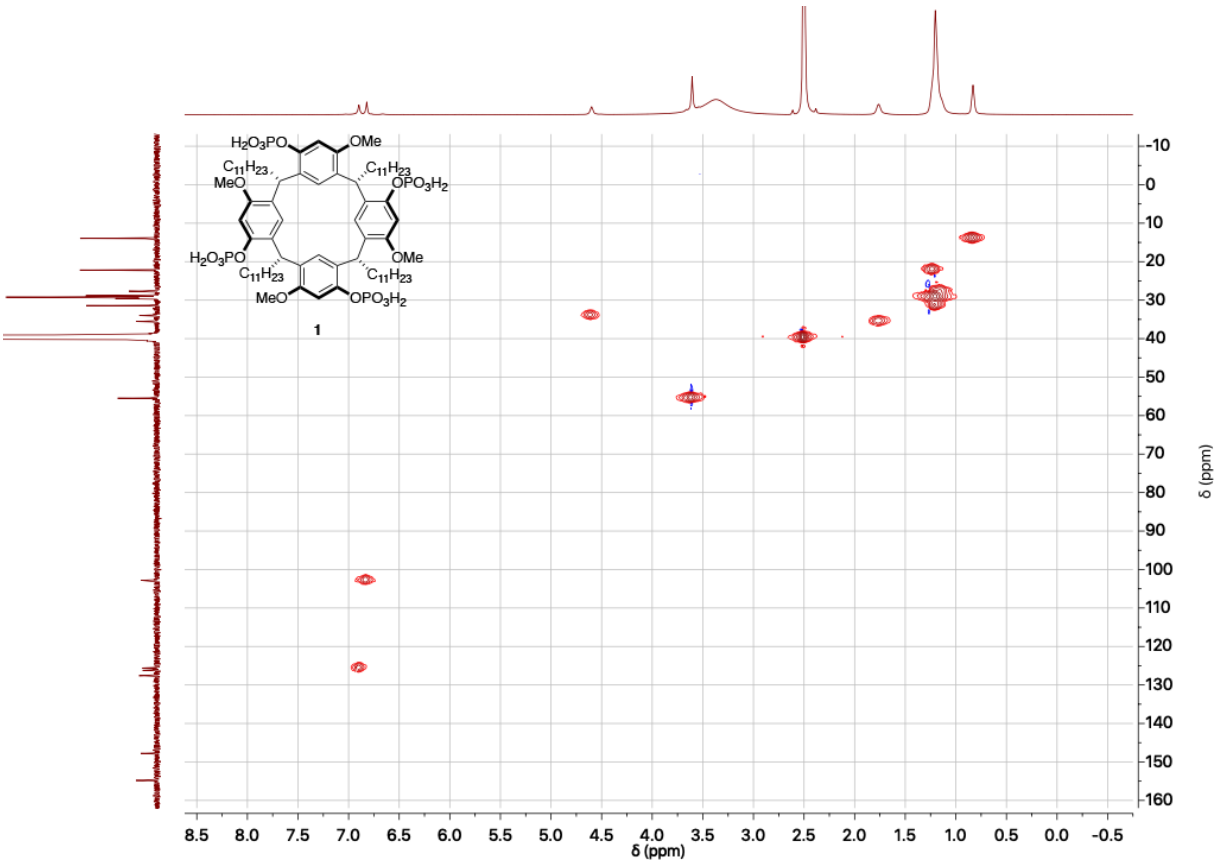

1-HMBC (DMSO-d_6, 298 K)

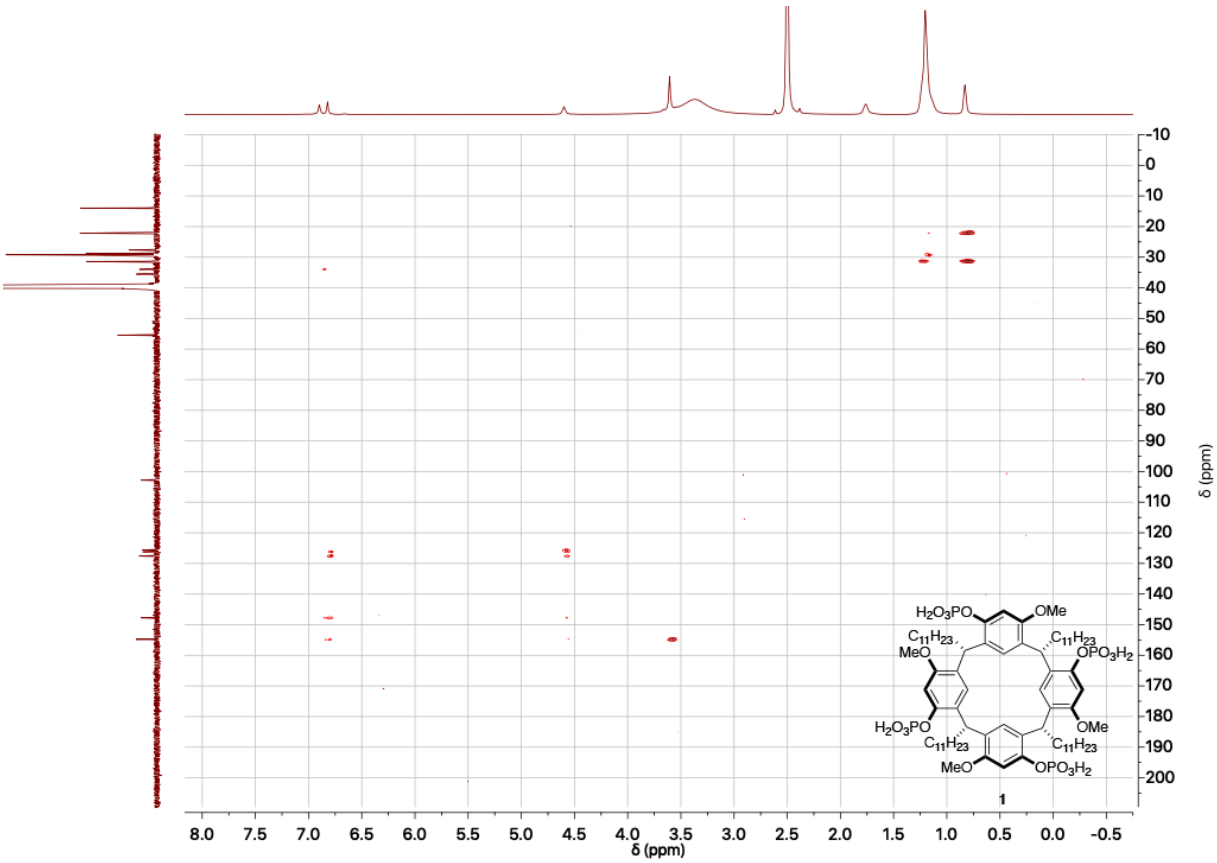

1-COSY (THF-d_8, 298 K)

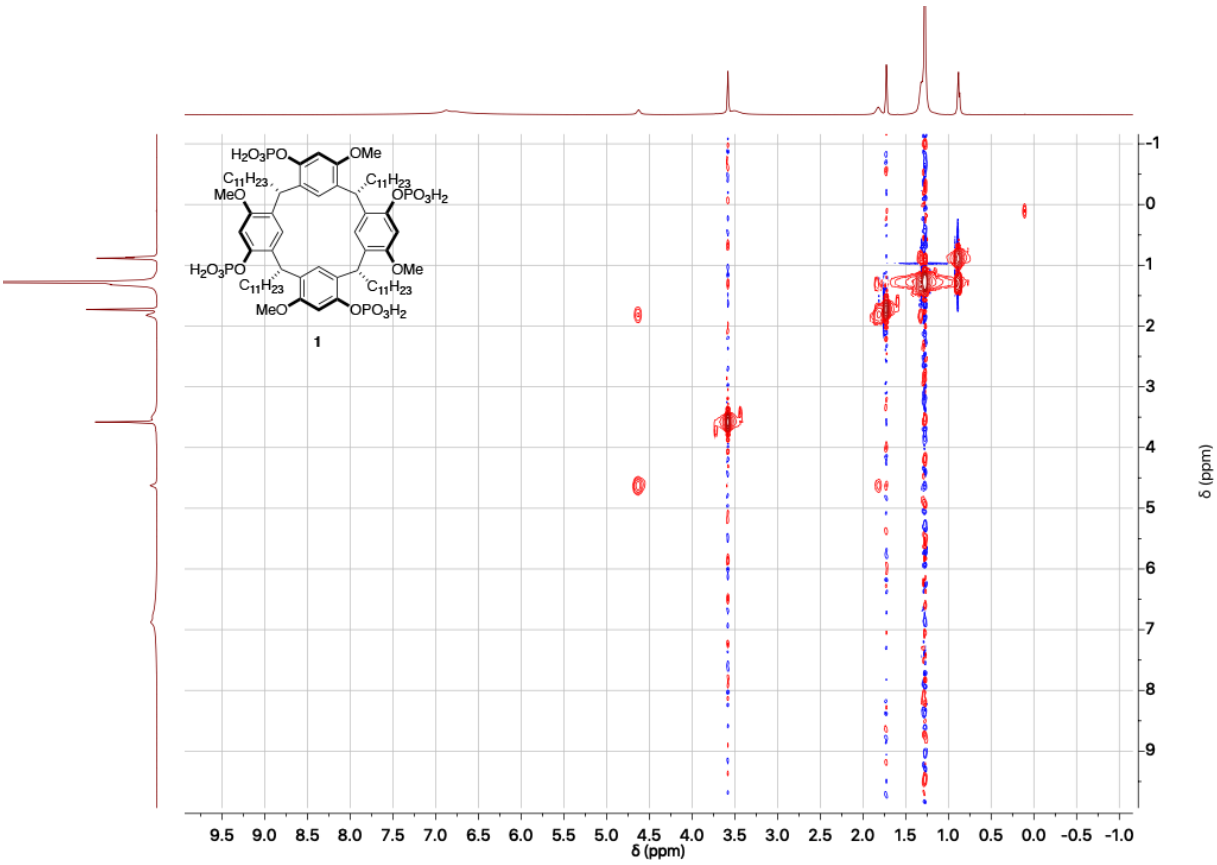

1-NOESY (THF-d_8, 298 K)

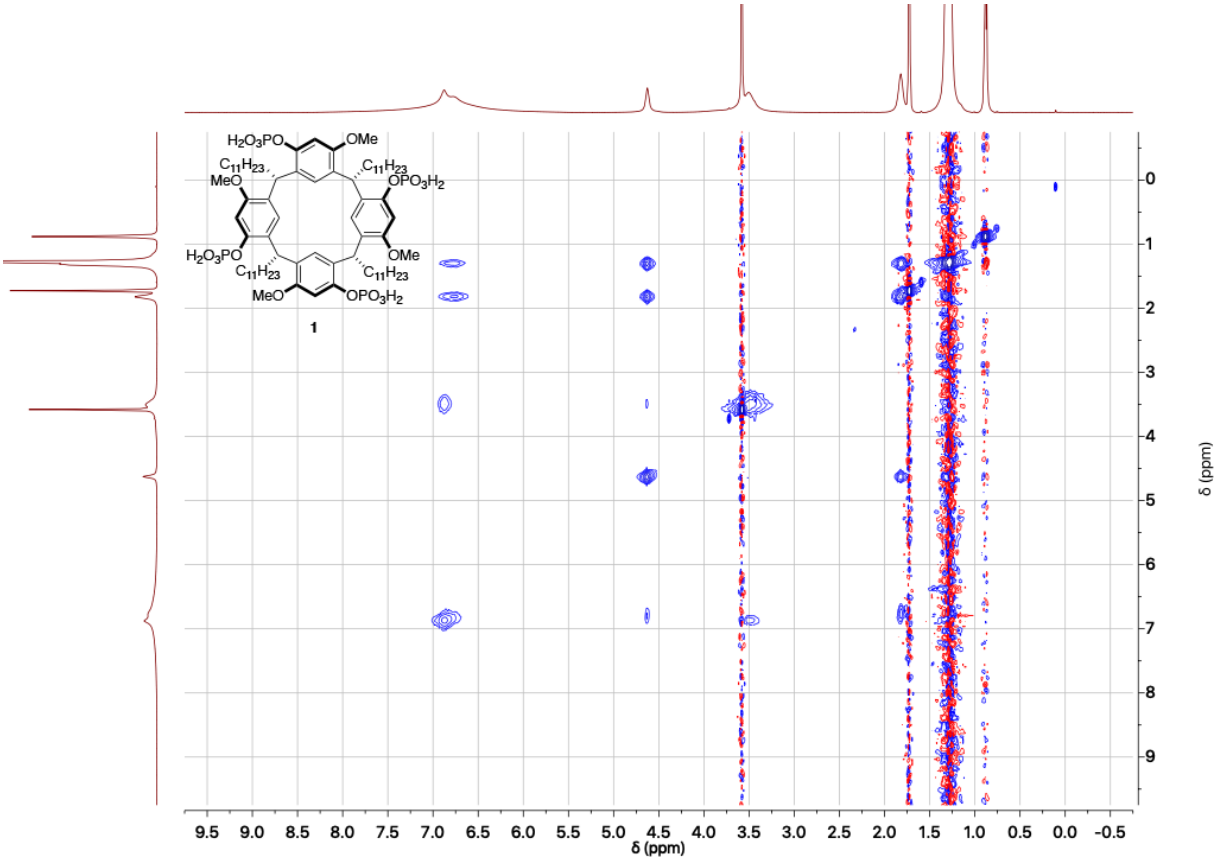

1-HMQC (THF-d_8, 298 K)

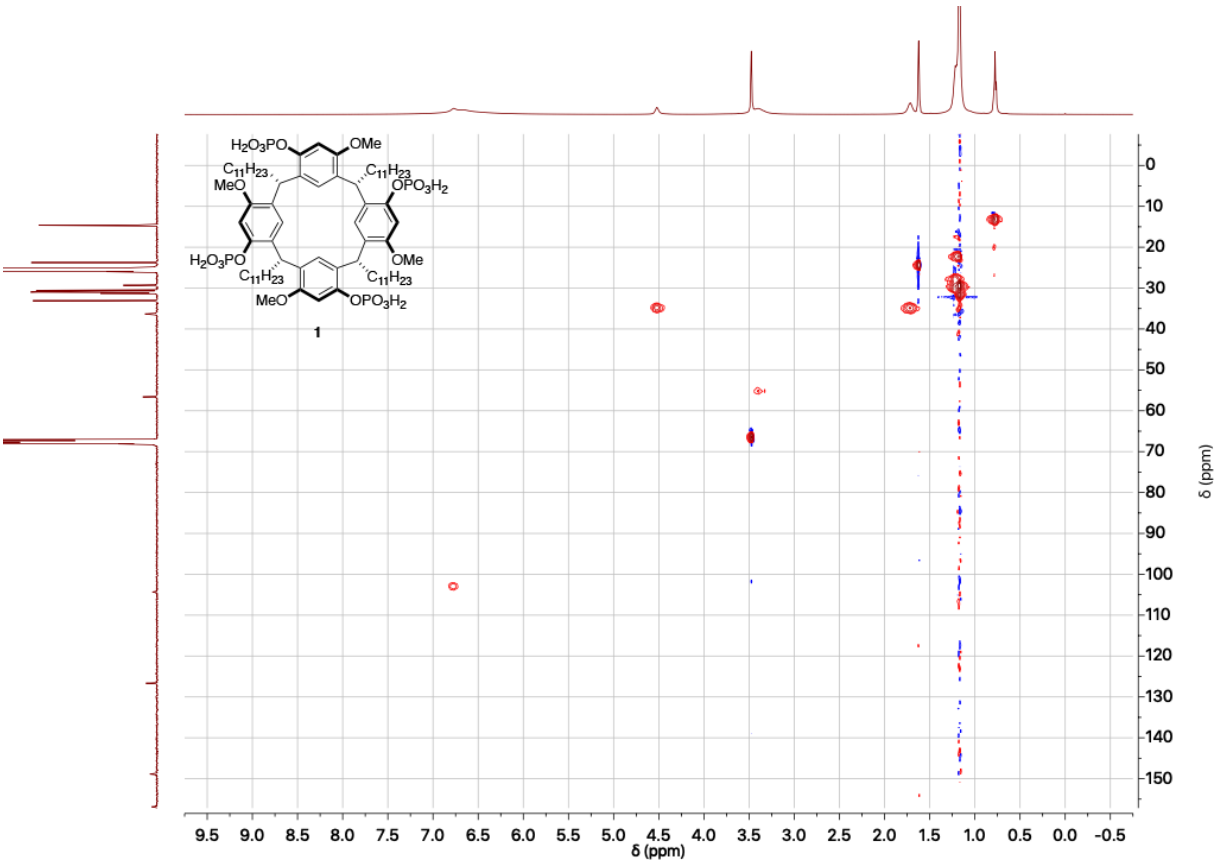

1-HMBC (THF-d_8, 298 K)

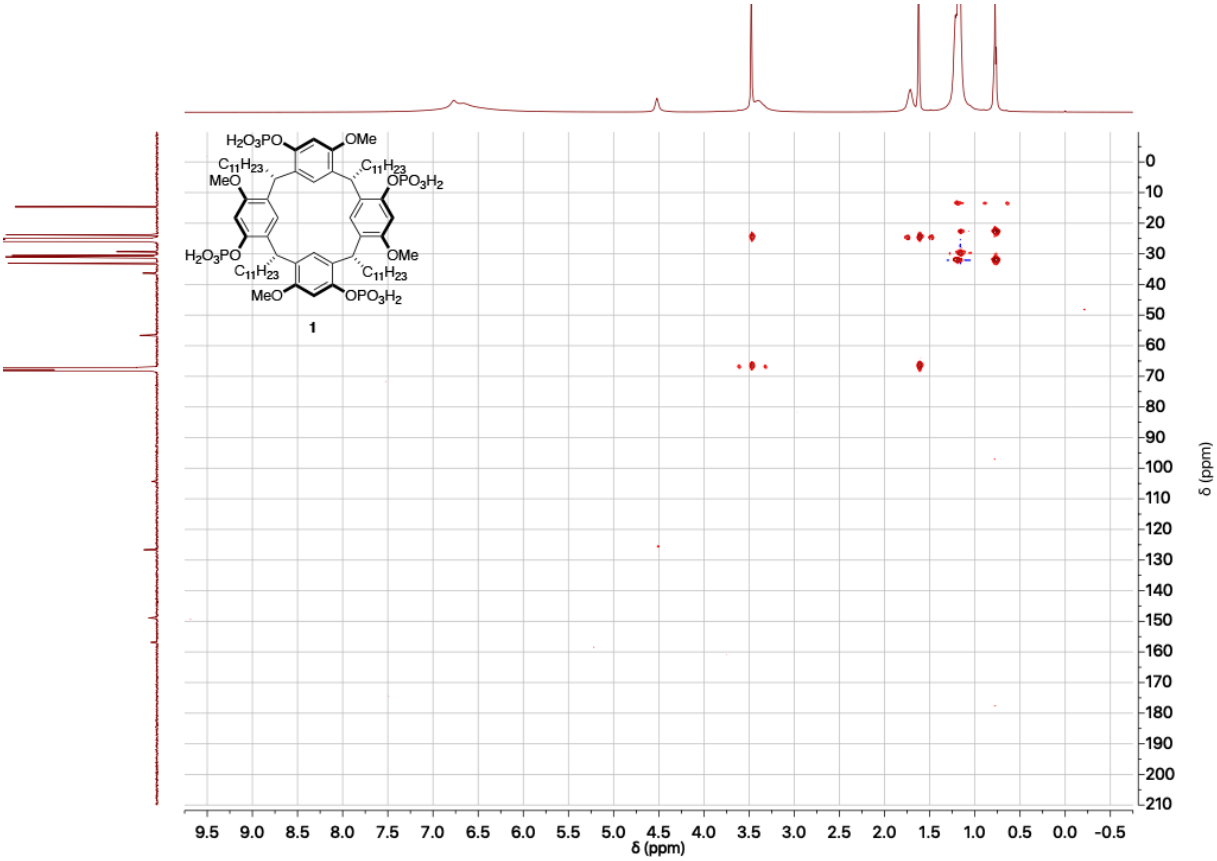

2-COSY (DMSO-d_6, 298 K)

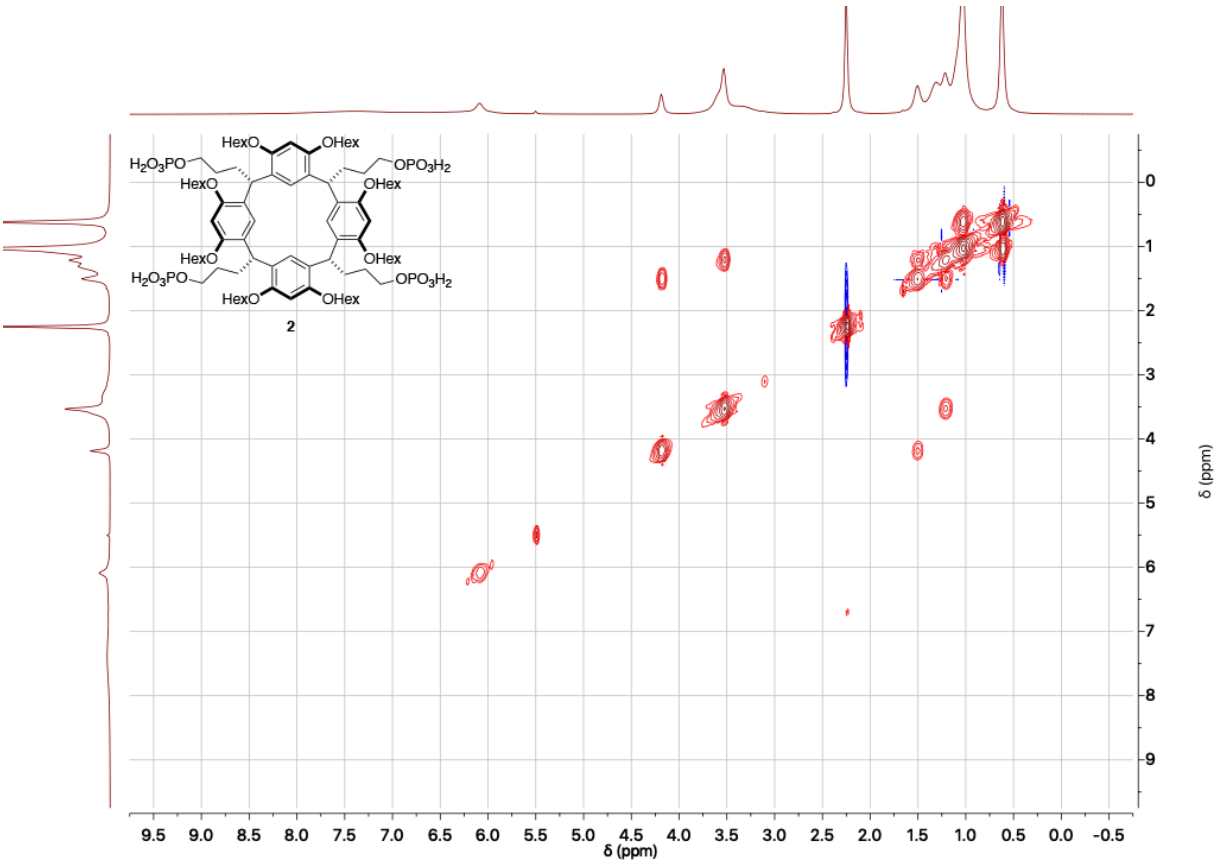

2-NOESY (DMSO-d_6, 298 K)

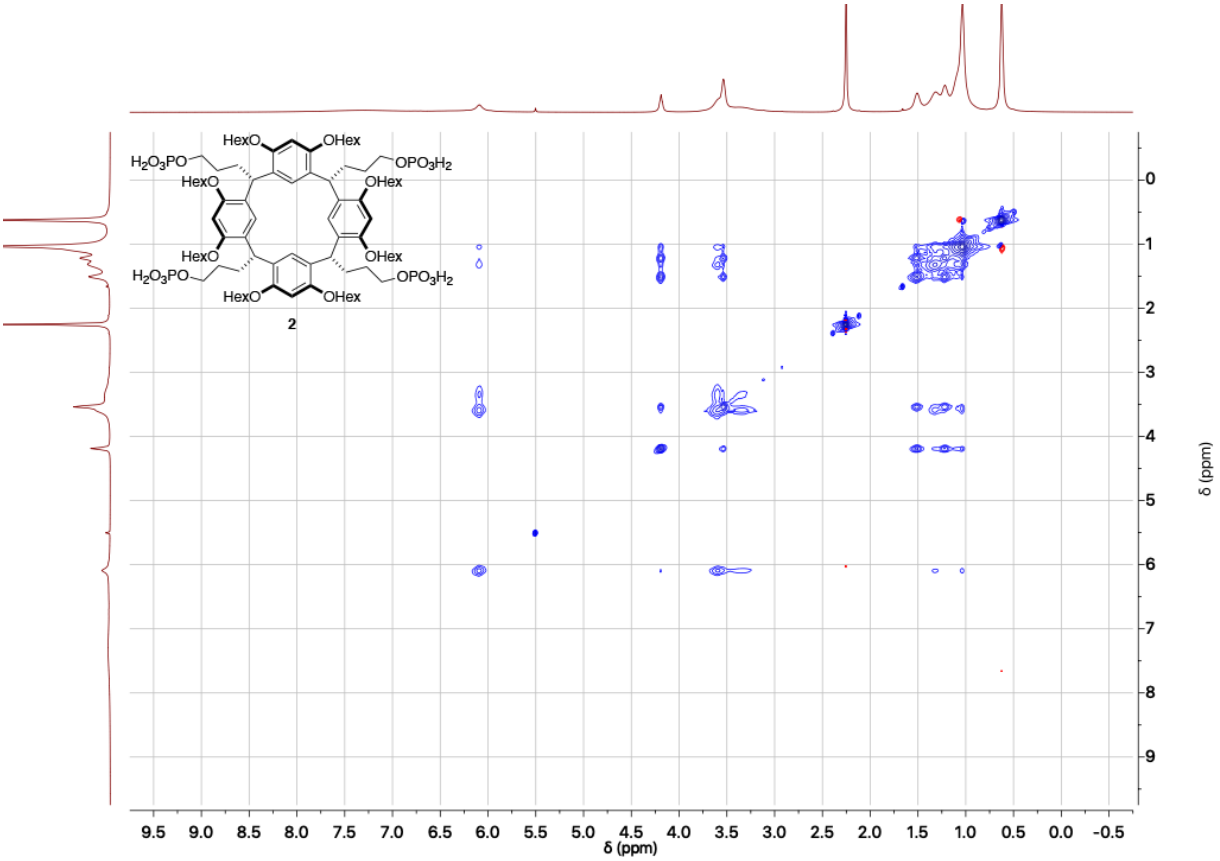

2-HMQC (DMSO-d_6, 298 K)

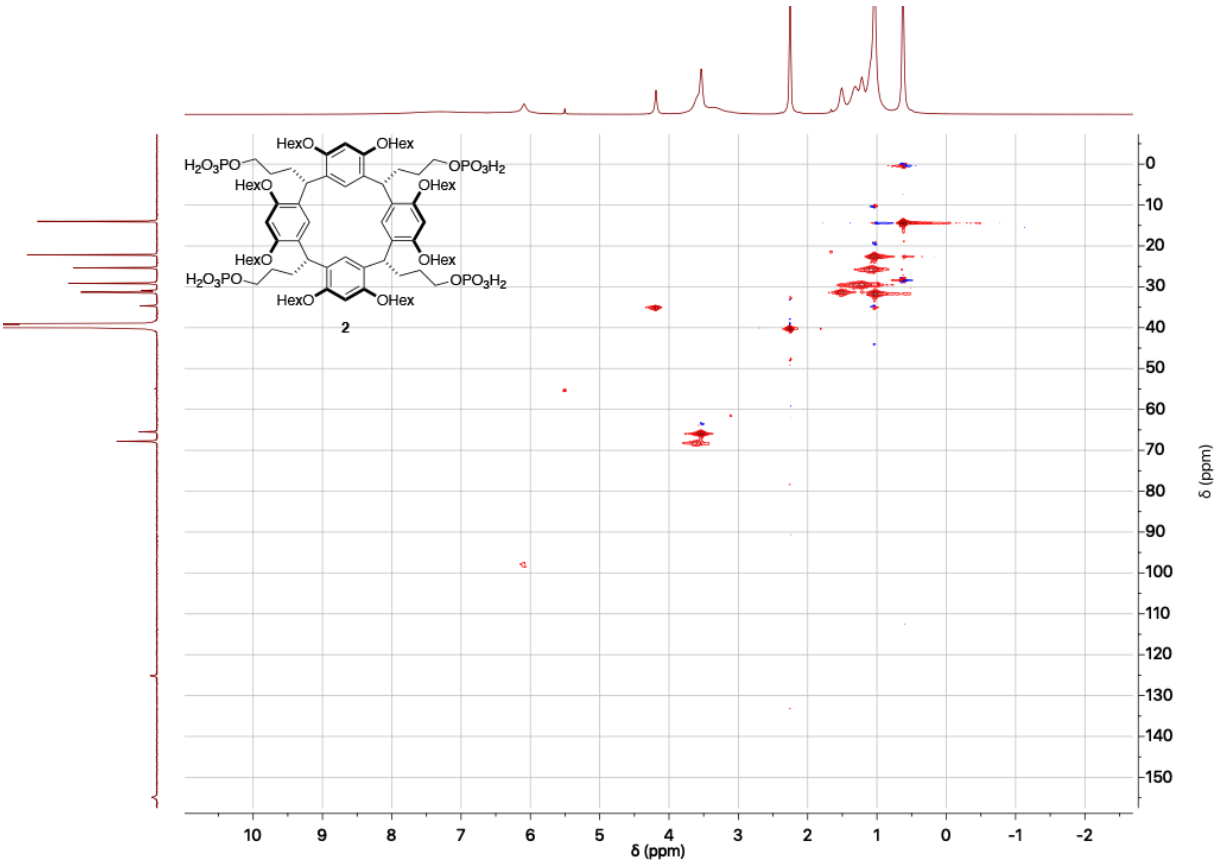

2-HMBC (DMSO-d_6, 298 K)

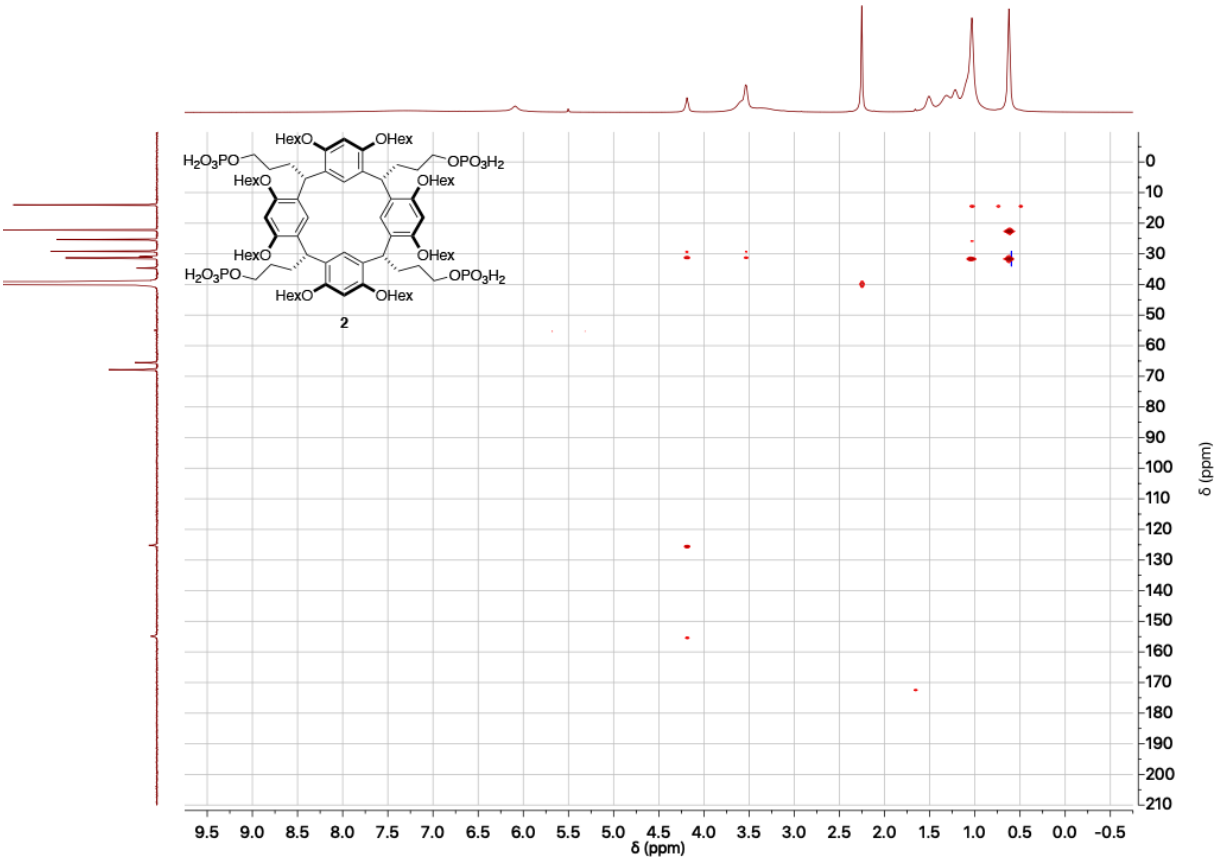

2-COSY (THF-d_8, 298 K)

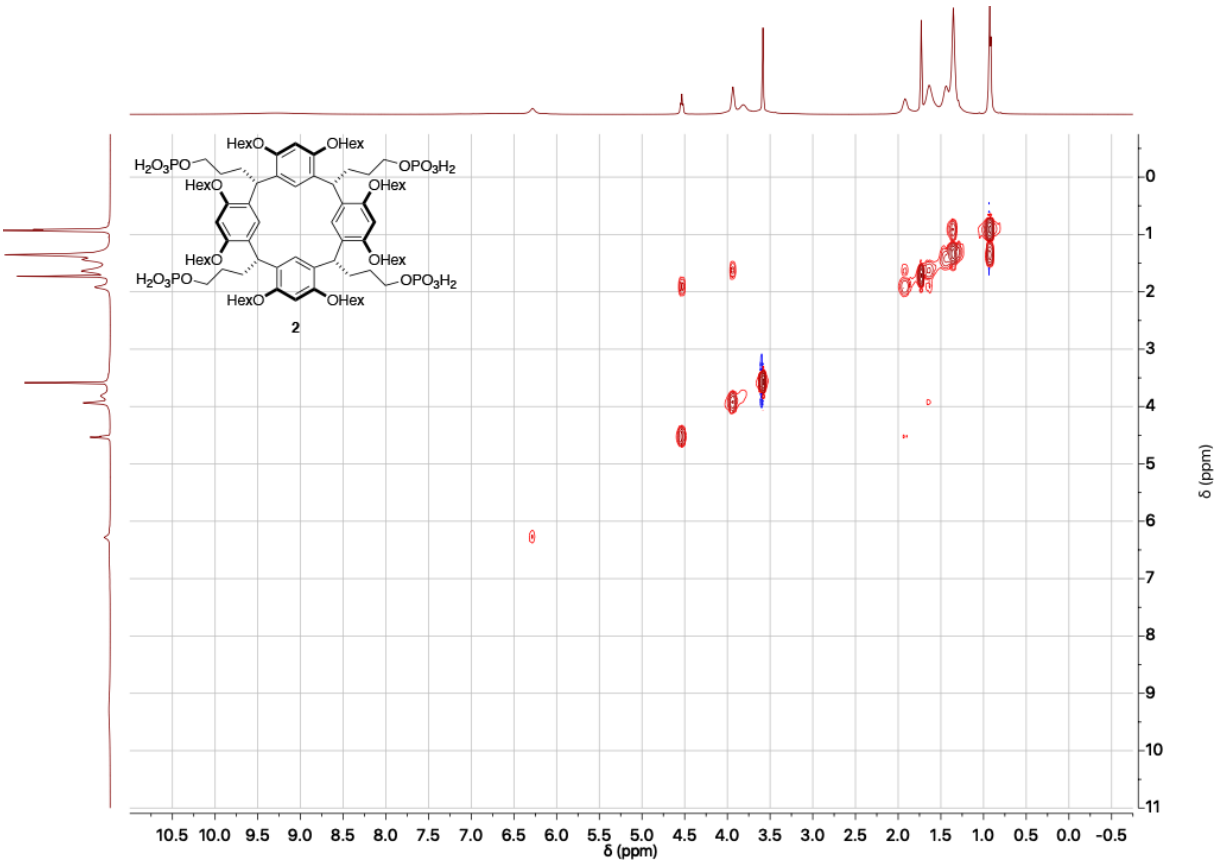

2-NOESY (THF-d_8, 298 K)

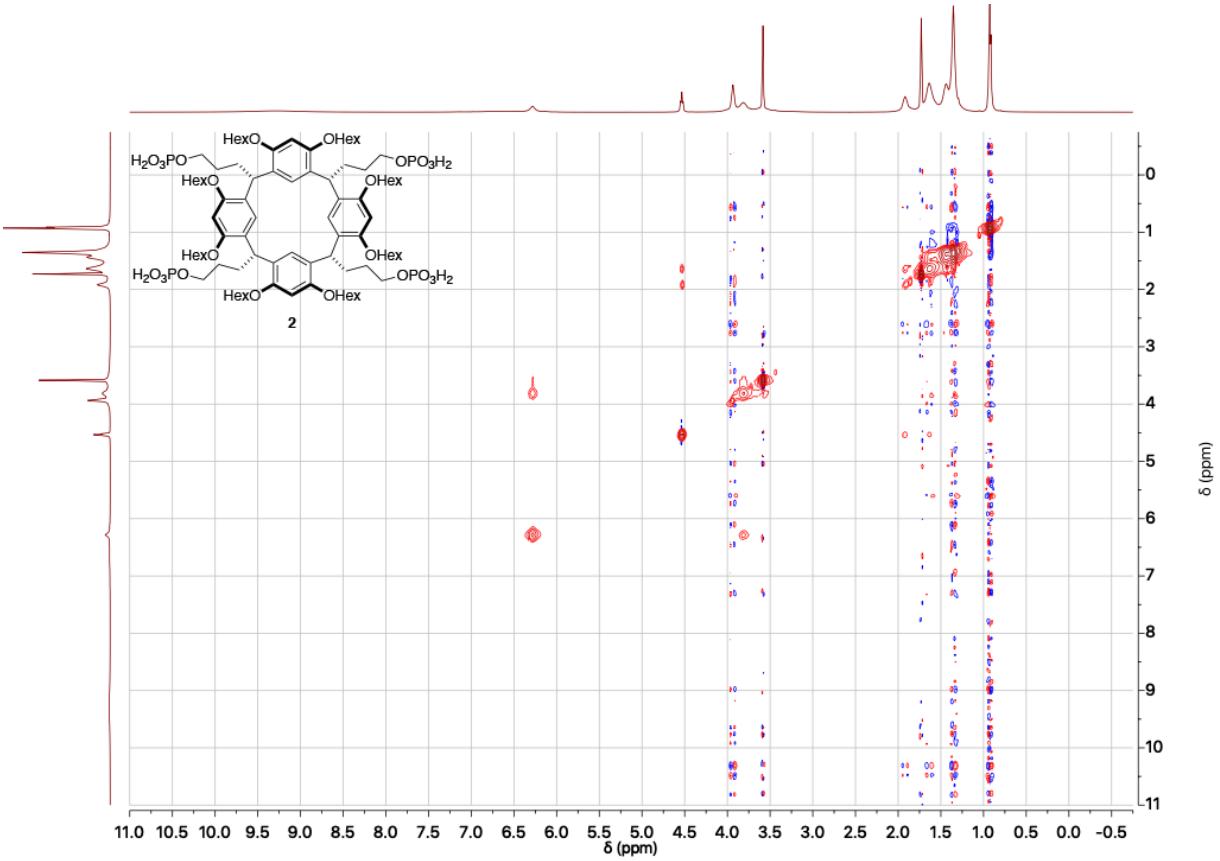

2-HMQC (THF-d_8, 298 K)

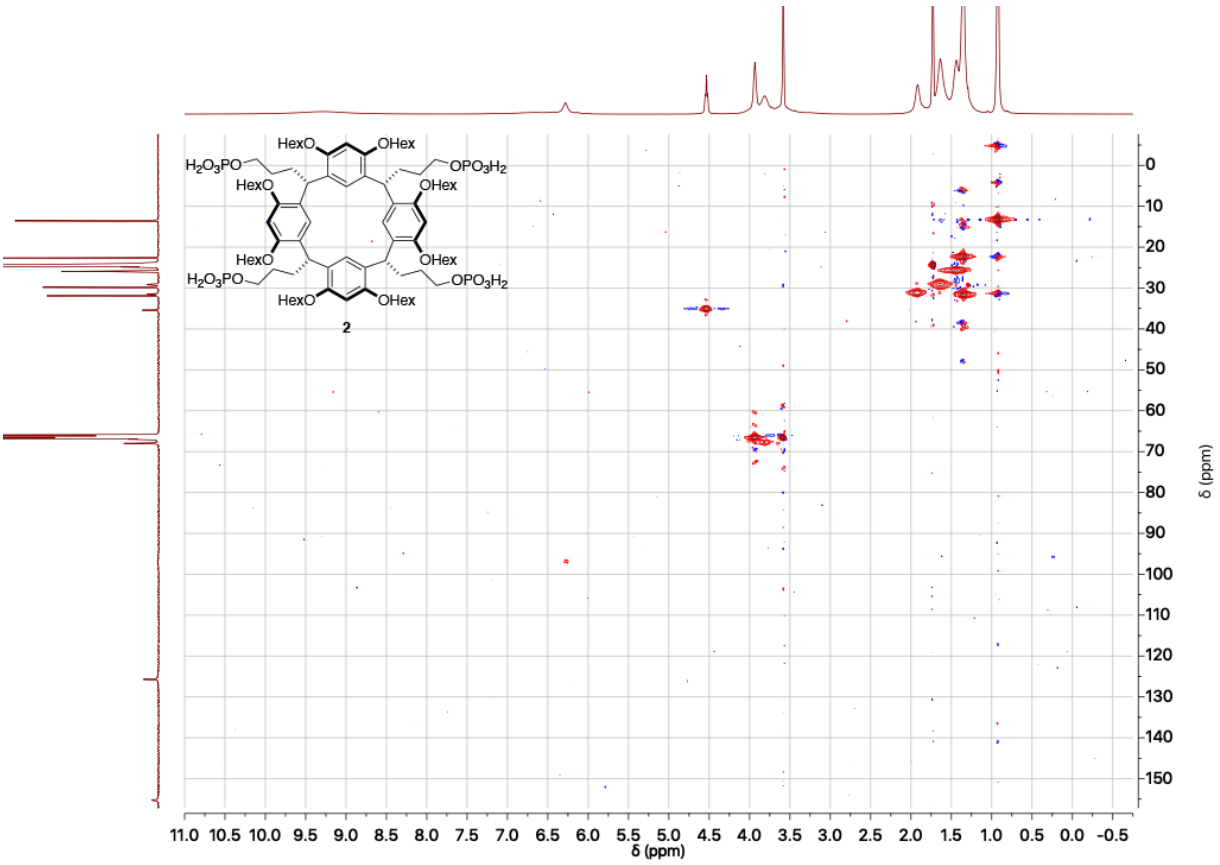

2-HMBC (THF-d_8, 298 K)